THE IMPACT OF WATER AND C3A ON PORTLAND

CEMENT HYDRATION

By

J. BRET ROBERTSON

Bachelor of Science in Civil Engineering

Oklahoma State University

Stillwater, OK

2008

Master of Science in Civil Engineering

Oklahoma State University

Stillwater, OK

2010

Submitted to the Faculty of the

Graduate College of the

Oklahoma State University

in partial fulfillment of

the requirements for

the Degree of

DOCTOR OF PHILOSOPHY

July, 2020

THE IMPACT OF WATER AND C3A ON PORTLAND

CEMENT HYDRATION

Dissertation Approved:

Dr. M. Tyler Ley
_____
Dissertation Adviser

Dr. Stephen Cross
_____

Dr. Bruce Russell
_____

Dr. Nicholas Materer
_____

Name: JOHN BRET ROBERTSON

Date of Degree: JULY, 2020

Title of Study: THE IMPACT OF WATER AND C3A ON PORTLAND CEMENT HYDRATION

Major Field: CIVIL ENGINEERING

Abstract: The water-cement ratio (w/cm) is one of the most influential parameters to determine the quality of concrete. A new test method, the Phoenix, has been developed that uses external heat to evaporate the water from the concrete before it has hardened. The method, calculation, and practical applications of this new test method are presented. This work also compares how the w/cm impacts fresh and hardened property measurements from slump, unit weight, surface resistivity, compressive strength, and the Phoenix. This work shows the accuracy of each measurement technique to determine changes in w/cm in field concrete. This work will aim to investigate how long a sample can be tested after mixing and obtain an accurate result and how long a sample can remain in the kiln before the materials decompose and change the results. These are important questions that limit the timing in the test method. Over 400 mixtures in the laboratory and field were conducted to validate the Phoenix and develop practical applications. In addition to a new test method, Tricalcium aluminate (C_3A) particles were also evaluated using X-ray nano-computed tomography (nCT) and nano X-ray fluorescence (nXRF). When these are combined, a technique named nano-tomography assisted chemical correlation (nTACCo) will be utilized to investigate three C_3A particles. C_3A plays a major role in the early hydration of Portland cement. Insights into C_3A dissolution and hydration product formation are important steps in understanding Portland cement hydration. The microstructural and chemical composition changes are directly observed, quantified, and discussed.

TABLE OF CONTENTS

Chapter   Page

LIST OF TABLES

LIST OF FIGURES

Figure   Page

CHAPTER I

INTRODUCTION

1.1 Introduction

There is not a widely used test to evaluate the water-to-cementitious ratio (w/cm) within a fresh

concrete mixture, even though modern concrete has been used for over a century. The w/cm is

arguably the most important parameter of concrete to determine the strength [1-3], consistency [4,

5], workability [6, 7], and durability [8, 9]. As water increases in a concrete mixture, the spacing

of the cement grains will also increase. This increase in grain spacing can improve the

workability for placing concrete but excessive water will decrease the performance of the

concrete. If the water content is too high, hydration products will have greater difficulty filling

the space between the cement grains [10]. This increase in porosity will also decrease the strength

[11], stiffness [5], and increase the amount of shrinkage from drying [7].

There has been some success from tests that use heating of the concrete to evaporate the water to

determine the w/cm. A test that uses a microwave oven was developed [12] and ultimately

became a standard [13]. The current version of the test requires 45 minutes. Furthermore, the

microwave test has been criticized for being inconsistent and the accuracy of the method has been

suggested to be +/- 0.03 to 0.05 of the actual w/cm [14]. This variability has been criticized as too

wide and therefore not useful.   A test method is needed that is efficient, rapid, and accurate to

establish a test that meets these criteria.

The presented method is known as the Phoenix and uses lab and field testing to establish a method to determine the w/cm. The Phoenix uses the actual batched materials and volumetric relationship to determine the w/cm of the batched mixture. Additional testing results for the air volume can be added to increase the accuracy of the w/cm calculation. Two versions of the Phoenix are used in this study. This work compares the Slump [15], Unit Weight (UW) [16], Compressive Strength [17], Surface Resistivity [18], and the Phoenix [19] to determine how accurately these tests can measure a change in the water content of the mixture. This is determined by preparing a concrete mixture with known water content and then measuring the changes in these results as known amounts of water are mixed into the concrete.

Two important questions are yet unanswered about the test method. The first is how long after mixing can a sample be investigated in the test and still obtain an accurate answer. This is important because water becomes bound and non-evaporable in hydration products unless exposed to temperatures greater than those in the test method. Second, can the temperature in the test cause further decomposition of the coarse or fine aggregates. This is important as this decomposition would be measured as weight change and so the test would interpret this as changes in the w/cm. To investigate this, this paper uses a variety of tests on the raw materials, paste, and ultimately concrete.

In addition to a new test method, Tricalcium aluminate (C_3A)[1] particles were also evaluated using X-ray nano-computed tomography (nCT) and nano X-ray fluorescence (nXRF). When these are combined, a technique named nano-tomography assisted chemical correlation (nTACCo) has been used to study the hydration of various C_3S systems [20-22]. C_3A makes up between 0% and 16% of Portland cement clinker. Also, C_3A plays a major role in the early hydration of Portland cement. This means that insights into C_3A dissolution and hydration product formation are important steps in understanding Portland cement hydration. C_3A hydration is typically delayed

---

[1] Conventional cement chemistry notation is used throughout this paper: C = CaO, A = Al_2O_3, H = H_2O

by adding $CaSO_4$ to avoid flash setting. The microstructural and chemical composition changes are directly observed, quantified, and discussed.

1.2 Research Objectives

The main tasks of this research were to:

- Chapter 2: Establish a fresh w/cm test method that is efficient, rapid, and accurate called the Phoenix.

- Chapter 3: Determine the accuracy of slump, unit weight, compressive strength, resistivity, petrography, and the Phoenix concerning the impact of water on properties of concrete.

- Chapter 4: Prove sample testing times within the Phoenix test method.

  - Establish the maximum amount of time between when a sample is mixed and when it is tested.

  - Minimize the amount decomposition in samples tested.

- Chapter 5: Study C_3A hydration during early hydration periods.

CHAPTER II

DETERMINING THE WATER-TO-CEMENT RATIO OF FRESH CONCRETE BY

EVAPORATION

2.1 Introduction

Although modern concrete has been used for over a century, there is not a widely used test to

evaluate the water-to-cement ratio (w/cm) within a fresh concrete mixture. Where cement may

consist of any material purposely added to the concrete to react with the water. Examples include

Portland cement, fly ash, slag, silica fume, natural pozzolans, or any other material added to react

with water. The w/cm is arguably the most important parameter of concrete to determine the

strength [1-3], consistency [4, 5], workability [6, 7], and durability [8, 9].

As water increases in a concrete mixture, the spacing of the cement grains will also increase.

This increase in grain spacing can improve the workability for placing concrete but excessive

water will decrease the performance of the concrete. If the water content is too high, hydration

products will have greater difficulty filling the space between the cement grains [10]. This

increase in porosity will also decrease the strength [11], stiffness [5], and increase the amount of

shrinkage from drying [7]. Each increase of 0.01 w/cm can decrease the strength by 103 kPa [23].

Service life models predict that a 0.01 w/cm increase for typical concrete practices in Oklahoma

would decrease the expected life of the structure by one year [24]. If 0.02 m^3 of water is added

toa 6 m^3 mixture with 335 kg/m^3 of the binder, then this will increase the w/cm by 0.01. There

are many ways for excess water to be added to concrete without being recorded. Some examples include leftover wash water or excess material from the previous mixture. Another possible error is incorrect moisture content of the aggregate in the mixture. Water can also be added inadvertently while cleaning a truck or to increase the workability at the job site.

Many attempts have been made to measure the w/cm in fresh concrete. The methods fall into the following categories: mechanical separation, absorption, electrical conductivity, and heat transfer. The mechanical separation methods utilized either a heavy liquid [25] or flocculation [26] of the concrete to separate the water from the mixture. One mechanical flocculation method could obtain the cement and water content from titrations [27]. These mechanical separation techniques require a calibration curve produced from similar materials and the equipment used is not practical for field testing. Gamma-ray backscatter and absorption [28] or ultrasonic wave transmission [29] have also been used. The gamma ray testing was not popular due to the careful training and handling required to run the equipment and the ultrasonic technique was determined to not be accurate for fresh concrete. Other methods used electrical conductivity [30, 31]. The technique measures the electrical resistivity in the fresh concrete to determine the w/cm. Many variables influence the reading of the probes including, aggregate size, temperature, admixtures, temperature, paste content, binder chemistry, and water content.

There has been some success from tests that use heating of the concrete to evaporate the water. A test that uses a microwave oven was developed [12] and ultimately became a standard [13]. A sample is weighed and placed in the microwave. After cooking for a fixed period, the sample is removed, crushed, weighed, and returned to the microwave. These steps are repeated until the sample does not change mass. The difference between the mass of the wet sample and the mass of the dry sample are used to calculate the total water. This information can be combined with the mass of cement in the mixture to determine the w/cm. The sample size in this test is only 1500 g or about one-third of a typical 4x8 cylinder. This small sample size is needed because a microwave oven is not able to remove the water in a timely manner. The current version of the

test requires 45 minutes. Furthermore, the microwave test has been criticized for being inconsistent and the accuracy of the method has been suggested to be +/- 0.03 to 0.05 of the actual w/cm [14]. This variability has been criticized as too wide and therefore not useful. For all of these reasons, these tests have not been adopted as an industry standard. Ultimately, a test is needed that is efficient, rapid, and accurate. The aim of this patent is to establish a test that meets these criteria. The presented method is known as the Phoenix and uses lab and field testing to examine 364 laboratory mixtures and 27 field mixtures with 23 aggregates, 9 portland cements, 5 supplementary cementitious materials (SCM), and 15 different admixtures. The results are repeatable, accurate, and the test can be completed in the field.

2.2 Experimental Methods

2.2.1 Materials

A summary of laboratory mixtures investigated are shown in Table 2-1 and the field mixtures can be seen in Table 2-2. Testing was completed for 364 laboratory mixtures and 27 field mixtures. Multiple w/cms from 0.30 to 0.60 are investigated for each aggregate source. These concrete mixtures used a type I cement that met the requirements of ASTM C150 [32]. The oxide and Bogue calculations for this cement can be seen in Table 2-3. A summary of the aggregate investigated is in Table 2-4. All aggregate used met ASTM C33 [33] specification and are used in commercial concrete mixtures. Multiple coarse and fine aggregate sources were used with a specific gravity between 2.42 and 2.85 and absorption between 0.20 and 4.69%. Seventeen coarse aggregates that were granite, limestone, and river rock were used. Six fine aggregates that were either natural or manufactured sand were also investigated.

Table 2-1. SSD Mixture Proportions.

w/cm	Cement kg/m3	Coarse kg/m3	Fine kg/m3	Water kg/m3	Coarse Aggregate Type	Fine Aggregate Type
0.36	390	1115	809	141	Granite 1	Natural Sand 1
0.39	390	1098	795	152	Granite 1	Natural Sand 1

6

0.42	390	1074	787	164	Granite 1	Natural Sand 1
0.45	390	1061	768	176	Granite 1	Natural Sand 1
0.48	390	1044	754	187	Granite 1	Natural Sand 1
0.42	390	1020	736	203	Granite 2	Natural Sand 1
0.45	390	1074	787	164	Granite 2	Natural Sand 1
0.48	390	1061	768	176	Granite 2	Natural Sand 1
0.39	390	1044	754	187	Granite 3	Natural Sand 1
0.45	390	1020	736	203	Granite 3	Natural Sand 1
0.39	362	1086	794	141	Granite 4	Natural Sand 1
0.45	362	1061	762	163	Granite 4	Natural Sand 1
0.42	362	1023	734	189	Limestone 1	Natural Sand 1
0.45	362	1083	826	141	Limestone 1	Natural Sand 1
0.48	362	1061	790	163	Limestone 1	Natural Sand 1
0.45	362	1017	767	189	Limestone 2	Natural Sand 2
0.36	362	1112	660	152	Limestone 3	Natural Sand 1
0.39	362	1098	647	163	Limestone 3	Natural Sand 1
0.42	362	1083	635	174	Limestone 3	Natural Sand 1
0.45	362	1062	619	189	Limestone 3	Natural Sand 1
0.48	362	1098	756	163	Limestone 3	Natural Sand 1
0.50	362	1068	736	182	Limestone 3	Natural Sand 1
0.55	362	1023	706	199	Limestone 3	Natural Sand 1
0.60	362	1003	688	218	Limestone 3	Natural Sand 1
0.44	362	1103	765	160	Limestone 3	Natural Sand 1
0.45	362	1068	830	163	Limestone 3	Manufactured Sand
0.45	362	1148	794	131	River Rock 1	Natural Sand 1
0.36	362	1133	781	141	River Rock 2	Natural Sand 1
0.45	362	1112	772	152	River Rock 2	Natural Sand 1
0.30	362	0	0	109		
0.40	362	0	0	145		
0.50	362	0	0	182		
0.60	362	0	0	217		

Table 2-2. Field testing materials batched.

Truck	Cement (kg/m³)	Fly Ash C (kg/m³)	Fly Ash F (kg/m³)	Slag (kg/m³)	Coarse (kg/m³)	Fine (kg/m³)	Water (kg/m³)	Coarse Aggregate Type	Fine Aggregate Type	Admixtures
1	316	78			889	897	166	Limestone 5	Natural Sand 2	AEA, WRA, Accelerator
2	338				1059	820	153	Limestone 5	Natural Sand 2	AEA, WRA
3	333				1061	815	156	Limestone 5	Natural Sand 2	AEA, WRA
4	333				1100	743	147	Limestone 6	Natural Sand 3	AEA, WRA
5	333				1113	739	145	Limestone 6	Natural Sand 3	AEA, WRA, Retarder
6	334				1102	749	145	Limestone 6	Natural Sand 3	AEA, WRA, Retarder
7	333				1095	745	140	Limestone 6	Natural Sand 3	AEA, WRA, Retarder
8	333				1095	745	140	Limestone 6	Natural Sand 3	AEA, WRA, Retarder
9	331				1086	742	142	Limestone 6	Natural Sand 3	AEA, WRA, Retarder
10	267	66			1114	788	131	Limestone 2	Natural Sand 2	AEA, WRA, Retarder
11	269	66			1159	784	131	Limestone 2	Natural Sand 2	AEA, WRA, Retarder
12	266	66			1140	784	131	Limestone 2	Natural Sand 2	AEA, WRA, Retarder
13	332				1109	787	147	Limestone 6	Natural Sand 3	AEA, WRA, Retarder
14	332				1106	74	145	Limestone 6	Natural Sand 3	AEA, WRA, Retarder
15	333				1100	743	146	Limestone 6	Natural Sand 3	AEA, WRA, Retarder
16	333				1113	739	142	Limestone 6	Natural Sand 3	AEA, WRA, Retarder
17	334				1102	749	140	Limestone 6	Natural Sand 3	AEA, WRA, Retarder
18	333				1102	749	143	Limestone 6	Natural Sand 3	AEA, WRA, Retarder
19	235		53	73	1056	737	130	Limestone 11	Natural Sand 4	AEA, HRWRA
20	230	59			1042	841	138	Limestone 8	Natural Sand 4	HRWRA
21	336				1038	769	161	Limestone 8	Natural Sand 4	AEA
22	235		55	73	1055	736	135	Limestone 11	Natural Sand 4	AEA, HRWRA
23	333				1054	785	147	Limestone 8	Natural Sand 4	AEA, HRWRA, accelerator
24	354	59			507	1203	208	Limestone 7	Natural Sand 4	-
25	226	60			991	878	141	Limestone 8	Natural Sand 4	AEA, HRWRA
26	283	72			1001	821	149	Limestone 9	Natural Sand 4	AEA, HRWRA
27	178			180	878	915	155	Limestone 10	Natural Sand 5	AEA, HRWRA

Table 2-3. Type I cement oxide analysis.

Oxide (%)	SiO_2	Al_2O_3	Fe_2O_3	CaO	MgO	SO_3	Na_2O	K_2O	TiO_2	P_2O_5	C_3S	C_2S	C_3A	C_4AF
Cement	21.1	4.7	2.6	62.1	2.4	3.2	0.2	0.3	-	-	57	18	8.2	7.8

Table 2-4. Tested aggregate summary.

Aggregate Type	Size	Specific Gravity	Absorption (%)	State
Granite	Coarse	2.75	0.46	OK
Quartzite-Granite	Coarse	2.75	0.51	GA
Granite	Coarse	2.59	1.06	MN
Quartzite-Granite	Coarse	2.66	0.66	MN
Dolomitic Limestone	Coarse	2.42	4.69	IA
Limestone	Coarse	2.67	0.70	OK
Limestone	Coarse	2.67	0.64	OK
Limestone	Coarse	2.85	0.76	OK
Limestone	Coarse	2.70	0.68	OK
Limestone	Coarse	2.76	0.72	OK
Limestone	Coarse	2.62	0.40	KS
Limestone	Coarse	2.63	1.70	KS
Limestone	Coarse	2.67	0.30	KS
Limestone	Coarse	2.67	1.80	KS
Limestone	Coarse	2.69	0.70	KS
Glacial Till	Coarse	2.67	1.52	MN
Glacial Till	Coarse	2.68	0.81	MN
Manufactured Sand	Fine	2.76	1.05	OK
Natural Sand	Fine	2.62	0.64	OK
Natural Sand	Fine	2.61	0.76	OK
Natural Sand	Fine	2.64	0.34	OK
Natural Sand	Fine	2.62	0.40	KS
Natural Sand	Fine	2.62	0.20	KS

2.2.2 Concrete Mixture procedure and testing

Since the focus is to obtain an accurate w/cm, it was important to very accurately measure and account for the moisture in the aggregates. To do this, a standard laboratory method was used to prepare the samples. It has been described previously but is repeated here for the convenience of the reader [34].

"The aggregates for each mixture were collected from outside stockpiles and brought into a temperature-controlled room at 22°C for at least 24 hours before mixing. Aggregates were placed in a mixing drum, spun for a period of time, and a representative sample was taken to determine the moisture content to apply a moisture correction to the mixture.

At the time of mixing, all aggregates were loaded into the mixer along with approximately two-thirds of the mixing water. This combination was mixed for three minutes to allow the aggregate surface to saturate and ensure the aggregates were evenly distributed. Next, the cement, fly ash, and the remaining water was added and mixed for three minutes. The resulting mixture rested for three minutes while the sides of the mixing drum were scraped. After the rest period, the desired admixtures were added and the mixer was turned on and mixed for two minutes."

The moisture content was obtained according to ASTM C566 [35] The fresh properties were measured and samples were created to complete the w/cm test. For the test, two samples were investigated simultaneously by the same operator for each mixture. Samples obtained for the microwave oven test were run in accordance with AASHTO T 318. The AASHTO T 318 test required 45 minutes to complete.

Some mixtures were hand mixed in small batches below 0.1 cubic feet. The aggregate used for the small mixtures was moisture corrected in the same way as the larger mixtures. To achieve accurate batch water, water was added to a dry bowl and weighed. All the materials were then added to the bowl with water and each mixed until thoroughly blended in the following order,

admixture (if used), cement, fine aggregate, and coarse aggregate. This material was then sampled for the testing. Two samples were investigated simultaneously.

Field testing was completed for twenty-seven concrete mixtures from four concrete plants in Oklahoma and Kansas. The majority of the samples were taken on job sites that were constructing a bridge or pavement. The remaining samples were taken from ready-mix plants before the concrete was transported to the job-site. The field testing batched values can be seen in Table 2-12.

2.2.3 Sample Size Selection

It was important to determine a satisfactory sample volume to use within the test. If the sample size investigated is too small, then the test will not give representative results. However, if the sample size used is too large then the increased volume in the test will increase the time required to complete the test. It is important to find a sample size that will give accurate results but will not take an excessive time to complete.

To investigate this concrete mixture with 0.45 w/cm were sampled with a variety of volumes. The unit weight and the average measured w/cm was found. The method and calculation for the measured w/cm are presented in future sections of this paper. The results are presented in Table 2-5.

According to ASTM C138, the single-operator standard deviation between measuring UW of concrete is 10.4 kg/m^3. This precision and bias are based on 7079 cm^3 volume. If this precision could be obtained with a smaller volume, then that would represent a satisfactory volume for the proposed test. The test was completed in waterproof plastic molds for all samples except for the sample that was 7079 cm^3, which was tested in an aluminum unit weight bucket. Further, the sample with a volume of 694 cm^3 matches the volume used in the microwave oven test. The plastic molds for the testing were created by taking larger molds and then cutting them so that

11

they were the desired volume. The volume of these plastic molds was checked by filling with water, measuring the mass, and finding the volume based on the density.

Based on this testing 1648 cm^3 is the lowest volume to show a satisfactory coefficient of variation for the density and the water to cement ratio. Again, it is important to pick a volume that was as small as possible but still provides a representative density and accurate estimate of the water content to minimize the time required by the test and also be representative of the concrete mixture. The 7079 cm^3 sample was not able to be tested in the water to cement test because of the large size. The coefficient of variation for the sample with 5559 cm^3 volume had a higher standard deviation and coefficient of variation than expected for the density. This was the tallest sample investigated and so this might have made it more challenging to consolidate the material. Despite the higher variability in density, the coefficient of variation of the water to cement testing matched the volumes of 1648 cm^3 and greater.

Table 2-5. Multiple size volumes tested for three, 0.45 w/cm mixtures.

Number Of Samples	Cylinder Size (in.)	Sample Volume (cm³)	Average Density (kg/m³)	Standard Deviation (kg/m³)	Density COV (%)	Average Measured w/cm	Standard Deviation	Measured w/cm COV (%)
9*	3x6	694	2412.4	51.3	2.1	0.42	0.022	5.2
9	4x4	824	2410.8	22.4	0.9	0.44	0.021	4.8
9	4x6	1236	2425.2	12.6	0.5	0.45	0.022	4.9
9	4x8	1648	2428.4	4.8	0.2	0.45	0.010	2.2
9	6x4	1852	2428.4	8.0	0.3	0.45	0.010	2.2
9	6x12	5559	2418.8	11.2	0.5	0.44	0.011	2.5
9	8x8.8	7079	2423.6	8.0	0.3			

*Sample is representative of microwave sample according to AASHTO T318

2.2.4 Phoenix Test Using Dual Heating Elements

The device used a heating element, an induction cooktop, pan, and a scale. The heating element temperature was ≈ 700 °C. The pan had a diameter of 23 cm and a depth of 8 cm. The 1500 Watt cooktop had a coil diameter of 20 cm. A scale with 0.01-gram accuracy and 10 kg capacity was used. The device setup can be seen in Figure 2-1. Conventional power was used in the laboratory and a generator was used in the field testing.

Figure 2-1. Phoenix with dual heating elements for laboratory testing.

2.2.5 Phoenix Test Using a Furnace

The device used a furnace, pan, and scale. The maximum temperature of the furnace was 815°C.

The pan used was 17.8 cm wide by 22.9 cm long with a depth of 4.4 cm. The furnace is 3600

Watt with a loading chamber covered by a hinged door as seen in Figure 2-2. The loading

chamber utilizes heating elements that surround the chamber to decrease heating and cooking

times. Some of the heating elements can be seen in Figure 2-3. The furnace applied heat from

both the top and bottom of the sample. A scale with 0.1-gram accuracy and 21 kg capacity was

used. A 240 Volt outlet with 20 amps was required to run the setup.

Figure 2-2. Phoenix with a furnace.
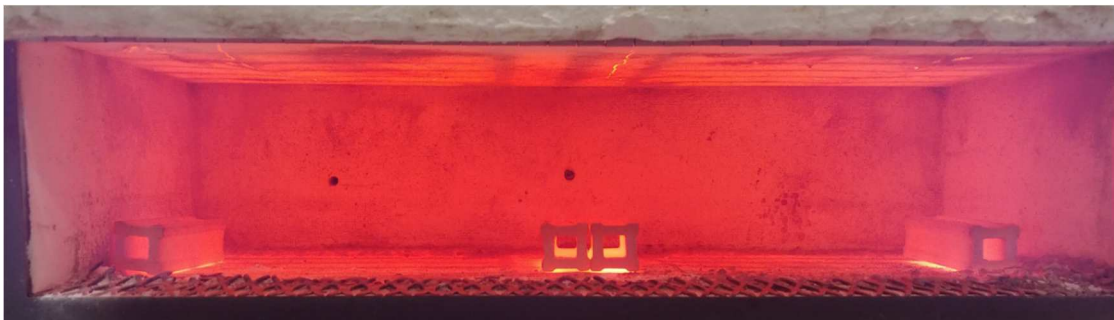
Figure 2-3. Heating chamber when the furnace is on.

2.3 Test Method

2.3.1 Phoenix Test Using Dual Heating Elements

The first step in the method is to gather concrete mixture of information. The concrete mixture

information required includes the mass of the batched materials, aggregate properties, binder

specific gravities, and the total volume of the batch. For the aggregate properties, the specific

gravity and absorption for each coarse and fine aggregate are needed.

The air volume in the concrete should be obtained by either using ASTM C231 [36] or based on

the theoretical density calculation according to ASTM C138 [16]. The ASTM C138 method to

obtain air is described in the calculations section.

Next, the mass and volume of the empty mold are recorded. This testing used a plastic 4x8

cylinder mold that met the volumes required for accurate and fast results. Fresh concrete is

sampled from the mixture in accordance with ASTM C172 [37]. All samples are prepared

according to ASTM C31 [38]. The mold is filled, finished, and weighed with fresh concrete. The

sample is then discharged into the pan and the mold is thoroughly emptied with a spatula. The

mass of the empty mold is compared to the mass before starting the test. The mass should be

within 10 g of the empty mold. This helps the operator determine that they have removed enough

material from the form to complete an accurate test. The volume of the tested material can be

calculated using Equation 10.

The material is placed in the pan so that it has a uniform thickness. The thickness of the material

in the pan should be 19 mm +/- 13 mm. The mass of the pan full of fresh concrete is recorded and

placed into the test device. The cooktop is turned to the highest setting. The heating element is

preheated for 10 min to reduce the time needed to complete the test. With these conditions, the

test can be completed in 30 minutes. Figure 2-4 shows a mass loss for three samples over time.
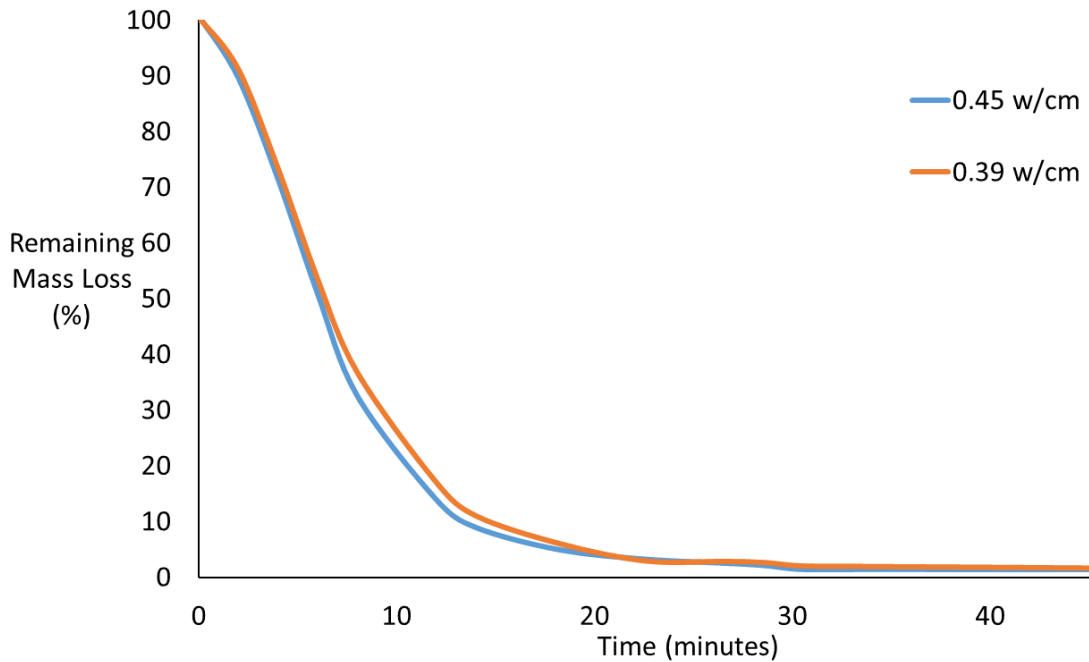
Figure 2-4. Percent remaining mass loss of concrete over time.

The sample can be kept under the heating element unattended and weighed at any point after 30 minutes. To determine when the sample is dry, the combined mass of the pan and concrete should be 2 grams or less of the previous measurement from at least two minutes of heat exposure. This represents a 0.05% change of the initial concrete mass. The final mass of the pan and concrete are recorded. This represents the total water evaporated, including the absorbed water in the aggregates. The concrete can then be removed, and the pan can be cleaned.

2.3.2 Phoenix Test Using a Furnace

The test method is the same as the dual heating elements, except for the preheating procedure, cooking time, and cleaning. The cooktop and heating element has been replaced with the furnace. The furnace is preheated to 815°C and the pan is placed in the furnace. The cooking time is 15 minutes. The sample can be kept in the furnace unattended and weighed at any point after 15 minutes. To determine when the sample is dry, the combined mass of the pan and concrete should

be 2 grams or less of the previous measurement from at least two minutes of heat exposure. This represents a 0.05% change of the initial concrete mass.

After the final weight is recorded, the pan is submerged in water to rapidly cool the pan and concrete. Once cooled, the pan can be cleaned. Figure 2-5 shows the mass loss over time for one sample for both devices.
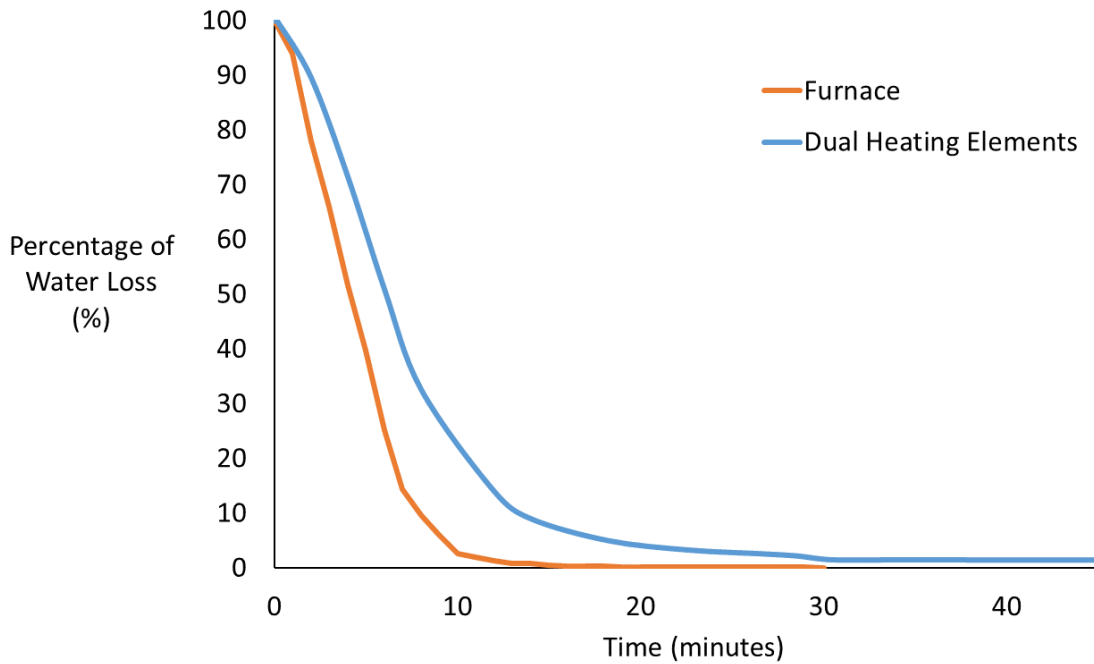
Figure 2-5. Percent remaining mass loss of concrete over time.

2.3.3 Moisture Content of Aggregate

The moisture content of aggregates can be determined according to ASTM C566 [27], using both test setups. The sample can be weighed and placed into the pan. The sample is then placed into the respective device. The sample can be checked in the dual heating elements after 15 minutes and the furnace after 5 minutes. The sample is thoroughly dry when further heating causes, or would cause, less than 0.1 % additional loss in mass [27].

2.3.4 Calculations

A summary of the variables for the test is in Table 2-6. The variable names assigned in Table 2-6 will be utilized for the calculation for the test method.

Table 2-6. Variable definitions for recorded values during the test method.

Description	Variable Name
Binder specific gravities	SG_{Binder}
Coarse aggregate absorptions	Abs_{Coarse}
Fine aggregate absorptions	Abs_{Fine}
Coarse aggregate specific gravities	SG_{Coarse}
Fine aggregate specific gravities	SG_{Fine}
Batched binder weight	M_{Binder}
Batched coarse aggregate weight	M_{Coarse}
Batched fine aggregate weight	M_{Fine}
Batch water weight	M_{Water}
Batched volume in mixer	V_{Batch}
Batched concrete air volume (See 4.1.1)	V_{Air}
Tare weight of cylinder	Cyl_{Tare}
Volume of cylinder	V_{Cyl}
Weight of cylinder filled with concrete	Cyl_{Full}
Weight of cylinder after emptied	Cyl_{Empty}
Weight of pan with fresh concrete	P_{fresh}
Weight of pan with dried concrete	P_{Dry}
Weight of binder in cylinder	Cyl_{Binder}
Weight of total absorbed water in cylinder	$Cyl_{WaterAbs}$

2.3.4.1 Air Volume

The air volume in the concrete can be found by using the measured density of the concrete. This density can be compared with the theoretical density from the batch information to obtain the air

content. This is performed according to ASTM C138 by using the mold in the proposed test method. The density of the concrete in the cylinder can be found as:

$$\text{Cyl Density} = (\text{Cyl}_{Full} - \text{Cyl}_{Tare}) / \text{V}_{Cyl} \qquad \{1\}$$

The theoretical density of the batched concrete can be found as:

Theoretical Density = Total Batched Mass / Absolute Volume Batched (Air Free)

where

$$\text{Total Batched Mass} = M_{Binder} + M_{Coarse} + M_{Fine} + M_{Water} \qquad \{2\}$$

and

Absolute Volume Batched (Air Free) = ((MBinder)/(SGBinder *1000)) + ((MCoarse)/(

SGCoarse * 1000)) + ((M_{Fine})/($SGFine$ * 1000)) + M_{Water} /1000 $\qquad \{3\}$

For the theoretical density calculation in lb/ft^3, the mass is replaced by batched weight and each 1000 is replaced by 62.4 lb/ft^3.

The theoretical air content can be found by finding the % difference between the theoretical density and the cylinder density. This can be found mathematically as follows:

Air Content (%) = ((Theoretical Density– Cyl Density) / Theoretical Density) * 100 $\quad\{4\}$

Or using equations, Air Content (%) = (({2} - {1}) / {2}) *100

The air content from ASTM C231 can also be used instead of this procedure.

2.3.4.2 Batched Absolute Volume Calculation

The absolute volume of concrete batched must be calculated for the fresh w/cm determination. This can be calculated with the batched masses and air volume from the batch information. This can be expressed mathematically as:

Absolute Volume Batched $= ((M_{Binder}) / (SG_{Binder} *1000)) + ((M_{Coarse}) / (SG_{Coarse} *$

$1000)) +$

$((M_{Fine}) / (SG_{Fine} * 1000)) + (M_{Water} / 1000) + (V_{Batch} * (V_{Air} / 100))$ {5}

2.3.4.3 Total Water Absorbed

As shown in Figure 2-4, all the water from the sample is removed from the concrete including the
absorbed water in the aggregates. Concrete mixtures are adjusted and batched by assuming the
aggregate are saturated surface dry. Although the aggregates are not usually in this condition
when placed into a mixer, it is assumed that the aggregates reach a saturated condition before the
concrete has set. Because the test evaporates all of the water from the concrete mixture, the
aggregate absorption must be accounted for in the calculations. To account for this the absorbed
water for each aggregate in the batch is calculated as follows:

Coarse Aggregate Absorbed Water $= (Abs_{Coarse} / 100) * M_{Coarse}$ {6}

and

Fine Aggregate Absorbed Water $= (Abs_{Fine} / 100) * M_{Fine}$ {7}

where

Total Absorbed Water = Coarse Aggregate Absorbed Water + Fine Aggregate Absorbed
Water

{8}

If there are multiple coarse and fine aggregate sizes in the mixture each could be added to these
values using the weight and absorption value for every additional aggregate to find the total
absorbed water.

2.3.4.4 Batched Density

The batched density is calculated by taking the sum of the batched masses divided by the absolute volume of the batch. This can be shown mathematically as:

$$\text{Batched Density} = \text{Total Batched Mass} / \text{Absolute Volume Batched} \qquad \{9\}$$

Or using equations, Batched Density = {2} / {5}

2.3.4.5 Cylinder and Pan Calculations

As mentioned before, the mass of material remaining in the mold should be < 10 g of the empty cylinder mass. The material that was placed in the pan is used to obtain the volume in the test. This can be shown mathematically as:

$$\text{Cylinder Volume Tested} = ((Cyl_{Full} - Cyl_{Empty}) / (Cyl_{Full} - Cyl_{Tare})) * V_{Cyl} \qquad \{10\}$$

Next, the water lost in the test is calculated. This is found by the difference between the mass of the pan with fresh concrete from the mass of the pan with dry concrete. This can be shown mathematically as:

$$\text{Water Loss Mass} = P_{fresh} - P_{Dry} \qquad \{11\}$$

2.3.4.6 Binder and Absorbed water in the Cylinder

The estimated water in the concrete cylinder represents the total water in the sample including the absorbed water in the aggregates. Next, the volume of the sample tested is divided by the absolute volume batched. This can be seen mathematically as:

$$\text{Volume Ratio} = \text{Cylinder Volume Tested} / \text{Absolute Volume Batched} \qquad \{12\}$$

Or using equations, as Volume Ratio = {11} / {5}

The volume ratio is a scale factor to reduce the material weights from a larger volume to the volume in the mold. Multiplying the volume ratio with a batch weight will represent the weight in the mold for that material. This will be used to determine the weight of the binder in the cylinder.

The weight of the binder in the cylinder can be found by multiplying the volume ratio with M_{Binder}. This can be seen mathematically as:

$$\text{Cyl}_{Binder} = \text{Volume Ratio} * M_{Binder} \qquad\qquad \{13\}$$

where Volume Ratio is equation {12}.

The total absorbed water for the batch has been calculated in equation {8}. This value needs to be adjusted to the water absorbed in the sample tested. The $\text{Cyl}_{WaterAbs}$ is the volume ratio multiplied by the total absorbed water. This can be seen mathematically as follows:

$$\text{Cyl}_{WaterAbs} = \text{Volume Ratio} * \text{Total Absorbed Water} \qquad\qquad \{14\}$$

Or using equations, $\text{Cyl}_{WaterAbs} = \{12\} * \{8\}$

2.3.4.7 W/cm Calculations

At the completion of the test the water loss from the sample represents the total water in the cylinder, this includes the absorbed water in the aggregate. For the w/cm calculation, the total water minus the aggregate absorbed water represents the adjusted water. The w/cm is determined by dividing the water loss mass minus the $\text{Cyl}_{WaterAbs}$ by the Cyl_Binder mass. This can be seen mathematically as follows:

$$\text{Measured w/cm} = (\text{Water Loss Mass} - \text{Cyl}_{WaterAbs}) / (\text{Cyl}_{Binder}) \qquad\qquad \{15\}$$

Or Measured w/cm = ({11} − {14}) / {13}

The measured w/cm is the result of this fresh concrete w/cm test method. The measured w/cm can

be compared with the batched w/cm. The batched w/cm is calculated by dividing the M_{Water} by

M_{Binder}.

2.4 Results and Discussion

2.4.1 Laboratory Results

2.4.1.1 Phoenix Test Using Dual Heating Elements

To determine the effectiveness of the proposed test, 231 lab mixtures with nine coarse aggregates,

three fine aggregates at five different w/cm were tested. Figure 2-6 shows the average and one

standard deviation for each measured w/cm versus the batched w/cm. In this graph, all of the

data is combined at each w/cm. A line of equality is included on the graph to show an exact

match of the batched and the measured w/cm. The two lines on either side represent a +/- 0.02

w/cm. This shows a reasonable range for the w/cm variation. The microwave oven test result is

also shown in Figure 2-6. The microwave testing was done on one of the concrete mixtures that

corresponded with the introduced w/cm method.
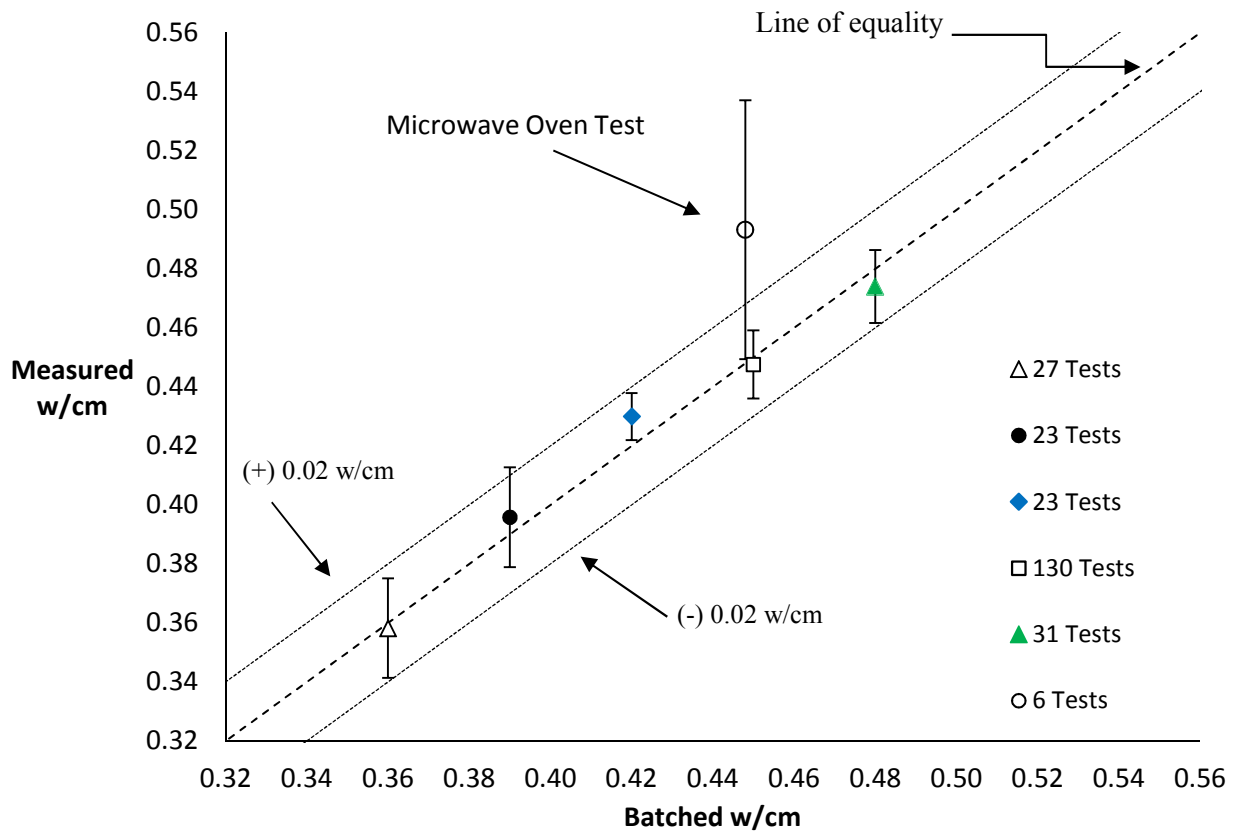
Figure 2-6. dual heating element device average and one standard deviation of all batched and measured w/cm test results. An AASHTO T 318 microwave oven test at 0.45 w/cm has also been included for comparison. The microwave oven test data was from mixtures batched with 0.45 w/cm. The point has been slightly offset on the x-axis to better show the error compared with the 0.45 data.

The same data from Figure 2-6 is plotted again in Figure 2-7 but for the individual mixture combinations. The average and one standard deviation are shown for each data set. The data points have been offset on the X-axis to the results easier to read.

Table 2-7. Summary of fresh w/cm with dual heating element device, sorted by coarse aggregate type.

Tests	Batched w/cm	Average Measured w/cm	Difference Batched and Measured	Standard deviation	COV (%)	Coarse Aggregate Type	Fine Aggregate Type
4	0.36	0.38	-0.020	0.026	6.9	Granite 1	Natural Sand 1
13	0.36	0.36	0.000	0.013	3.5	Limestone 3	Natural Sand 1
3	0.36	0.35	0.010	0.010	2.9	Limestone 3	Natural Sand 2
4	0.36	0.34	0.020	0.012	3.6	River Rock 2	Natural Sand 1
11	0.39	0.40	-0.010	0.015	3.6	Granite 1	Natural Sand 1
4	0.39	0.38	0.010	0.024	6.4	Granite 3	Natural Sand 1
4	0.39	0.39	0.000	0.017	4.2	Granite 4	Natural Sand 1
4	0.39	0.41	-0.020	0.012	2.9	Limestone 3	Natural Sand 1
6	0.42	0.43	-0.010	0.008	2.0	Granite 1	Natural Sand 1
6	0.42	0.43	-0.010	0.008	1.9	Granite 2	Natural Sand 1
4	0.42	0.43	-0.010	0.004	0.9	Limestone 1	Natural Sand 1
7	0.42	0.43	-0.010	0.011	2.6	Limestone 3	Natural Sand 1
8	0.45	0.44	0.010	0.011	2.5	Granite 1	Natural Sand 1
2	0.45	0.43	0.020	0.012	2.7	Granite 1	Manufactured Sand
4	0.45	0.44	0.010	0.009	2.0	Granite 1	Natural Sand 2
7	0.45	0.44	0.010	0.011	2.4	Granite 2	Natural Sand 1
6	0.45	0.45	0.000	0.008	1.8	Granite 3	Natural Sand 1
4	0.45	0.46	-0.010	0.005	1.1	Granite 4	Natural Sand 1
6	0.45	0.46	-0.010	0.012	2.5	Limestone 1	Natural Sand 1
16	0.45	0.44	0.010	0.023	5.1	Limestone 2	Natural Sand 1
65	0.45	0.45	0.000	0.015	3.2	Limestone 3	Natural Sand 1
6	0.45	0.45	0.000	0.010	2.2	River Rock 1	Natural Sand 1
6	0.45	0.44	0.010	0.011	2.4	River Rock 2	Natural Sand 1
7	0.48	0.49	-0.010	0.011	2.3	Granite 1	Natural Sand 1
4	0.48	0.47	0.010	0.004	0.9	Granite 2	Natural Sand 1
10	0.48	0.47	0.010	0.015	3.1	Limestone 1	Natural Sand 1
10	0.48	0.47	0.010	0.020	4.2	Limestone 3	Natural Sand 1
			0.001	**0.012**	**3.0**		

Bold indicates the average for all tests
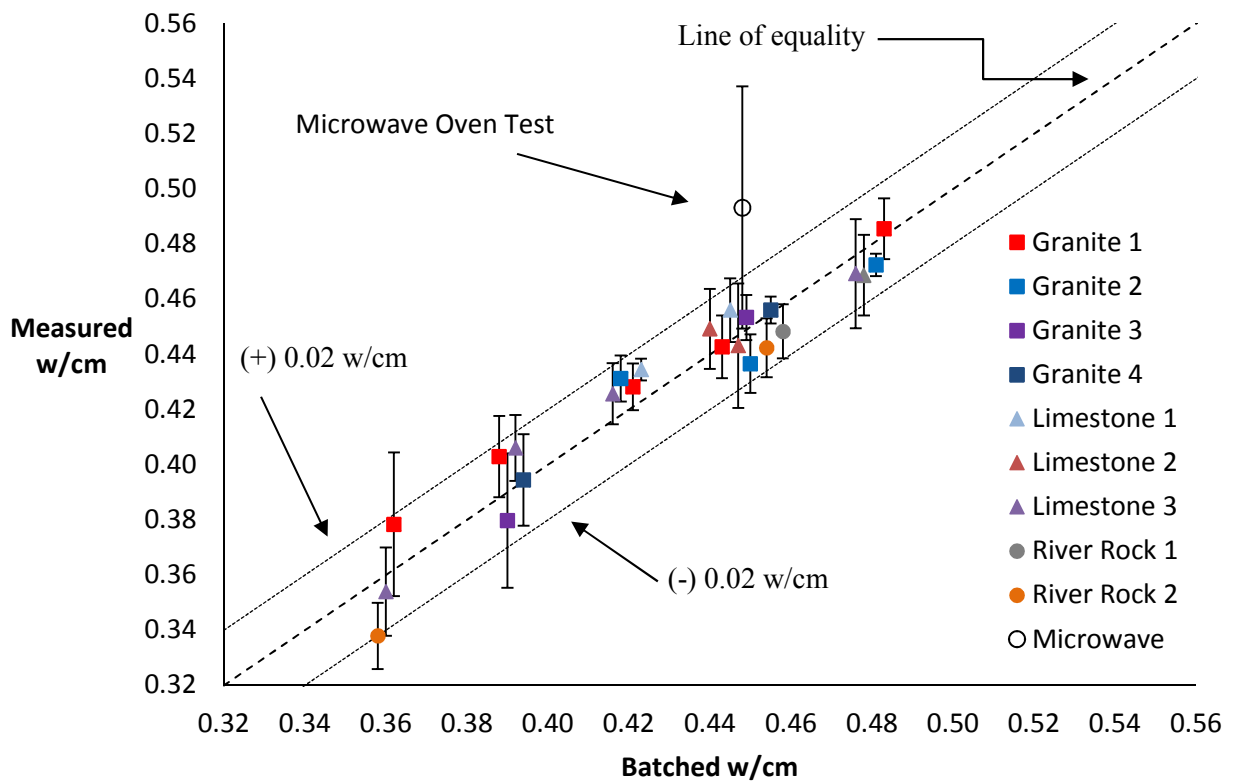
Figure 2-7. A comparison of the batched w/cm and measured w/cm for different mixtures. An average and one standard deviation are shown. The data at each tested w/cm have been staggered for easier viewing.

The average standard deviation for all measured w/cm for the 231 mixtures is 0.012 for w/cm between 0.36 and 0.48 for a variety of different materials. The average coefficient of variation (COV) for all the tests is 3.0%. This shows the test is precise. The results from Figure 2-6 show that the average results are within 0.01 from the batched w/cm and from table 2-7 the average difference between the batched and measured w/cm is 0.001. This shows that on average there is little difference between the batched and measured w/cm. The aggregate type and w/cm do not seem to influence the results for the materials and mixtures investigated. This is an improvement over the AASHTO T 318 test results as the difference in the measured and batched w/cm was 0.043, and the standard deviation was 0.044 w/cm with a COV of 8.9%. This variability is similar to the value reported by Hover, Bickley, and Hooton [14]. The standard deviation of the

27

introduced w/cm test is roughly three times smaller than the standard deviation of the microwave oven test.

2.4.1.2 Laboratory Results, Phoenix Furnace and Device Comparison

To evaluate the furnace, 133 mixtures were tested. Paste and concrete were evaluated, and the results can be seen in Table 2-8. The concrete mixtures used Limestone 3 and Natural Sand 1. Figure 2-8 shows the average and one standard deviation for each measured w/cm versus the batched w/cm. In this graph, all of the data is combined at each w/cm. A line of equality is included on the graph to show an exact match of the batched and the measured w/cm. The two lines on either side represent a +/- 0.02 w/cm. This shows a reasonable range for the w/cm variation.

Table 2-8. Summary of furnace results.

Tests	Batched w/cm	Average Measured w/cm	Difference Batched and Measured	Standard deviation	COV (%)	Coarse Aggregate Type	Fine Aggregate Type
16	0.30	0.31	-0.010	0.006	1.8	-	-
16	0.40	0.41	-0.010	0.004	0.9	-	-
11	0.44	0.45	-0.010	0.008	1.9	Limestone 3	Natural Sand 1
16	0.45	0.46	-0.010	0.007	1.5	-	-
10	0.45	0.44	0.010	0.013	2.8	Limestone 3	Natural Sand 1
8	0.48	0.47	0.010	0.008	1.6	Limestone 3	Natural Sand 1
12	0.50	0.51	-0.010	0.010	2.0	-	-
12	0.50	0.50	0.000	0.009	1.7	Limestone 3	Natural Sand 1
6	0.55	0.55	0.000	0.014	2.6	Limestone 3	Natural Sand 1
12	0.60	0.61	-0.010	0.009	1.5	-	-
14	0.60	0.60	0.000	0.012	2.0	Limestone 3	Natural Sand 1
			-0.004	**0.009**	**1.8**		

Bold indicates the average for all tests
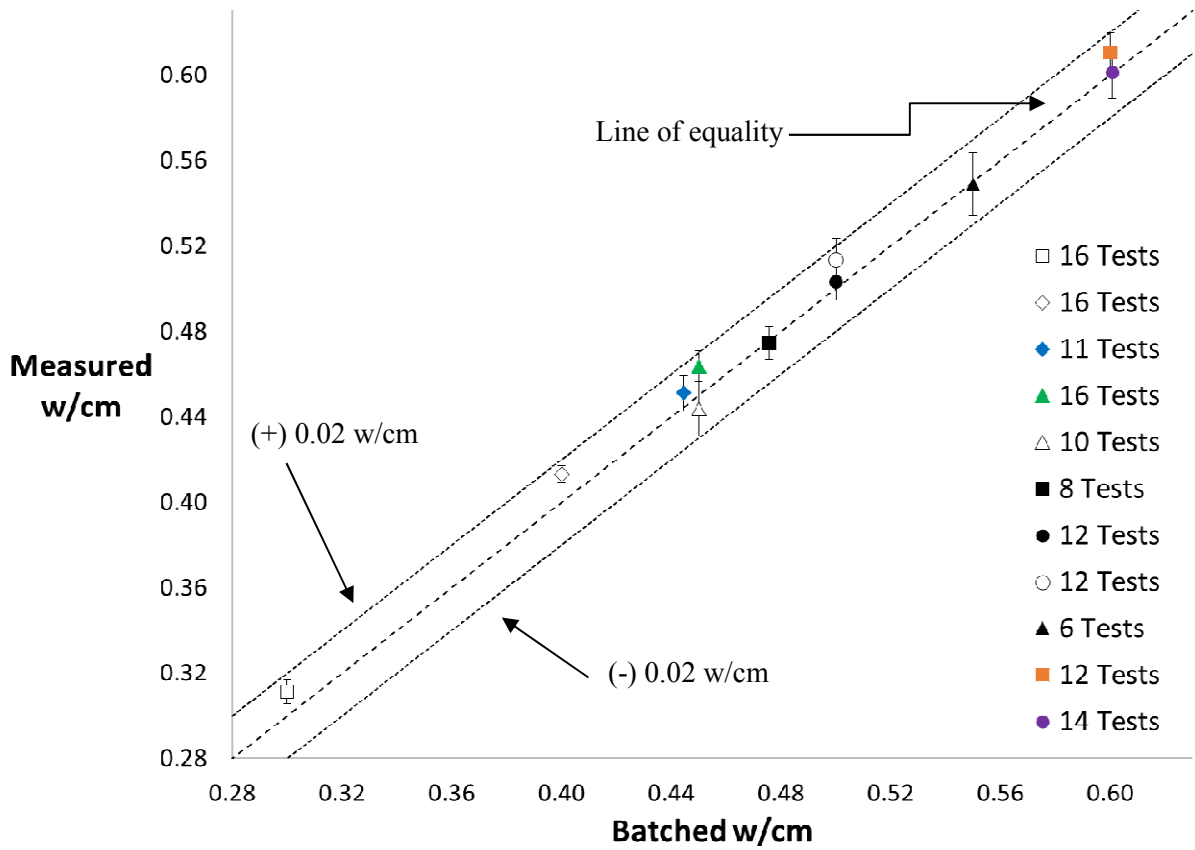
Figure 2-8. Furnace average and one standard deviation results.

For the furnace results, the average standard deviation for all measured w/cm is 0.009 for w/cm

between 0.30 and 0.60. The average coefficient of variation (COV) for all 133 tests is 1.8%. This

shows the test is precise and accurate, regardless of the test setup.

The combined results for both test setups can be seen in Figure 2-9. This figure shows that both

devices are precise, accurate, and can be utilized to achieve similar results. Both devices have an

average measured w/cm values within 0.01 of the batched w/cm. The COV of the furnace is 1.8%

compared with the dual heating elements with a COV of 3%. Table 2-9 shows the average results

for each test setup and also the average values for all the laboratory tests.
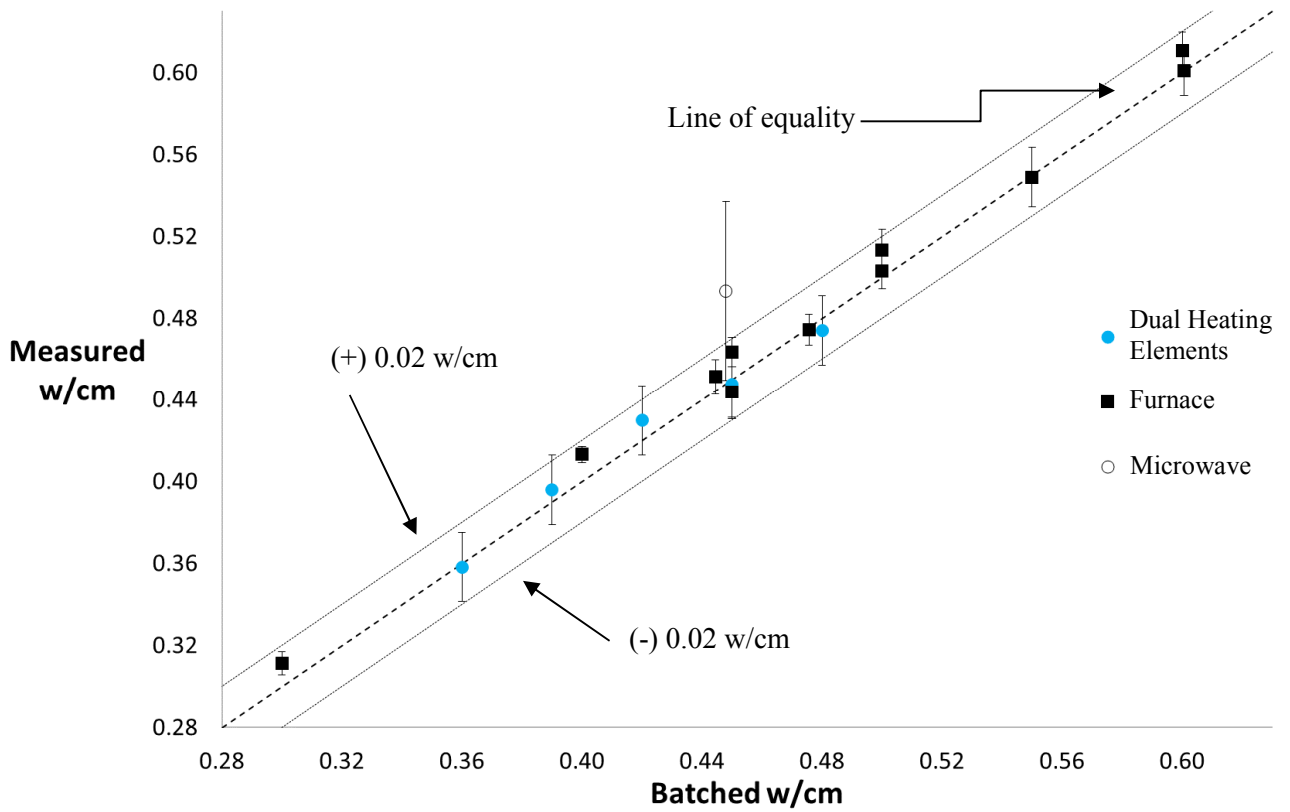
Figure 2-9 Combined average and one standard deviation results from each test setup.

Table 2-9 Average for all laboratory test results.

	Number of Tests	Average Difference Batched and Measured	Standard deviation	COV (%)	Time Required to complete test (min)
Dual Heating Elements	231	0.001	0.012	3.0	30
Furnace	133	-0.004	0.009	1.8	15
Microwave	10	-0.045	0.044	8.9	45

2.4.2 Field Results

Table 2-10 shows the results from 27 field concrete mixtures tested with the dual heating

elements. Figure 2-10 compares the batched and measured w/cm for the field tests graphically.

Table 2-10. Field testing summary.

Truck Number	Batched w/cm	Average Measured w/cm	Difference Batched and Measured	Standard deviation*	COV (%)*
Truck 1	0.42	0.43	-0.01	0.005	1.2
Truck 2	0.45	0.45	0.00	0.009	2.0
Truck 3	0.47	0.46	0.01	0.004	1.0
Truck 4	0.44	0.44	0.00	0.013	3.0
Truck 5	0.44	0.44	0.00	0.004	1.0
Truck 6	0.43	0.47	-0.04	0.002	0.5
Truck 7	0.42	0.42	0.00	0.003	0.8
Truck 8	0.42	0.42	0.00	0.007	1.7
Truck 9	0.43	0.44	-0.01	0.003	0.6
Truck 10	0.39	0.39	0.00	0.007	1.8
Truck 11	0.39	0.39	0.00	0.002	0.6
Truck 12	0.39	0.39	0.00	0.004	1.0
Truck 13	0.44	0.46	-0.02	0.002	0.5
Truck 14	0.44	0.46	-0.02	0.016	3.4
Truck 15	0.44	0.48	-0.04	0.006	1.2
Truck 16	0.43	0.43	0.00	0.006	1.3
Truck 17	0.42	0.43	-0.01	0.008	1.8
Truck 18	0.43	0.44	-0.01	0.007	1.6
Truck 19	0.36	0.38	-0.02	0.003	0.9
Truck 20	0.48	0.49	-0.01	0.005	1.0
Truck 21	0.48	0.44	0.04	0.002	0.4
Truck 22	0.37	0.38	-0.01	0.006	1.4
Truck 23	0.44	0.42	0.02	0.005	1.2
Truck 24	0.50	0.54	-0.04	0.001	0.2
Truck 25	0.49	0.46	0.03	0.003	0.7
Truck 26	0.42	0.42	0.00	0.001	0.3
Truck 27	0.43	0.45	-0.02	0.003	0.8
			0.00	**0.010**	**1.2**

Bold values indicate the average for all tests
*Two samples tested per truck
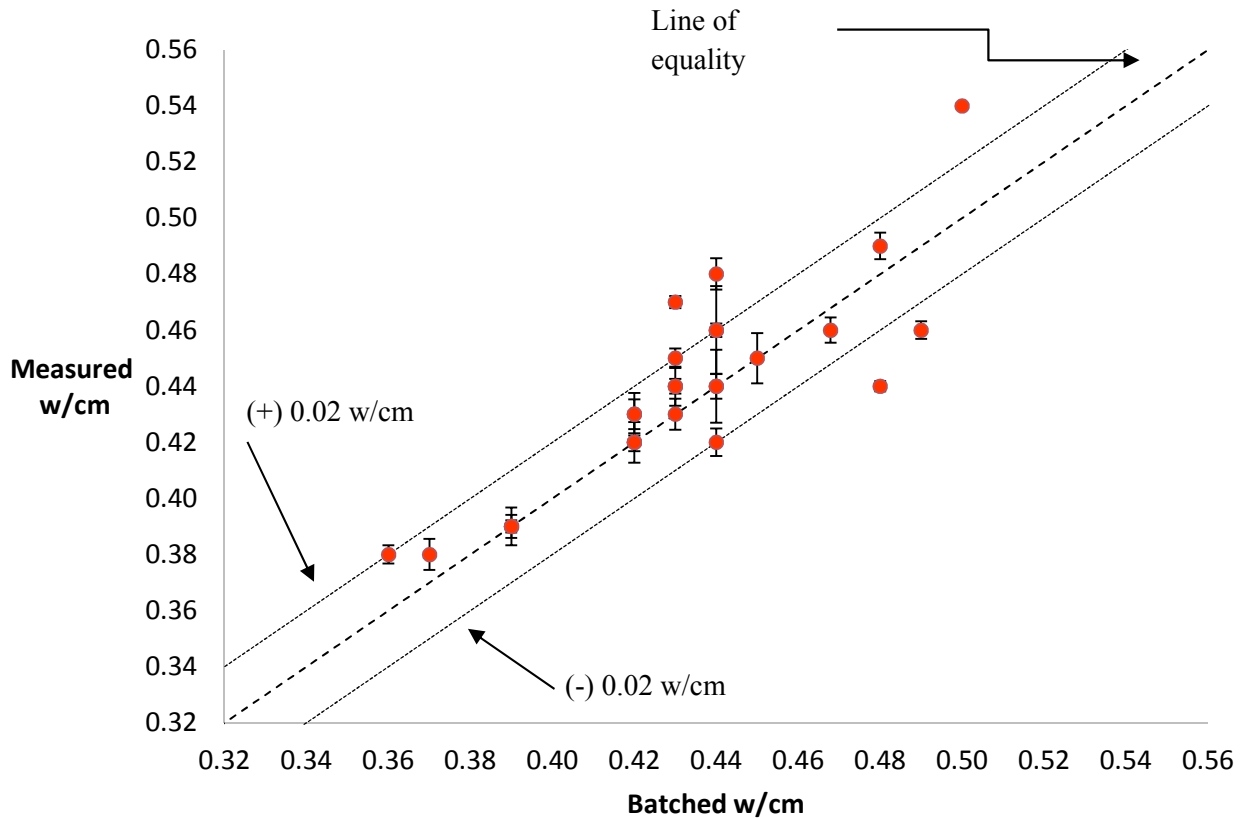
Figure 2-10. Field tests comparing the batched and measured w/cm. Two samples were tested and averaged per truck.

From Table 2-10 the average standard deviation was 0.010. This is very close to the 0.012 that was measured from the laboratory data. Also, the COV of the field data between the two measurements was 1.2%. This is lower than the 3.0% COV from the laboratory testing and shows that this test method can be used in the lab or the field. It should be noted that the standard deviation and COV for the field measurements were based on two tests per truck. While this is a low number of samples for each measurement, it was not possible to measure more with the time

and equipment available. Despite these reduced number of tests, the variance from both the lab and field are similar.

It was found that 15% of the field mixtures had a w/cm higher than 0.02 from batched w/cm. This was obtained from trucks at the batch plant and does not reflect the additional water that could be added before placement within the forms. Furthermore, these samples were not taken randomly. All concrete producers knew that the concrete was being sampled and this may have an impact on the quality of concrete that was provided for the testing. Despite these limitations, this test shows promise in being able to detect excess water in both laboratory and field concrete mixtures.

An example of the usefulness of the test can be shown by comparing two mixtures used for a bridge pier. The results from the testing and specifications are shown in

Table 2-11 [39]. Because there is no specified test method to measure w/cm of fresh concrete, the specification limits the maximum slump of the concrete to 18 cm because of concerns for excess water. Both trucks were rejected because the slump was above the specified value; however, the testing shows that the measured w/cm for Truck 7 was within the allowable limits of the specification. This shows that there are many variables that impact the slump of concrete beside the w/cm. This also shows the value in more directly measuring the desired property instead of relying on indirect measurement methods for specifications.

Table 2-11. Truck 6 and 7 field testing results.

Truck Number	Batched w/cm	Average Measured w/cm	Measured Slump (cm)	Air Content (%)	Specified w/cm	Maximum Slump (cm)	Specified Air Content (%)
Truck 6	0.43	0.47	23	4.7	0.25-0.44	18	6±1.5
Truck 7	0.42	0.42	20	8.1	0.25-0.44	18	6±1.5

Table 2-12. Field testing batch tickets.

Truck	Batch Size (m^3)	Cement (kg)	Fly Ash C (kg)	Fly Ash F (kg)	Slag (kg)	Coarse (kg)	Fine (kg)	Water (kg)
1	10.5	2533	628			7140	7203	159
2	10.5	2712				8500	6586	147
3	10	2549				8110	6232	143
4	10	2545				8410	5679	135
5	10	2545				8509	5652	133
6	10	2554				8428	5724	133
7	10	2549				8373	5697	129
8	10	2549				8373	5697	129
9	10	2533				8301	5670	130
10	10	2041	508			8518	6024	120
11	10	2057	508			8863	5996	120
12	10	2037	508			8718	5996	120
13	10	2538				8482	6015	134
14	10	2538				8455	567	133
15	10	2545				8410	5679	134
16	10	2545				8509	5652	131
17	10	2554				8428	5724	128
18	10	2549				8423	5729	131
19	6	1080		245	333	4844	3379	72
20	9	1585	404			7167	5788	114
21	8	2055				6350	4704	118
22	8	1436		336	445	6450	4504	99
23	7.5	1912				6046	4500	101
24	7	1894	315			2712	6436	133
25	6.25	1082	288			4736	4196	81
26	3	649	166			2295	1882	41
27	8	1091			1100	5371	5597	113

2.4.3 Practical Significance

The concrete industry does not have an established method to determine the w/cm of fresh

concrete. This work presents a test method that has improved on previous methods and the results

are accurate for a wide range of materials and mixtures. The inputs for the test can be easily

determined with basic mixture design information and the unit weight of the fresh concrete. The results in the lab and field show promise.

Each presented method shows an improvement in the time required to obtain an accurate test result compared to the microwave test, AASHTO T318. The dual heating elements device has a time requirement of 30 minutes and the furnace has a time requirement of 15 minutes compared with 45 minutes for the microwave test.

This test method can benefit owners, contractors, and producers. Owners are interested in obtaining a durable concrete and the w/cm is helpful for determining this. Contractors want consistent products for construction and producers need tools to help them with the quality control of their materials. Being able to verify the fresh concrete w/cm in a timely manner would be of significant benefit to the industry. Currently, concrete with a high w/cm would not be identified until compressive strength testing or some other hardened property such as surface resistivity [18] or rapid chloride permeability [40] testing is completed. Unfortunately, this would take days or weeks to complete the testing after the concrete has hardened. Since the suggested test method can identify concrete mixtures with excess water then this will allow better control of the durability, strength, and consistency of the concrete before the mixture is placed. This would allow the concrete to be adjusted to reach the desired properties before it has been placed. This would benefit the entire concrete industry and improve the service life of our concrete structures.

2.5 Conclusion

A test method is presented that measures the w/cm of the fresh concrete. Testing was performed for 364 laboratory mixtures and 27 field mixtures. The mixtures used 17 coarse aggregates and 6

fine aggregates with specific gravities between 2.42 and 2.85 and absorption between 0.20 and 4.69%. The method uses information about the mass of the ingredients, aggregate properties, and the unit weight of concrete. The following conclusions can be drawn:

- A volume > 1236 cm^3 was needed to precisely and accurately determine the density and water to cement ratio of fresh concrete. This is important because a minimum volume of material is needed in a testing protocol.

- The tested sample was simultaneously used to determine the density and water to cement ratio of fresh concrete. The accuracy of the water to cement ratio is highly dependent on the tested sample density.

- A maximum temperature of 815°C was used to accurately determine the water to cement ratio of fresh concrete. Temperatures that exceed this would evaporate more than water.

- The material was tested at a uniform thickness of 19 mm +/- 13 mm. This ensures a consistent testing time.

- By using heat from multiple faces and an insulated chamber the water content of the sample could be found within 15 min.

- For the laboratory mixtures with w/cm between 0.30 and 0.60, the average measured w/cm was within 0.01 from the batched w/cm and on average the difference was 0.001 for the dual heating elements and 0.004 for the furnace.

- For six mixtures with a batched 0.45 w/cm, the AASHTO T 318 microwave oven test was within 0.045 w/cm while the introduced test method was within 0.015 w/cm for the dual heating elements and 0.013 for the furnace.

- The average standard deviation and COV for the laboratory and field mixtures were comparable. The dual heating elements had a standard deviation of the water to cement ratio of 0.012 and COV of 3.0% and the furnace a standard deviation of 0.009 and COV of 1.8% for laboratory and field standard deviation of 0.010 and COV of 1.2%.

- The COV of the introduced w/cm for dual heating elements and furnace was approximately three and five times lower respectively than the AASHTO T-318 microwave oven test (3.0% and 1.8% compared to 8.9%). This is likely caused by the larger volume of sample investigated in both devices.

- For the field testing, 15% of the mixtures were found to have a 0.02 w/cm or higher than the batched w/cm.

This shows that this proposed test method could provide a useful tool to measure the w/cm of fresh concrete in about 30 minutes for the dual heating elements and in about 15 minutes for the furnace with a sample size that is not excessive but provides an accurate measurement. The test also has the potential to directly measure the amount of water within the concrete and not make an estimate of the value based on an indirect measurement from the slump test. The implementation of this test in the quality control of concrete has great potential to improve the quality and performance of concrete structures.

CHAPTER III

MEASURING THE CHANGE IN WATER TO CEMENT RATIO IN FRESH AND

HARDENED CONCRETE

3.1 Introduction

The water-to-cementitious ratio (w/cm) of concrete mixtures influences the strength, workability,

durability, serviceability, cracking, setting time, bleed rate, and even the color of the concrete [1-

9, 41, 42]. Modern specifications for structural concrete construction commonly require a specific

maximum w/cm limit or range for the w/cm at placement depending on the application [43].

While this w/cm is typically specified, it is difficult to ensure that the w/cm of the delivered

concrete is within the specified limit(s), because there are no established test methods to measure

this in the field. The goal of this paper is to compare how accurately and rapidly test methods can

determine a change in the w/cm of concrete. These findings can be used to establish a new

approach to concrete quality control testing.

Currently, the concrete batch ticket is the most common method to report the w/cm of a concrete

mixture. Unfortunately, the reported values on the batch ticket may not accurately represent the

quantity of water within the concrete. Previous field testing shows that 15% of mixtures have a

w/cm > 0.02 over the reported value on the batch ticket [19].

The water content in a concrete mixture can be variable because water is added at the job site, improper adjustment for the moisture within the aggregate, not accounting for the leftover washout water in a concrete truck, and not properly batching the water at the plant [44, 45]. It is common in the concrete industry to indirectly measure the impact of the water on the properties of the concrete. Some indirect methods that have been used to measure w/cm are slump [15], unit weight (UW) [16], compressive strength [17], resistivity [18], and petrography [46]. Unfortunately, these test measurements can be affected by variables that are not related to water. Some of these challenges and the reported coefficient of variation (COV) are summarized in Table 3-. The COV is a useful way to compare the expected variation of a test method. The COVs were either determined in this study or are from published literature. While understanding the variation of the test is important, it does not give insight into the accuracy of the test to determine the w/cm of the concrete mixtures. Determining the accuracy of some of these tests will be a focus of this work.

Table 3-1. Challenges with test methods to measure the w/cm.

Test	Challenges for w/cm estimate	COV(%)
Slump	Constant water content can produce a wide range of slump measurements [47]. Water added to mixtures may not increase slump [5, 11, 15].	13.4 [A]
UW	Water content is assumed based on the values in the mixture design. Differences in batch weights and air content change the volumetric relationship to estimate the water content [5, 11, 42].	3
Compressive strength	Use of three-point curve to estimate w/cm based on compressive strength. Requires a history of mixture data. Field cylinders are prone to inconsistencies in making, curing, and testing [5, 7, 11, 41, 42, 48].	3.2
Resistivity	The use of supplementary materials and admixtures introduces a wide variation in permeability at a constant w/cm [49]. Sample storage temperature and moisture are important [50].	7.0
Petrography	No standardized test methods to determine w/cm. Various methods are utilized that include absorption, scratching, polarized light, and optical fluorescence. Subjective results that occur weeks or months after placement [51, 52].	
Phoenix [B]	Requires equipment that is not standard, and a generator is needed for field use. Still under investigation for different materials [19, 53, 54].	1.8
Microwave [B]	The sample size is small causing a high variation of results [14].	8.9 [C]

[A] [55]

[B] Indicates a direct test method.

[C] [19, 53, 54]

Two tests use heat to directly measure the water in the fresh concrete. These tests are the microwave [13] and the Phoenix [19]. The Phoenix is a novel test method that can quickly and accurately determine the w/cm of fresh concrete to 0.02 w/cm in both the laboratory and field [19]. This test uses a dual heating device that provides 700 °C to quickly evaporate water from the sample. The sample volume reduces variability by using a 1648 cm^3 (4x8" cylinder) cylinder mold. The Phoenix uses the actual batched materials and volumetric relationship to determine the w/cm of the batched mixture. Additional testing results for the air volume can be added to increase the accuracy of the w/cm calculation. Two versions of the Phoenix are used in this study. A summary of the limitations of the microwave and the Phoenix is also included in Table 1. This work compares the Slump [15], Unit Weight (UW) [16], Compressive Strength [17], Surface Resistivity [18], and the Phoenix [19] to determine how accurately these tests can measure a change in the water content of the mixture. This is determined by preparing a concrete mixture with known water content and then measuring the changes in these results as known amounts of water are mixed into the concrete.

3.2 Experimental Methods

3.2.1 Materials & Mixture Design

A summary of the field mixtures investigated can be seen in Table 3-2**Error! Reference source not found.**. Multiple w/cms from 0.28 to 0.54 were investigated with the same coarse and fine aggregate sources. These concrete mixtures used a Type I-II Portland cement that met the requirements of ASTM C150 [32]. An ASTM C618 Class C fly ash was used with a 20% replacement by weight[56]. The coarse and fine aggregate tested met ASTM C33 specifications [33] and had a specific gravity of 2.78 and 2.61 respectively and both had an absorption of 0.6%. All of the mixtures used either a polycarboxylate superplasticizer meeting ASTM C1017 or a mid-range water reducer meeting ASTM C494 [57, 58]. None of the mixtures contained an air-

entraining admixture to help reduce the amount of variability in the results. Each mixture design

is commercially used at the ready-mix plant used for the testing.

Table 3-2. Field Mixtures at SSD before water additions

Truck	Cement Type I-II kg/m³	Fly Ash Class C kg/m³	Coarse Aggregate kg/m³	Fine Aggregate kg/m³	Water kg/m³	w/cm
1	335	83	1071	966	17	0.34
2	332	82	1096	897	15	0.31
3	362	83	1080	890	15	0.28
4	332	84	1070	877	20	0.39
5	332	84	1071	821	19	0.38
6	335	84	1067	832	18	0.35
7	265	67	867	672	16	0.41
8	427	0	1067	807	21	0.42

3.2.2 Batching & Sampling the Concrete

The concrete was batched in a dry batch plant and the resulting concrete met the standards of ASTM C94 [59].

Eight ready mix trucks were used. Each truck was checked for unwanted water left in the drum. This was done using a fifteen-foot telescoping pole with a camera and light attached. The video was streamed to a connected device beside the truck. The camera was inserted into the drum where concrete is typically discharged, and the pole was extended until it could see until the back of the drum.

After the truck was checked for excess water, the aggregates were tested for moisture content according to ASTM C566 [60]. The empty truck was then loaded according to ASTM C94 [23]. This plant would discharge one material at a time from hoppers with control gates into the truck. The drum of the truck would spin while each material was introduced. Once the truck was

batched, the truck drum was spun for 100 revolutions to mix the concrete. If water was added to the mixture after the initial mixing, then the truck was spun for 30 revolutions to mix the concrete.

3.2.3 Procedure for Retempering Trucks

For this testing, a mixture was batched with a w/cm of between 0.28 and 0.42 and then water was added to increase the w/cm by 0.04 several times. This addition of water is known as retempering and it is a common practice on job sites to adjust the workability. After the initial mixing samples were taken to measure the slump, unit weight, Phoenix, compressive strength, and surface resistivity. These same samples were taken after the trucks were retempered. Due to removing and testing concrete from the truck and then adding water to increase the w/cm, the volume of concrete had to be determined. Before water was added to a truck, the new volume was used to calculate the amount of water required to increase the w/cm by 0.04. The additional water then increased the remaining volume in the truck before concrete was removed for the next series of tests. This is shown visually in Figure 3-1, with the concrete volume in the truck represented by the Y-axis and the w/cm on the X-axis. The w/cm of the mixture was increased by adding water to the truck using a known mass of water in buckets. This process was repeated 3 to 4 times for each truck.
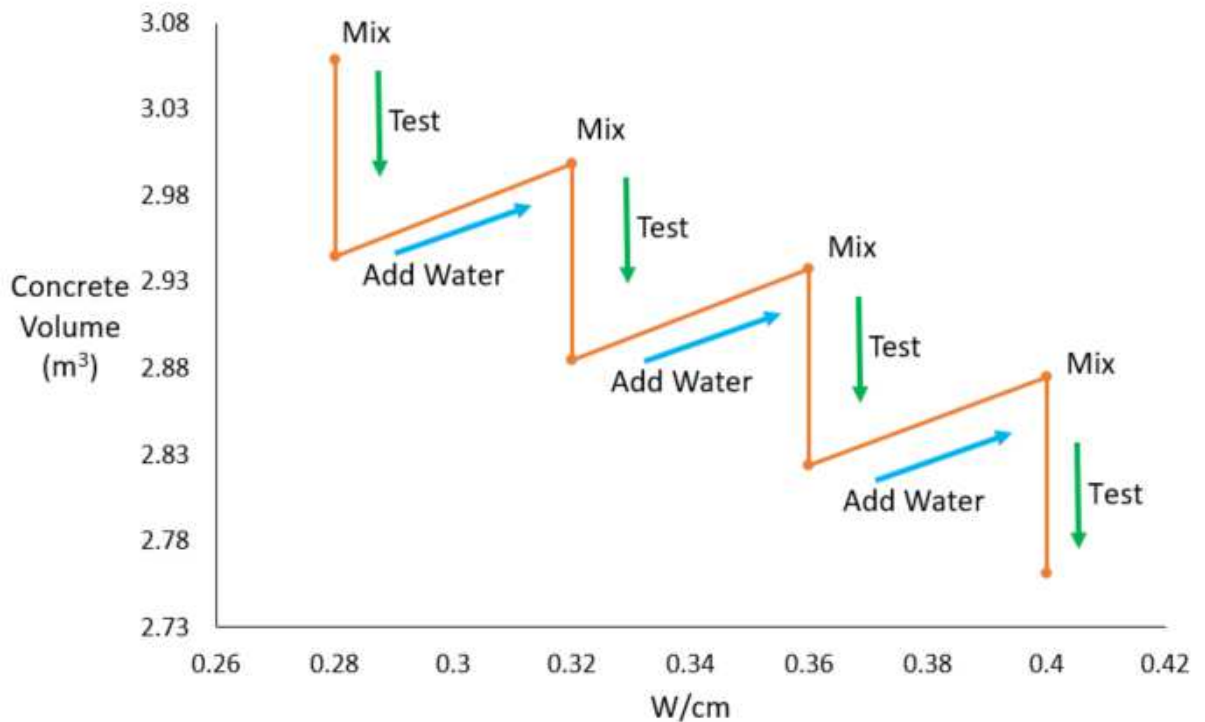
Figure 3-1. Concrete volume change in the truck after testing and adding water to increase the w/cm.

3.2.4 Sampling Concrete

The batched truck was then brought to the testing area. The testing area was located on the batch plant property directly across from the truck washout area. This eliminated a haul distance or timing issue of the tested material. The batch ticket was collected, all the batch weights and volume were recorded. The truck was spun for an additional 30 cycles and concrete was discharged into a wheelbarrow. Samples were taken according to ASTM C172 [37].

Prior to testing the concrete, a wheelbarrow was filled with 0.11 m^3 (4 cubic feet) of water and marked for reference. Each time concrete was sampled the wheelbarrow was filled to this mark. While this may not represent 0.11 m^3 of concrete because of differences in consolidation; it is a consistent method that was used to discharge approximately the same volume of concrete for each test.

3.2.5 Fresh and Hardened Property Testing

The sampled concrete was tested for Slump [15], Air Content [36], and Unit Weight [16]. Six specimens, consisting of 100 mm x 200 mm (4x8) cylinders were made for Surface Resistivity [16] and Compressive strength Strength Testing [15] at 7 and 28 days. In addition, two Phoenix tests [19] were also performed.

Two different Phoenix devices were used for the testing. Both devices were fundamentally the same but one of the devices had improvements in speed, reduced power, and safety. The results from both devices are compared.

3.2.6 Phoenix Procedure

The Pheonix test method consists of making and weighing a 4x8 cylinder of fresh concrete. A cylinder is used to ensure that a constant volume is tested each time. After emptying the concrete, the mass of the cylinder mold is measured to ensure the mold was properly emptied. The concrete is emptied into a pan with a uniform thickness of 19 mm +/- 13 mm. The pan is weighed before and after being heated to determine the water loss from the concrete. To determine when the sample is dry, the combined mass of the pan and concrete should be 2 grams or less of the previous measurement from at least two minutes of heat exposure. This represents a 0.05% change in the initial concrete mass. The final mass of the pan and concrete are recorded. This represents the total water evaporated, including the absorbed water in the aggregates.

To calculate the w/cm the mass of the materials batched, aggregate specific gravity, aggregate absorption, binder specific gravities, the air volume, and the total volume of the batch is needed. The air volume in the concrete should be obtained by either using ASTM C231 [36] or based on the theoretical density calculation according to ASTM C138 [16]. Detailed calculations and validation testing can be found in previous publications [19, 53, 54].

3.2.7 Phoenix Test Devices

Two different devices were used in this study. A summary of both methods is provided in Table 3-3. More information about the different methods is contained in Chapter 2. Since both methods are comparable their results are combined for comparison with the other test methods.

Table 3-3. Phoenix test device summary.

	Average Difference			Time
	Batched and Measured	Standard deviation	COV (%)	Required to complete test (min)
Dual Heating Elements	0.001	0.012	3.0	30
Furnace	-0.004	0.009	1.8	15

3.2.8 Statistical Significance of Field-Testing

Statistical significance was determined by comparing results from both a t-test and the overlap of the 95% confidence intervals. This was chosen because the t-test is used to determine if there is a significant difference between two means of data [61-64]. If the two data sets are different that would mean the increased w/cm is noticed by the test method. The two data sets would be assumed to be different and the t-test would determine if this is true or false. In addition, the 95% confidence intervals were calculated to show the difference between the means of the data sets. This creates an interval for each mean that will provide a direct comparison to evaluate if two intervals are different from each other [65-67]. By combining both the means and the interval of the data it provides a useful approach to determine the statistical significance of a test method to determine a change in the w/cm. This is discussed in more detail in several publications [61, 64, 68-72].

This work aims to determine if a test method can determine with statistical significance, changes in the w/cm by 0.04, 0.08, and 0.12. This is done by combining the results from the t-test and the

95% confidence interval. The analysis used the measured variation for the Phoenix, compressive strength, and surface resistivity from this work; however, to analyze the slump and UW published precision values are used. The standard deviation for Slump is 9mm and UW is 10.4 kg/m^3 [15, 16, 73].

3.3 Results and Discussion

3.3.1 Truck Testing Results from Retempering

To compare the impacts of retempering, Figure 3-2 shows the Phoenix results for 31 tests from eight trucks with sequential water additions. The measured w/cm is the average of two tests with one standard deviation shown using error bars. The measured w/cm is represented by the y-axis and the batched w/cm is represented by the x-axis. The dashed line on the graph is the line of equality that represents if the measured and batched w/cm match exactly. The two lines on either side represent a +/- 0.02 w/cm. Based on lab testing this 0.02 w/cm limit gives a good estimate of the accuracy of the test method [19, 53, 54].
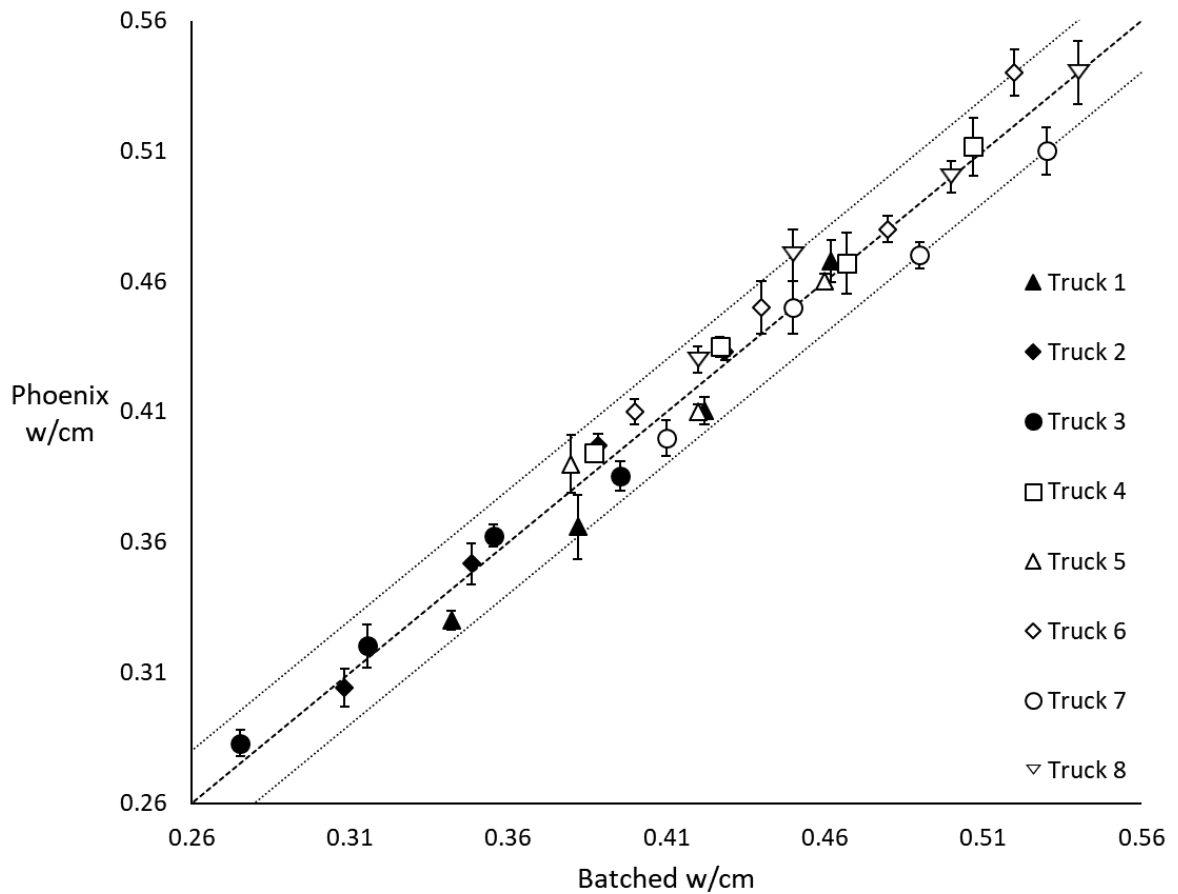
Figure 3-2. Truck summary of average measured w/cm with one standard deviation compared with batched w/cm with water additions.

The concrete mixtures had a w/cm ranging from 0.28 to 0.54 and all the measured w/cm in their mixtures were within +/- 0.02 w/cm of the batched values. It was found that 88% of the measurements are within 0.01 w/cm of the batched w/cm values. This shows that it is possible to very accurately batch a concrete mixture to a consistent w/cm and measure water additions in the field with the Phoenix.

3.3.2 Comparison of Field-Testing Results for Quality Control

Another important inquiry from this work is to determine if common quality control testing can be used as indirect tools to accurately measure when water was added to the concrete trucks.

Since the water was added in known 0.04 w/cm increases then the change in a measured property can be shown versus the known change in water content. Figure 3 and Figure 4 show the change in the test result for the w/cm increase.   These results are shown as box plots to help the reader better understand the distribution of the data and the amount of overlap between measurements. Ideally, there would be minimal overlap for the different water additions. Each data point is an average of multiple tests except for the slump and unit weight which is only one test. Two Phoenix tests, three compressive, and surface resistivity measurements are used.
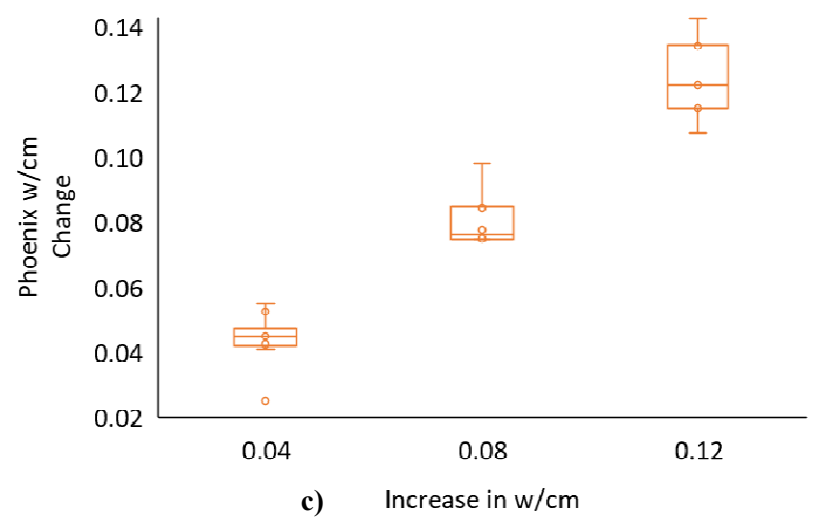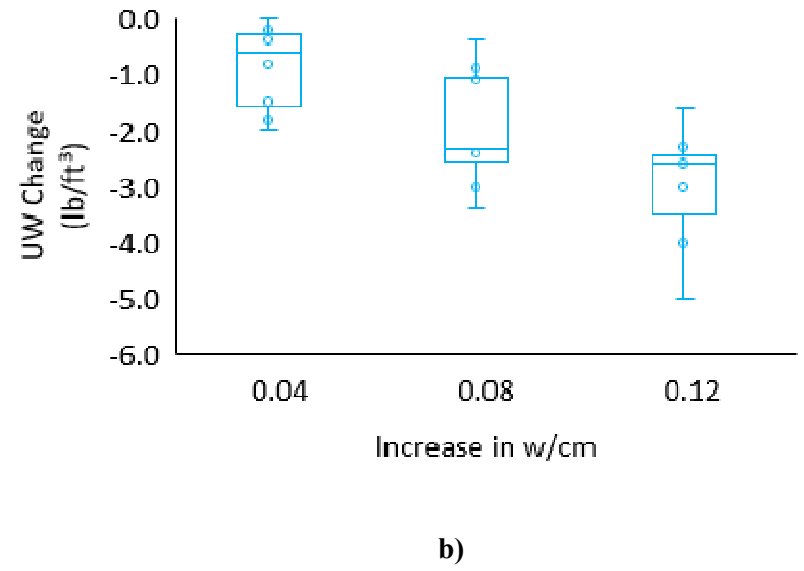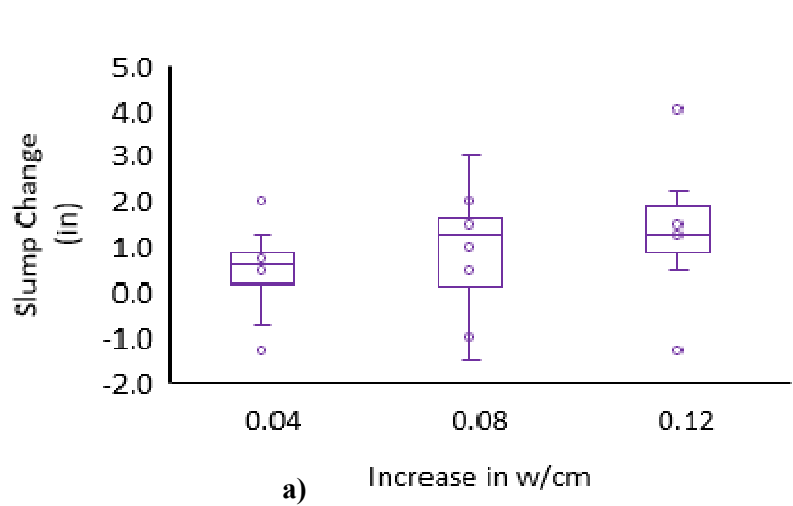
Figure 3-3. Average measured change from the initial test for each truck includes (a) slump change, (b) UW change, and (c) Phoenix w/cm change.

Figures 3-3a and 3-3b show that as water is added to the mixtures the means of the UW and

slump values change but the quartile lies overlap. This means there is not a significant change in

the measurements for the changes in the w/cm observed. However, the Phoenix measurements

showed distinct changes as water is added to the mixtures. None of the test results was more than

0.02 w/cm from the expected value as shown in Figure 3-2. The data for the Phoenix has a higher

separation and there is no overlap of the box pots as w/cm increased. The statistical significance

of these measurements will be discussed more in a later section but the lack of overlap of the box

plots shows that the variability of the test is small enough to make meaningful measurements.
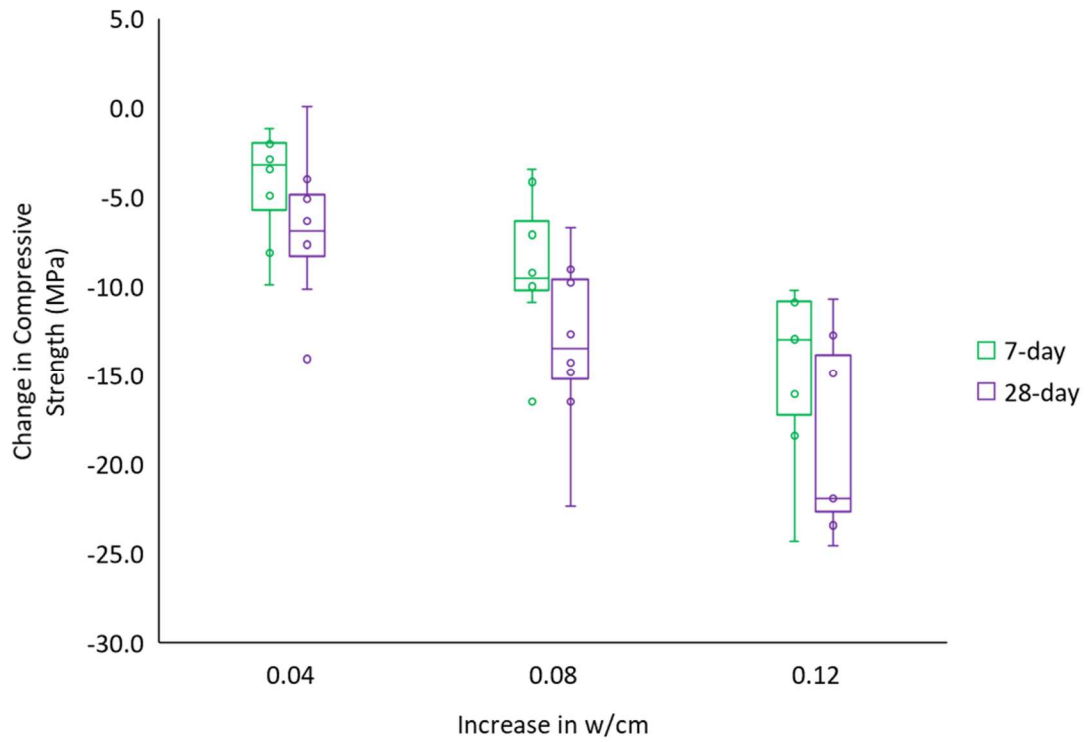
a)
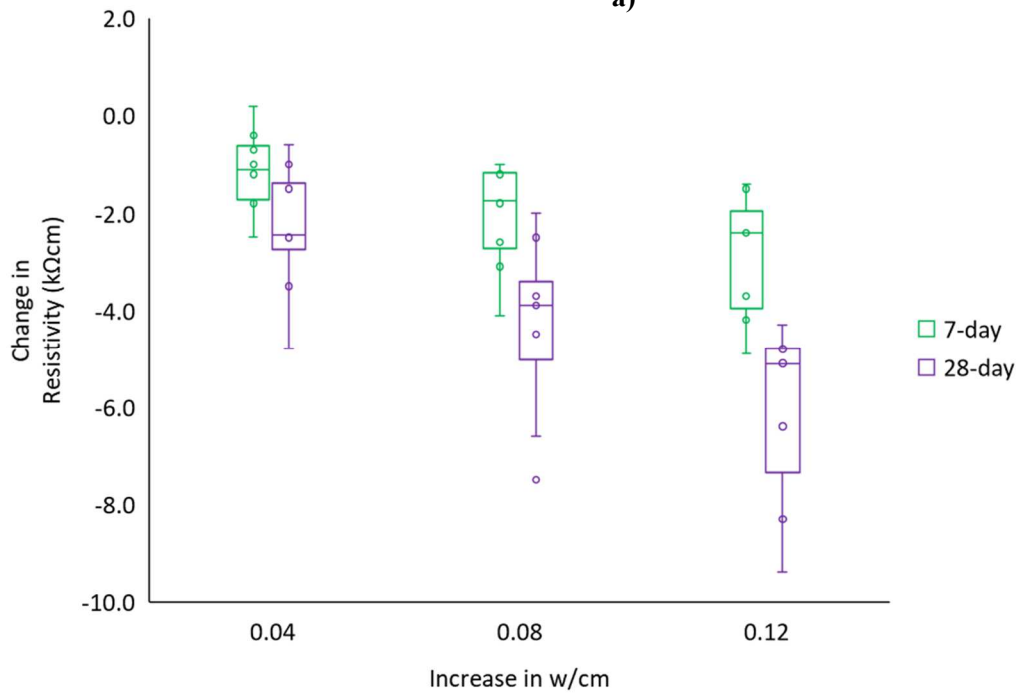
b)

Figure 3-4 shows that as the w/cm increased than both the 7 and 28-day surface resistivity and compressive strength decreased.

The compressive strength and surface resistivity plots also show a large overlap of the box plots at all increases of w/cm. This means that for some of the samples the changes being measured are within the expected variation of the test method. This will be discussed more in determining the statistical significance of the measurements.

3.3.3 Statistical Significance of Field-Testing Results

The t-test and 95% confidence interval results are provided in the Appendix. A summary table of the results is given in Table 3-4. Table 3-4 shows the percentage of statistically significant tests that passed both the t-test and 95% confidence interval.

Table 3-4. Phoenix, Compressive Strength, and Resistivity Test Performance (based on Percentage of tests statistically significant)

	Increase in w/cm			Average % of statistically significant tests
	0.04	0.08	0.12	
Slump	0%	0%	0%	0%
UW	0%	0%	0%	0%
Phoenix w/cm	63%	75%	50%	63%
7-day Compressive strength	0%	0%	0%	0%
7-day resistivity	63%	25%	25%	38%
28-day compressive strength	0%	0%	0%	0%
28-day resistivity	63%	38%	50%	50%

The means of the slump, UW tests, and compressive strength tests were not found to be different within statistical significance and so these tests are not reliable in determining changes of the w/cm for the materials and mixtures investigated. The Phoenix has the highest statistical significance and was able to show a statistically significant change for on average 63% of the tests investigated. The surface resistivity showed statistical significance for only 38% of the mixtures at 7-days and this increases to 50% of the tests after 28-days. This highlights how the surface resistivity test needs increasing curing time to accurately determine the changes in the w/cm of 0.04.

3.3.4 Practical Significance

This work examines the ability for fresh and hardened test methods to measure changes in w/cm of 0.04. A combination of the t-test and the 95% confidence interval shows that the slump, UW, and compressive strength are not able to determine a change in the w/cm of 0.04. This suggests that these test methods are not a reliable method to determine changes of the w/cm in fresh concrete.

Both the Phoenix and the surface resistivity test can determine if the w/cm increases by 0.04 for a concrete mixture. The Phoenix shows the highest number of statistically significant measurements of the tests investigated. The Phoenix has other advantages as it can measure the changes to the w/cm in fresh concrete in 15 min on a job site or at a batch plant. This could allow changes to be made to the concrete mixture to bring it within specification. This means the Phoenix is the most reliable test method investigated and has the potential to be used in the field to investigate concrete mixtures.

The surface resistivity was the only hardened test method that was able to determine statistically significant changes of the w/cm within 0.04. The number of statistically significant measurements increased with curing to 28 d. Unfortunately, after 28 d it would be too late for meaningful changes to be made to the hardened concrete or to change the construction practices. More work should be done at times between 7d and 28d to see how the surface resistivity test performs. However, these measurements are not likely to be as useful as the Phoenix as the test method can be completed in fresh concrete and it shows a greater number of statistically significant measurements than a 28-day measurement with the surface resistivity.

3.4 Conclusion

This study used the slump, unit weight, compressive strength, surface resistivity, and the Phoenix to measure the change in the w/cm of fresh concrete of 0.04 for 31 different field concrete mixtures with a w/cm from 0.28 to 0.54.

The following is concluded:

- Concrete batch plants and field water adjustments can be used to produce concrete mixtures with a w/cm of a range of +/- 0.02 w/cm of a target value.

- The slump, unit weight, and compressive strength at 7-day and 28-day did not provide a statistically significant measure of the change in the w/cm of the concrete mixture of 0.04.

- The Phoenix measurements are within +/- 0.01 w/cm of the target value for 88% of the measurements and 100% of the measurements are within +/- 0.02 w/cm of the target value.

- The Phoenix is able to observe a change in w/cm of 0.04 for 63% of the investigations.

- The 28-day surface resistivity test is statistically significant for 50% of the mixtures investigated and 7-day surface resistivity is statistically significant for 38% of the mixtures.

The results highlight that the slump, unit weight, and compressive strength are not able to reliably identify a 0.04 w/cm change in fresh concrete. The Phoenix however shows great promise to be a new method to help producers develop consistent concrete with reliable w/cm. While hardened properties are useful, they are not able to change construction practices because they cannot be used to adjust fresh concrete. This work highlights that many of our current test methods do not correctly identify critical changes to the w/cm of concrete mixtures. The development of new test methods could help benefit the consistency of the concrete industry and improve the service life and reliability of our in-place structures.

CHAPTER IV

DEVELOPMENT OF TIME & TEMPERATURE TESTING LIMITS FOR A FIELD WATER-

TO-CEMENT RATIO TEST

4.1 Introduction

Measuring w/cm is important in concrete because it influences the strength, workability,

durability, serviceability, cracking, setting, bleed rate, and even color of the concrete [1-6, 8, 9,

41, 42, 74]. Many attempts have been made to measure the w/cm in fresh concrete and have been

reported in previous literature [12, 13, 19, 25-31, 54]. One test that shows promise is the Phoenix

[19, 54]. The Phoenix aims to measure the water-to-cementitious ratio (w/cm) in fresh concrete

[19, 54]. Samples are placed into an 815°C furnace and water is evaporated from the sample. This

high heat removes all the water in as little as 15 min to obtain an average w/cm estimate within

+/- 0.02 for 364 laboratory mixtures [19, 53, 54]. Work in the field has shown the Phoenix

reliably measures w/cm within +/- 0.02 over 93% of the time for 58 mixtures [19, 53, 54, 75].

Two important questions are yet unanswered about the test method. The first is how long after

mixing can a sample be investigated in the test and still obtain an accurate answer. This is

important because water becomes bound and non-evaporable in hydration products unless

exposed to temperatures greater than those in the test method. Second, can the temperature in the

test cause further decomposition of the coarse or fine aggregates. This is important as this

decomposition would be measured as weight change and so the test would interpret this as changes in the w/cm. To investigate this, this paper uses a variety of tests on the raw materials, paste, and ultimately concrete.

4.1.1 Non-Evaporable Water in Concrete

When concrete is hydrating, some of the hydration products will contain water in the chemical bonds [5, 7, 41, 76, 77]. The water within these bonds is not easily removed and this is called non-evaporable water. While products are forming during hydration water exists in multiple states [7, 41, 77]. Previous studies have identified the amount of non-evaporable water in concrete based on w/cm [7, 41, 48, 78, 79]. Thermogravimetric analysis (TGA) and quasi-elastic neutron scattering have been used to quantify non-evaporable water in cement pastes [7, 41, 76]. As the non-evaporable water increases over time, the Phoenix may not be able to remove this water and so it can not accurately determine the w/cm. Samples with known w/cm will be produced and TGA and the Phoenix results will be used to investigate the change in the amount of non-evaporable water at different amounts of hydration. The goal of the work will be able to establish the maximum amount of time between when a sample is mixed and when it is tested and still achieve accurate results.

4.1.2 High-Temperature Decomposition of Hydration Products and Aggregates

When concrete reaches an internal temperature of 120°C, dehydration of hydration products occurs until complete melting into a liquid at 1300°C [7, 41, 80-83]. Two distinct phase changes occur in concrete and paste as temperatures increase. At 135°C, the dehydration of ettringite and CSH occur [7, 41, 80, 81]. At 750°C $CaCO_3$ and CO_2, dehydrate [7, 41, 80, 81]. More detailed information on other phase changes is given in the methods. TGA and X-ray Diffraction (XRD) have been used to identify phase changes and components in cement paste at temperatures up to 1100°C [7, 41, 82, 84]. Concrete aggregates can also decompose at higher temperatures. Calcium carbonate and siliceous aggregates experience phase changes above 200°C [85, 86]. Carbonate

aggregates including limestones have a mass loss from CO2 at 700°C, some dolomitic limestones can lose as much as 50% of the original mass of the material after 900oC [85, 86]. Siliceous aggregates including granite could have multiple mass losses from the phase changes of the quartz contained in the material [85, 86].

The Phoenix removes the total water of the mixture as short as 15 min [19, 53, 54]. The test uses a specially designed furnace set to 815°C and the samples remain within the furnace until the water is evaporated. After the water is evaporated the sample is weighed. If the sample remained in the furnace after the water evaporated, decomposition could start as the temperatures increase. If the decomposition is large enough, the Phoenix w/cm calculation would be affected.

The TGA of raw materials and paste samples are tested to determine at the temperature and the magnitude of the mass change occurs beyond 200°C. The performance in the Phoenix will also be investigated to determine by leaving samples in the furnace for extended periods. A comparison will be made between the TGA and Phoenix for samples tested at similar temperatures. A time limit will be established to minimize the amount decomposition in a sample that is tested with the Phoenix. This will allow samples to be tested so the accuracy of the Phoenix is maintained.

4.1.3 Research statement

This work aims to establish two important times within the Phoenix test method. This work will investigate how allowing extended periods before testing concrete will affect the w/cm calculation of the Phoenix. The work also aims to investigate the decomposition of the mixture when samples are kept in the furnace for long periods. Both limits will serve as important measures for the measurement of w/cm by evaporation.

4.2 Experimental Methods

4.2.1 Materials & Mixture Design

The ten concrete mixtures and one paste used for the testing are outlined in Table 4-. All of these mixtures were designed with a 0.45 w/cm. The paste mixture was used for isothermal calorimetry

and TGA testing. The concrete mixtures were tested by the Phoenix. The laboratory mixtures used multiple coarse aggregates and one natural sand. A summary of the aggregate type, specific gravity, and absorption can be seen in Table 4-2. All aggregates met ASTM C33 [33] specification and are used in commercial concrete mixtures. These mixtures use a type I cement that met the requirements of ASTM C150 [17]. The oxide and Bogue analysis for this cement can be seen in Table 4-3. This cement was also tested by TGA.

Table 4-1. Mixture Design at SSD

Coarse Aggregate Type	Cement kg/m^3	Coarse kg/m^3	Fine kg/m^3	Water kg/m^3
none*	362	-	-	163
Dolomite	362	1083	790	163
Dolomitic Limestone 1	362	1068	788	163
Dolomitic Limestone 2	362	1080	788	163
Gabbro	362	1121	791	163
Granite 1	362	1035	789	163
Granite 2	362	1062	790	163
Granite 3	362	1080	788	163
River Rock 1	362	1068	788	163
River Rock 2	362	1074	786	163
Sandstone	362	1017	791	163

Note: *indicates a paste mixture.

Table 4-2. Aggregate Type and Properties

Type	SG	Abs %
Dolomite	2.71	0.7
Dolomitic Limestone 1	2.67	0.6
Dolomitic Limestone 2	2.70	0.6
Gabbro	2.81	0.2
Granite 1	2.59	1.1
Granite 2	2.66	0.7
Granite 3	2.70	0.4
River Rock 1	2.67	1.5
River Rock 2	2.68	0.8
Sandstone	2.55	1.2
Natural Sand	2.62	0.6

Table 4-3. Type I cement oxide analysis

Oxide	SiO_2	Al_2O_3	Fe_2O_3	CaO	MgO	SO_3	Na_2O	K_2O	C_3S	C_2S	C_3A	C_4AF
Cement (%)	21.1	4.7	2.6	62.1	2.4	3.2	0.2	0.3	56.7	17.8	8.2	7.8

4.2.2 Mixture Procedure and Testing

All mixtures were hand mixed in small batches below 0.1 cubic feet. This method was described previously but is repeated here for the convenience of the reader [19]. The aggregate used was moisture corrected according to ASTM C566 [60]. To achieve accurate batch water, water was added to a dry bowl and weighed. All the materials were then added to the bowl with water and each mixed until thoroughly blended in the following order, cement, fine aggregate (if used), and coarse aggregate (if used). This material was then sampled for the testing.

4.2.3 Isothermal Calorimetry Testing

Isothermal calorimetry was utilized on cement paste to determine the heat given off during hydration. Isothermal calorimetry testing was performed according to ASTM 1702 [87]. Three paste mixtures were tested with an 8-channel standard volume calorimeter with TAM Air from TA instruments. Comparison samples use a volume of water with a matching specific heat to the sample. To determine the appropriate mass of water, the sum of the product of the mass of each material by the individual specific heat is divide by the specific heat of water.

To prepare the calorimeter, the comparison sample of water is placed into the reference chamber at least 30 min before mixing. Samples of 2.9 grams of fresh paste were placed into 20 mL glass ampoules. The ampoules were placed into the calorimeter sample chamber and monitored for 24 h. The rate of heat evolution was measured and a typical plot of the results can be seen in Figure 4-1.
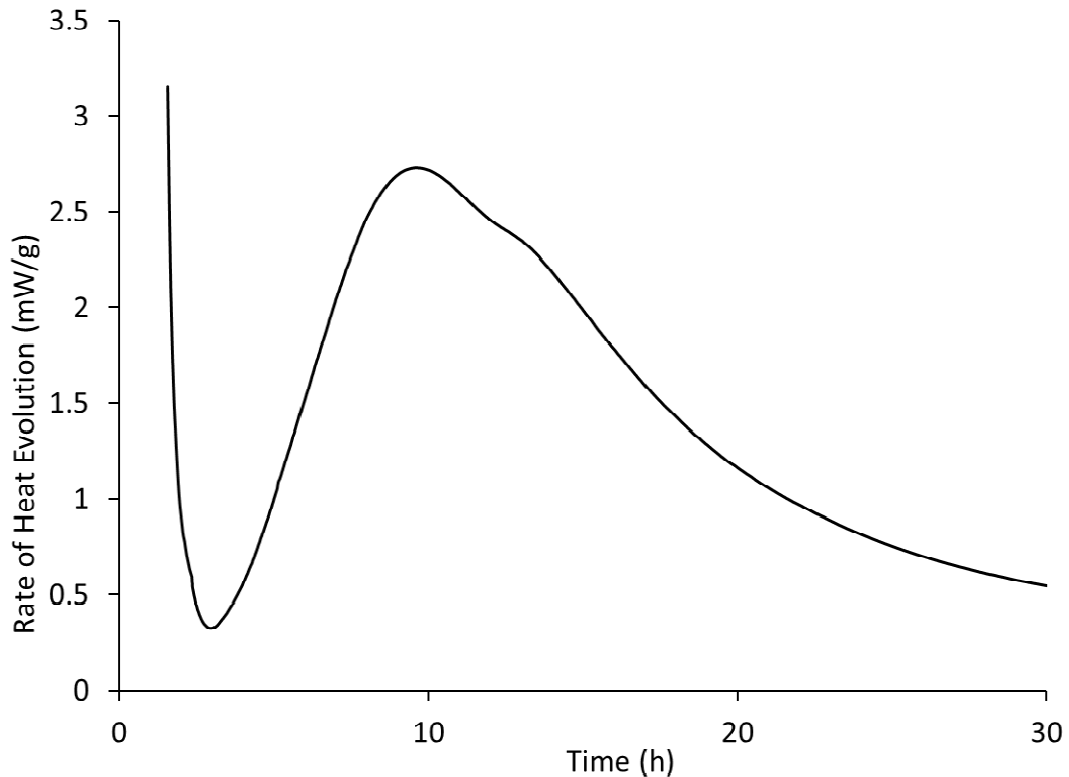
Figure 4-1. Example of the rate of heat evolution in OPC through the first 30 h.

4.2.4 Phoenix Testing

The Phoenix test method has been described in Chapter 2, but the method is repeated here for the convenience of the reader [19, 54]. A 100 mm diameter by 200 mm tall (4x8 inch) cylinder mold is filled, finished, and weighed with fresh concrete. Using a spatula, the sample is then emptied into a pan of 17.8 cm wide by 22.9 cm long with a depth of 4.4 cm. The material is placed in the pan so that it has a uniform thickness of 19 mm +/- 13 mm. The mass of the pan full of fresh concrete is recorded and placed into the test device. A scale with 0.1 gram accuracy and 21 kg capacity was used. The mass of the empty mold is compared to the mass before starting the test and mass should be within 10 g of the empty mold.

The furnace is 3600 Watt and can be seen in Figure 4-2. The furnace used heating elements that surround the chamber. Once the furnace is preheated to 815°C, the pan is placed in the furnace. The sample can be kept in the furnace unattended and weighed at 15 min. To determine when the

sample is dry, the combined mass of the pan and concrete should be 2 grams or less of the previous measurement from at least 2 min of heat exposure. This represents a 0.05% change in the initial concrete mass. The final mass of the pan and concrete are recorded. This represents the total water evaporated, including the absorbed water in the aggregates. The concrete can then be removed, and the pan can be cleaned.

Figure 4-2. Phoenix furnace testing device.

4.2.4.1 Determining the Impact of Non-evaporable Water Content

Sixteen concrete mixtures were tested with the Phoenix furnace to evaluate when non-evaporable water would influence the measurement of the w/cm. These mixtures used the dolomitic limestone 1 mixture seen in Table 4-1. The first two mixtures were tested in the Phoenix, at 15 min after mixing. For the remaining tests, the initial mass was measured after mixing to ensure

no water was lost to evaporation then the sample was added to the furnace at either 2, 3, 5, 6, 7, 8, or 9 h after mixing. These times were chosen so that they would be heated in the furnace at different points of the hydration. This will show at which point the non-evaporable water influences the w/cm measurement of the Phoenix.

4.2.4.2 Determining the Impact of Decomposition of Hydration Products and Aggregates

Each of the 10 coarse aggregate mixtures was repeated twice and dolomitic limestone 1 was repeated an additional two tests, a total of 22 mixtures. The dolomitic limestone 1 concrete mixture was tested in the furnace for 180 min to establish when aggregate decomposition occurs. Once determining a test length of 1 h was enough to observe aggregate decomposition, the remaining Phoenix tests were left in the furnace for up to 1 h. Each remaining coarse aggregate was tested with two repeated mixtures and was checked by weighing the sample multiple times to allow multiple periods to be investigated. These tests will show how much the decomposition of the mixture will affect the w/cm calculation for the Phoenix.

4.2.5 Thermogravimetric Analysis (TGA) Testing

For TGA testing, raw materials and cement paste were analyzed. Three samples were tested as raw materials including dolomitic limestone 1, natural sand, and Type I cement. Three tests were also done on cement paste samples that were tested at the following ages from mixing, 15 min, 3 h, and 9 h.

The TGA monitors the mass loss of material while increasing temperature [41, 88-91]. A differential scanning calorimeter (DSC) analysis was also used to measure the heat flow into the sample to interpret the heat energy consumed [88-92]. DSC measures how much energy a sample absorbs or releases during heating or cooling. Simultaneous TGA-DSC measures both heat flow and weight changes as a function of temperature or time in a controlled atmosphere [88-92]. The information obtained allows differentiation between endothermic and exothermic events which

have no associated weight loss [88-92]. A comparison will be made with TGA and Phoenix

results for samples tested at the same ages.

Concrete also has distinct phase changes and in turn expected mass loss while tested with TGA

[41, 80-83]. A list of changes in concrete during heating can be seen in Table 4-4.

Table 4-4. Changes in Concrete during Heating [41, 80-83].

Temperature Range	Description of Heat Changes in Fresh Concrete
20-200°C	Capillary water loss and reduction in cohesive forces as water expands
	Ettringite dehydration (80-150°C)
	C-S-H dehydration (135-150°C)
	Gypsum decomposition (150-170°C)
	AFm dehydration (185-200°C)
300-400°C	Decomposition of some siliceous aggregates (350°C)
400-500°C	Portlandite decomposition (460-540°C)
	$Ca(OH)_2 \rightarrow CaO + H_2O$
600-800°C	Further C-S-H dehydration due to phase change (600-750°C)
800-1000°C	Dolomite decomposition (840°C)
	Calcite decomposition (930-960°C)
	$CaCO_3 \rightarrow CaO + CO_2$, carbon dioxide release
1200-1300°C	Concrete components begin melting
1300-1400°C	Remaining cement-based composite exists only in a liquid state

A Mettler Toledo TGA/DSC 3+ was utilized to determine the temperature and percentage of

mass loss for the concrete raw materials and paste mixtures. All of the samples were heated under

a nitrogen atmosphere from 25°C to 1000°C at a constant rate of 10°C per min.

The TGA can only analyze one sample at a time and replicate samples were desired for

comparison. To avoid inconsistencies from multiple paste mixtures, samples were taken in

batches from a single mixture and aged. Once the target age was reached, the samples were flash-

frozen with liquid nitrogen. The samples were placed into a freezer at -18°C until they could be

tested in the instrument. Once removed from the freezer, samples were prepped in a nitrogen

environment and placed into a 70 µL pan. An isothermal hold at 23ºC in the furnace was

performed for 10 min before the TGA test began. This eliminates each sample starting the test at random temperatures after leaving the freezer.

4.3 Results and Discussion

4.3.1 Change in Non-Evaporable Water During Hydration

4.3.1.1 Isothermal Calorimetry and Phoenix Results

Results from the isothermal calorimeter and the percentage of water and w/cm as tested with the Phoenix are shown in Figure 4-3. The change in the amount of water and w/cm is shown in the left y-axis and the heat release is shown on the right y-axis. The x-axis represents the amount of time in hours from when mixing began. The black line represents the rate of heat release for a 0.45 w/cm paste. Each Phoenix measurement shows the percentage of water evaporated as well as an estimate for the w/cm at different periods. The tests at 15 min, 3 h, and 9 h are measured at the same time in both test methods. These are emphasized in the figure as they represent a tie between the two types of testing and they will be discussed in more detail later in the paper.
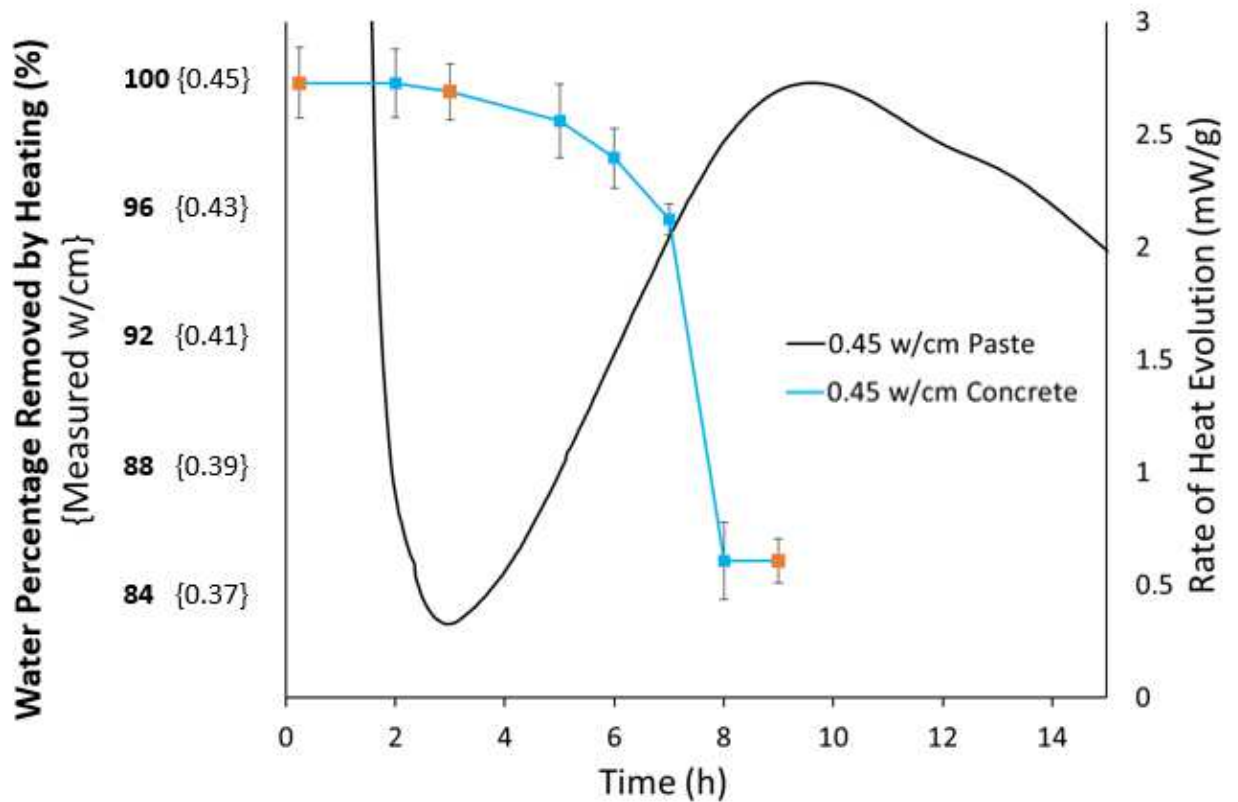
Figure 4-3. Isothermal calorimetry and Phoenix results versus time since mixing began. For samples delayed 15 min, 2 h, and 3 h, the measured w/cm is equal to the expected w/cm at 0.45. After 5 h, the accuracy of the Phoenix is reduced by 2% and this is the longest recommended time to determine the w/cm accurately. The samples delayed for 7 h show a decrease in the measured w/cm to 0.43. Samples delayed 8 and 9 h, decreased the water percentage by 15% and the measured w/cm to 0.38.

The isothermal calorimetry results show an increase in the rate of heat change between 2 and 4 h. This increase is known as the acceleration period. This occurs when the cement starts to rapidly dissolve and when hydration products start forming [11, 41, 42, 77]. As the acceleration period shows an increase in heat, an inverse relationship of decreasing w/cm is shown to occur at the same time. This shows the change in the non-evaporable water content of the materials over time.

It should be noted that the start and length of the acceleration period for a concrete mixture can change because of cement type, cement fineness, mixture proportions, temperature, SCMs, and admixtures [42]. This means that the length of time allowed before starting a test should be limited to the increase in the rate of heat evolution or the beginning of the hardening of the mixture. This data shows that a good estimate for most mixtures is close to 5h but a conservative estimate is 3h.

4.3.1.2 Thermogravimetric Analysis Results

The results for the TGA of the cement paste tests are shown in Figure 4-4. These times were chosen to match the Phoenix tests of the same age. The figure shows the mass loss percentage versus the temperature. The estimated w/cm is also included on the y-axis. The solid lines represent the average and the dashed lines represent the upper and lower standard deviation for the measurements. The vertical lines represent temperatures when phases are expected to dehydrate as outlined in **Table 4**.
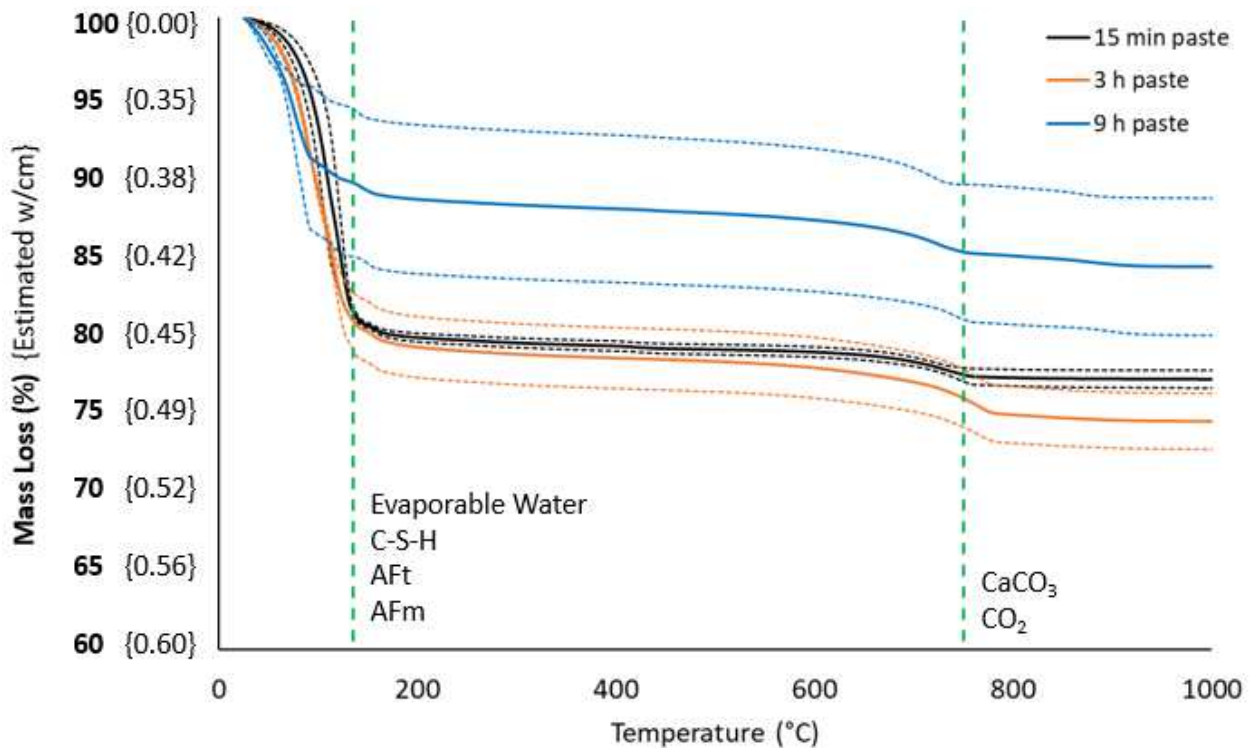
Figure 4-4. TGA results for cement pastes tested at different times after mixing.

At 135°C, the 15 min and 3 h paste have a similar mass loss at 20% or an estimated w/cm of 0.45. This is expected as the change in the mass loss is similar and is largely due to the loss of the evaporable water and decomposition of the early hydration products. This matches the findings from the Phoenix testing shown in Figure 4-3 where the 15 min and 3 h samples measured the same w/cm at 0.45.

However, the 9 h paste shows a mass loss of only 10%. This would estimate a w/cm of 0.38. The difference in performance between the 9 h paste and the 3 h and 15 min shows that at 9 h of hydration the amount of non-evaporable water increases. This matches the findings from the Phoenix. This likely occurs because with additional reaction will form more hydration products that will contain chemically bound water and water found in interlay CSH pores that are < 10 nm [41]. This water is likely related to the CSH and AFm constituents and is non-evaporable until these materials start to melt at 1200°C [41, 76, 82, 84]. Since these tests were limited to 1000°C these mass changes were not observed.

There is minimal change in any of the paste samples at 750°C. This shows that either the remaining constituents are present in small volumes or that they easily dehydrate at early ages. Regardless of the reason, these changes do not significantly impact the mass loss of the sample. The tests at 15 min, 3 h, and 9 h were completed in both the Phoenix and TGA. This shows that there is minimal change in the non-evaporable water from 15 min to 3 h, but there is a significant difference after 9 h of hydration. This confirms with two different techniques, two different sample sizes, and with both paste and concrete that the same behavior is occurring.

4.3.2 Decomposition of Aggregates

4.3.2.1 Thermogravimetric Analysis (TGA) Results

The TGA results for the raw materials and paste samples are shown in Figure 4-5. The figure shows the mass loss percentage versus the temperature. The solid lines represent the average of

all the samples tested for each material and the dashed lines represent the upper and lower

standard deviation.
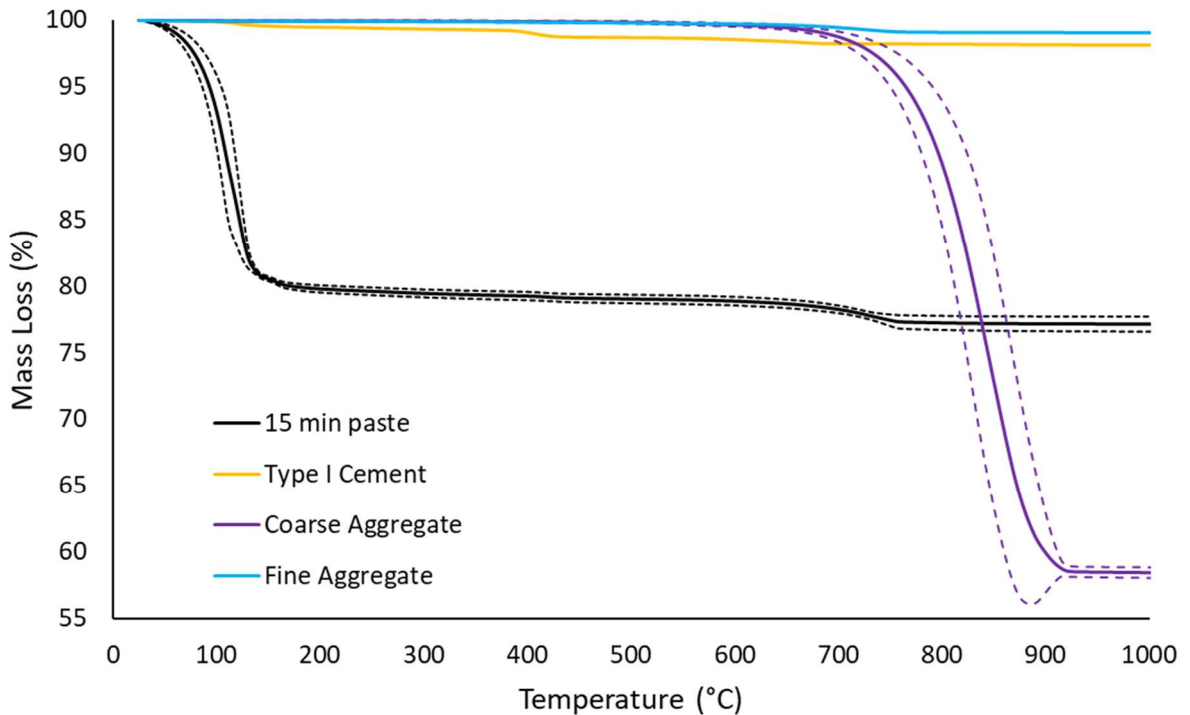
Figure 4-5. TGA results for raw materials and paste. Solid lines represent the average of the

specific pastes tested with the dashed lines representing the upper and lower standard deviation

from the average.

The anhydrous Portland cement and fine aggregate show less than 2% mass loss up to 700°C.

The fresh paste loses 20% of the mass at 135°C and then another 4% at 700°C.   For temperatures

> 700°C, the mass loss for the paste is < 2%. However, from 600°C to 900°C, the coarse

aggregate has a mass loss of 40% from thermal decomposition. This is likely from CO_2 leaving

the dolomitic limestone [85, 86].

Due to roughly 40% of a concrete mixture volume being made of coarse aggregate, the amount of

mass loss is significant enough to impact the results from the w/cm calculation in the Phoenix.

This shows that there is a time limit that the sample could stay in the Phoenix furnace and still be

an accurate method to determine w/cm.

4.3.2.2 Phoenix Results

The dolomitic limestone 1 concrete mixture was tested with the Phoenix using the furnace for up to 180 min. The mass loss and reported w/cm is given in Figure 4-6. The measurements between 15 min and 40 min give results within +/- 0.01 w/cm from the expected value. The last measurement before the rapid loss of mass at 40 minutes is marked on the graph as a blue dot. After 40 min, the mass loss increases rapidly and causes errors in the calculated w/cm. Based on the TGA data, once the internal temperature of the concrete reaches 600°C, the coarse aggregate would begin to decompose [85, 86]. The TGA data in Figure 4-5, shows that there would be a 2.5% loss in the mass of the paste from 200ºC to 800ºC. Since the paste is 28% of the mass of the concrete then this would be a total change of the concrete weight of 0.7%, which is negligible. This shows that the mass change at these higher temperatures appears to be from the decomposition of the coarse aggregates.

The results from the Phoenix tests with different coarse aggregate are summarized in Table 4-5. The lowest time in Table 4-5 is 40 min and so this is the suggested maximum amount of time that a sample can be left in the furnace and still achieve an accurate result from the test.
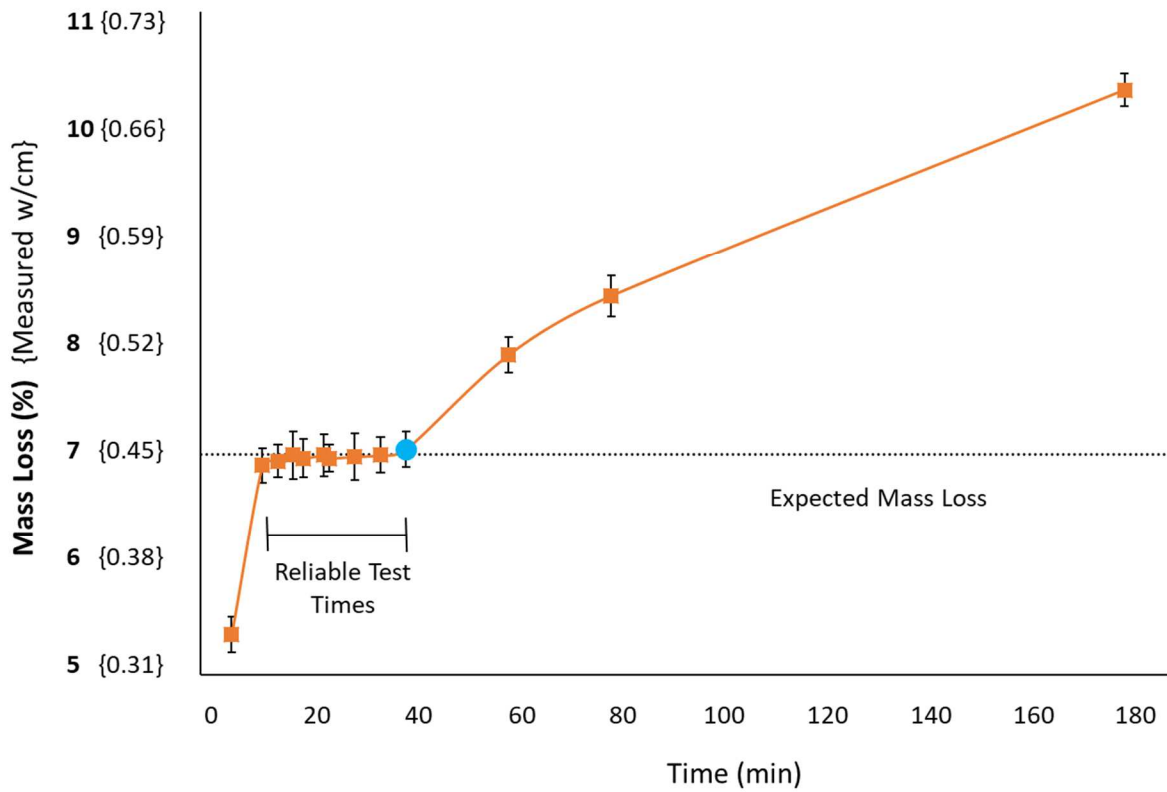
Figure 4-6. Phoenix results for a sample tested over time.

Table 4-5. Time of aggregate decomposition

Coarse Aggregate Type	Time of Decomposition (min)
Dolomite	40
Dolomitic Limestone 1	40
Dolomitic Limestone 2	45
Gabbro	50
Granite 1	40
Granite 2	45
Granite 3	50
River Rock 1	40
River Rock 2	45
Sandstone	45

4.3.3 Practical Significance

Previous research has shown the accuracy of the Phoenix for hundreds of mixtures [19, 54]. This study has found that the accuracy of the Phoenix could be affected if samples are not tested before the start of the acceleration period. For the materials used and for most conventional concrete, a test should be completed within 3 h of mixing for accurate measurements of the w/cm. Based on the mixture design and admixtures used, this timing can be extended or shortened and so heat release or setting time studies could be done to better understand when the heat release begins and testing should be done before this begins.

This study has also found that the accuracy of the Phoenix could be affected if samples are tested for extended periods in the furnace. This means that there is a maximum amount of time that the sample could be placed in the furnace. For the 10 coarse aggregates investigated, the samples should be removed and weighed before they have been cooked for 40 min.

There are many solutions to limit the maximum time limit in the test. For example, the furnace could be turned off after 20 min or the furnace could start at 815°C but not reheat above 500°C if a sample is inserted. Another solution is to use an internal scale that could be used in the furnace to constantly monitor the mass of the sample. This would prevent samples from reaching temperatures that cause decomposition of the aggregates.

4.4 Conclusion

This study investigates two important timing questions concerning a w/cm test method known as the Phoenix. The first question is how long after mixing a sample can the w/cm still be accurately measured. The second question is when samples are kept in the furnace after the test is complete, will the heat cause decomposition of the materials and modification of the results.

The following conclusions were found:

- The Phoenix test provided accurate w/cm results within +/-0.01 for 100% of the mixtures investigated if the test was completed before the increase in the rate of heat release known as the acceleration period. The acceleration period occurred after 3h for the mixtures investigated.

- The TGA analysis shows that there is approximately a 2.5% loss in the mass of the paste from 200ºC to 800ºC. This will cause a negligible mass loss for a concrete mixture.

- For the concrete mixtures investigated the primary material that decomposed after 600°C is the coarse aggregate.

- Based on concrete mixtures with the 10 coarse aggregates tested, the maximum amount of time that the sample should spend in the furnace is 40 min before decomposition begins.

This work further refines the Phoenix and robustness of the test to measure the w/cm of fresh concrete in about 15 min. This is an important measurement that is not currently possible in the quality control of cementitious materials.

CHAPTER V

THREE-DIMENSIONAL OBSERVATION OF THE MICROSTRUCTURE AND

CHEMISTRY OF TRICALCIUM ALUMINATE HYDRATION

5.1 Introduction

Tricalcium aluminate $(C_3A)^2$ makes up between 0% and 16% of Portland cement clinker and

plays a major role in hydration. The C_3A hydration is typically delayed by adding $CaSO_4$ to

avoid flash setting [7, 41, 42, 77]. Despite decades of research, the direct mechanism of delayed

C_3A hydration is still not clear [41, 93-105]. Research on hydrating C_3A has historically been

limited because of hydration products forming on the surface and not allowing direct observation

[100, 102, 105].

Multiple techniques have been used to gain insights into cement hydration despite the formation

of hydration products [106-122]. Synchrotron-based techniques using soft X-ray ptychography

imaging combined with scanning transmission X-ray microscopy (STXM), and X-ray adsorption

near-edge fine structure (XANES) have been used to study C_3A hydration [105, 123-129]. Also,

the combination of X-ray nano-computed tomography (nCT) and nano X-ray fluorescence

(nXRF) are combined as a technique named nano-tomography assisted chemical correlation

(nTACCo) has been used to study the hydration of various C_3S systems [20-22].

---

2 Conventional cement chemistry notation is used throughout this paper: C = CaO, A = Al_2O_3, H = H_2O

This study aims to extend the use of nTACCo to study the hydration of C_3A particles. This work will allow for a better understanding of C_3A and its role in cement hydration, nTACCo can identify the density, chemical composition, and locations of C_3A hydration products. These techniques are capable of non-destructive imaging at the nanoscale. Further, the sample preparation is minimal and the method allows multiple evaluations over time.

In this paper, nCT is used to investigate three C_3A multi-particle groups before and after 2 h and 10 h of hydration. The nCT measurements give direct observations of the surface and inner structure of the hydrated particles. Also, one particle was additionally scanned with nXRF and was investigated using nTACCo. The microstructural and chemical composition changes are directly observed, quantified, and discussed. The goal of this work is to study C_3A hydration during early hydration periods. These results will provide insights into the dissolution and formation of C_3A hydration products in early age hydration. These insights can be applied to improve knowledge concerning the hydration of Portland cement.

5.2 Methodology

5.2.1 Materials

The C_3A material used in this study was synthesized by Mineral Research Processing in Meyzieu, France. This material was characterized with inductively coupled plasma optical emission spectroscopy (ICP-OES) for elemental composition, X-ray diffraction (XRD) for crystalline phase abundance, automated scanning electron microscopy (ASEM) on the dispersed powder for particle size distribution (PSD), and isothermal calorimetry for the rate of heat release. The results from ICP-OES analysis using a dilution of 10 by mass and acidification with a 5 % nitric acid solution are shown in Table 5-1. The XRD analysis indicates this material is close to pure C_3A. The PSD measured by ASEM using 2000 individual particles suggests that 95% of the particles are less than 9 μm in size. The isothermal calorimetry heat flow curve can be seen in Figure 5-1, with vertical lines to indicate correlated imaging periods at 2 and 10 h. These periods correlate with the induction and

deacceleration periods of cement hydration [130-132],], These same periods have also been

investigated with C_3S hydration from previous research with nTACCo [20-22]. The calorimetry

experiment used a saturated lime (CH) and $CaSO_4$ solution with a water-to-solid (w/s) ratio equal to

five to match the conditions of the X-rays imaging experiments in this paper. This was chosen as it

supplies both Ca and SO_4 ions to the solution and is based on previous studies of the pore solution in

Portland cement [41, 74, 94, 97, 133-138].

Table 5-1. Elemental composition based upon a single analysis of C_3A

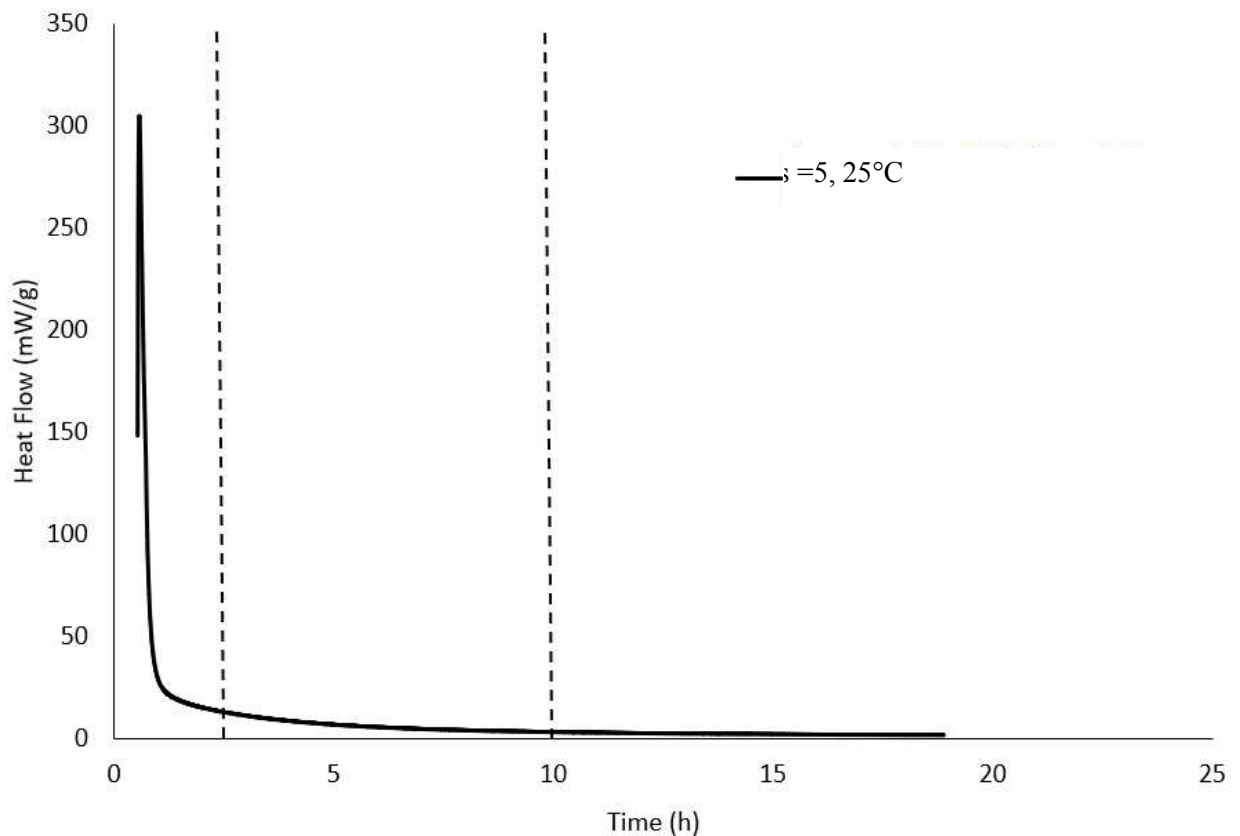| ICP elemental analysis (mol%)	Al	Ca	Fe	K	Mg	Na	P	Si
	36.8	61.7	0.1	<0.01	0.20	0.20	<0.01	1.1

Figure 5-1. Heat flow of C_3A hydrated with saturated CH and $CaSO_4$ solution from the isothermal

calorimeter.

5.2.2 Sample Preparation and Experimental Setup

Sample preparation for C_3A particles performed similar to previous nTACCo research publications and has been repeated here for the convenience of the reader [20-22]. The sample was prepared by gluing multiple C_3A particles on the tip of a tungsten needle with Devcon 5 min epoxy as shown in Figure 5-2. After the epoxy hardened, the C_3A particles were then investigated with a laboratory SkyScan 1172 μCT scanner to ensure epoxy did not coat the particles. A plastic cone that fits tightly to the needle was used as a solution container. The cup has a small hole that allowed the needle to penetrate through it. The cup fit tightly to the needle and stayed in place due to friction unless intentionally pulled up or down the needle. Additional C_3A powder was attached on the side of the needle to make the average w/s =5 within the cone volume. At the beginning of the experiment, an initial scan of the dry particle needle configuration was made with the cup at the lowest location. Next, the sample was placed in an ultra-high purity nitrogen environment and the cup was filled with saturated CH and $CaSO_4$ lime solution at 25 °C. The cup was then raised to submerge the sample in solution. The sample was then sealed in the nitrogen environment to avoid carbonation and allowed to hydrate for either 2 h or 10 h. The seal was removed after the prescribed hydration time, the solution was removed, and the sample was submerged in 99% isopropyl alcohol (IPA) for five minutes to arrest hydration. IPA was used because it has been suggested previously to have the least impact on the microstructure of hydrated samples [139, 140]. Previous work with these same materials and techniques has indicated no observed differences in the microstructure before and after using IPA to stop hydration [20-22]. The cup was then lowered, and the sample was placed back on the nCT scanner to obtain the final tomography scan. The nXRF scans were also completed on one of the particles for subsequent nTACCo analysis. A w/s of 5 was used because it allowed sufficient X-ray transmission for tomographic imaging. If pure water had been used, the mounted particle might have reacted too quickly to make meaningful measurements, therefore a solution containing saturated CH

and $CaSO_4$ solution was chosen instead. Past research with C_3A shows that this solution is representative of the pore solution that occurs in Portland cement [41, 74, 94, 97, 133-138].
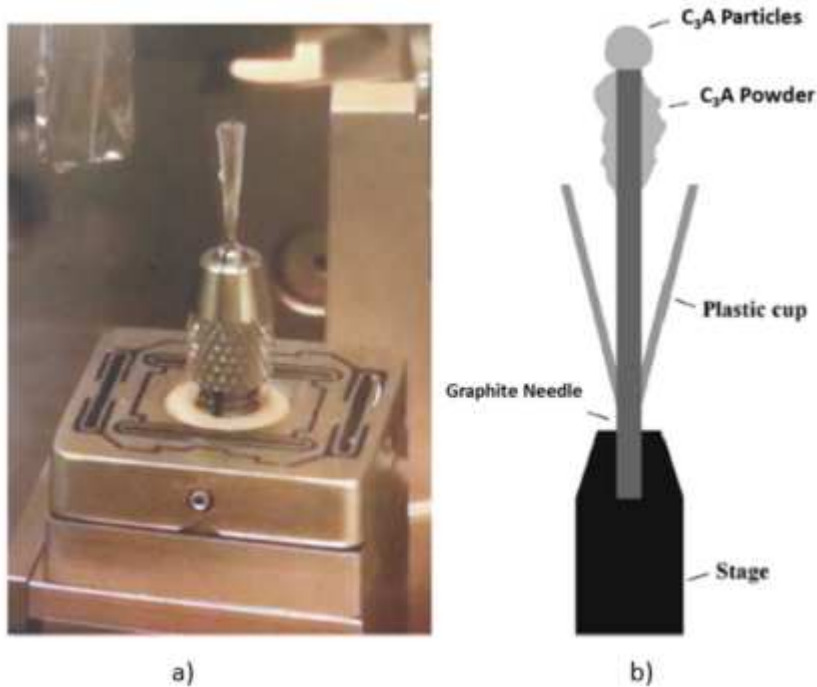
Figure 5-2. Overview of the assembled setup on the beamline of the experimental setup.

5.2.3 Nano-tomography (nCT)

Sample testing for C_3A particles was performed on the same nCT as previous nTACCo research publications and has been repeated here for the convenience of the reader [20-22]. The nCT scanner used in this experiment was a Zeiss 810 Ultra (Carl Zeiss X-ray Microscopy, CA, USA) with an X-ray energy level of 5.4 keV at the resolution of 65 nm per pixel. The instrument settings are given in Table 5-2 and more details can be found in Winarski et al. [127]. One nCT scan produces two different types of data sets. A radiograph is a 2D projection of the X-rays that pass through the sample in one direction. A tomograph is created from the reconstruction of all the radiographs from multiple angles. One tomograph is a 3D data set that contains several 2D virtual slice images through the sample. The grayscale value of a pixel represents the X-ray absorption of the material as a function of its local composition and density. With enough contrast, the segmentation of different phases can be

made by the direct threshold of their gray values. This allows the 3D structure of the material to be rendered. Because of the nanometric length scale of this experiment, any small shifting of the sample due to thermal expansion or imperfection of stage positioning could change the position of the sample in the nCT data sets. To compensate for these movements and allow the same region to be compared, the data from before- and after hydration scans need to be aligned. Usually, this alignment can be accomplished by using the mounting needle as a reference point. However, because individual particles may have independent movements that do not match the needle, these individual particles were first separated from the sample, and then their data were aligned individually. Dragonfly software version 3.6 from ORS was used to analyze the data [141]. An example of a data set for an individual particle is shown in Figure 5-4. The data in this study is reported with an uncertainty of 0.1 μm^3 [20-22]. This would be a volume of 300 voxels. A conservative estimate of the error caused by measurement and segmentation similar to other nanoscale materials with similar X-ray absorption of known size and geometry [20-22].

5.2.4 Analysis of Particle Reaction Depth

The depth of reaction of each particle was quantified by drawing a straight line from the reacted surface to the original centroid of the particle. When this line reaches anhydrous C_3A, the distance is recorded and this determines the depth of reaction. With this technique, every voxel on the reacted surface provides an independent measurement of the reaction depth. A histogram for the reaction depths was determined at 65 nm intervals. To examine the distribution of reaction depth for each selected particle, the histogram for all the voxels on the reacted surface is plotted as the "Reacted Surface" as shown in Figure 5-8.

5.2.5 Nano-X-ray Fluorescence

The nXRF measurements were made with an X-ray spot size smaller than 50 nm at the hard X-ray nano-probe beamline at sector ID-26 of the Advanced Photon Source (APS) and the Center of

Nanoscale Materials (CNM) at Argonne National Laboratory. The instrument settings are given in Table 5-2 and more details can be found in Winarski et al. [127].

Table 5-2. Summary of instrument settings for nCT and nXRF experiments.

	nCT	nXRF
Resolution	65 nm/pixel	50 nm/pixel
Numbers of radiographs from 0° to 180°	901	-
Exposure time	20 s	-
Source energy	5.4 keV	-
Dynamic ranges [a]	min -5000	-
	max 5000	-
Detector dwelling time	-	0.1 s
Scaler count time	-	0.1 s

[a] The data is displayed in FLOAT type.

X-ray fluorescence radiation is detected with a four-element silicon drift energy dispersive detector (Vortex ME4) [127]. Additional details can be found in other publications [22]. Fluorescence was analyzed using the software package MAPS [142]. Fitting and quantification of the fluorescence data were performed with thin-film standards (National Bureau of Standards, Standard Reference Material 1832 and 1833).

The nXRF technique has two limitations that make its interpretation challenging: 1) the X-ray beam penetrates through the material and causes X-ray fluorescence along its path, which makes it challenging to determine depth-dependent information in the sample; 2) a portion of the fluoresced X-rays are absorbed by the sample before it can reach the detector. Both of these limitations can be overcome by combining the structural information from nCT with the nXRF data sets. After aligning the two data sets, the nCT measurements can determine the travel path of the nXRF beam as well as the different materials the beam traverses within 65 nm. Next, the areas analyzed by nXRF are carefully chosen so that they are close to the EDS detector (<4 μm from the edge). By reducing the travel path of the X-rays, the absorption is reduced to about 10% for Si and 5% for Ca [143].

5.2.6 Data Fusion of nCT and nXRF (nTACCo)

Additional details about nTACCo are provided in earlier publications and have been repeated here [20-22]. An overview of the data fusion of nCT and nXRF is shown in Figure 5-3. The nCT and nXRF data are aligned by comparing 2D radiographs to match the particle boundary and areas of uniquely identifiable chemical composition. -The top radiograph shows where the nXRF scan took place on the particle. The bottom radiograph shows the cross-section at the slice location for the corresponding elemental map at the right side of the figure. The elemental map has two locations that were observed. Location A shows that the X-ray beam only passes through the hydration product. Location B shows the beam passes through both the hydration product and anhydrous C_3A. Because the data sets are aligned, information about the depth and the number of materials investigated can be determined for each point in the nXRF scan. For example, since point A on the nXRF scan only passes through the hydration product, the material concentration can be calculated using equation 1

$$D_{product} \ = \ C_A \ / \ L_A \tag{1}$$

Where the material will have a concentration, C_A, per unit area of the beam ($\mu g/\mu m^2$), and the length of travel, L_A, is expressed in μm. The concentration density ($D_{product}$) can then be calculated in $\mu g/\mu m^3$. This process was done for 487 locations in the sample to identify the average concentration density of the hydration product, represented as $\overline{Dproduct}$.

However, when repeating this process at location B, this location has two constituents along the length of the path of the X-ray beam, the length of anhydrous C_3A, L_{BX}, and the length of hydration product, L_{BY}. The aligned nXRF and nCT data can help determine the length of the X-ray beam through each constituent. Since the average concentration density of the hydration product was determined at and around location A, $\overline{Dproduct}$ can be used to estimate the concentration of the anhydrous C_3A (D_{C3A}). The concentration density of the anhydrous C_3A, D_{C3A}, can be found by subtracting the average concentration of the hydration product, $\overline{Dproduct}$, multiplied by the length of the path of the total hydration product (L_{BY}), from the total concentration at point B, C_B. This is then

divided by the depth of the anhydrous C_3A (L_{BX}) at that location. This is expressed mathematically in

equation 2.

$$D_{C3A} = \frac{C_B - (\overline{D_{\text{product}}} * (L_{BY}))}{L_{BX}} \tag{2}$$

This process was completed for 219 points and the average and one standard deviation can be seen in

Table 5-4. This process is then repeated at other locations for particle group 1, the locations can be

seen in Figure 5-9.
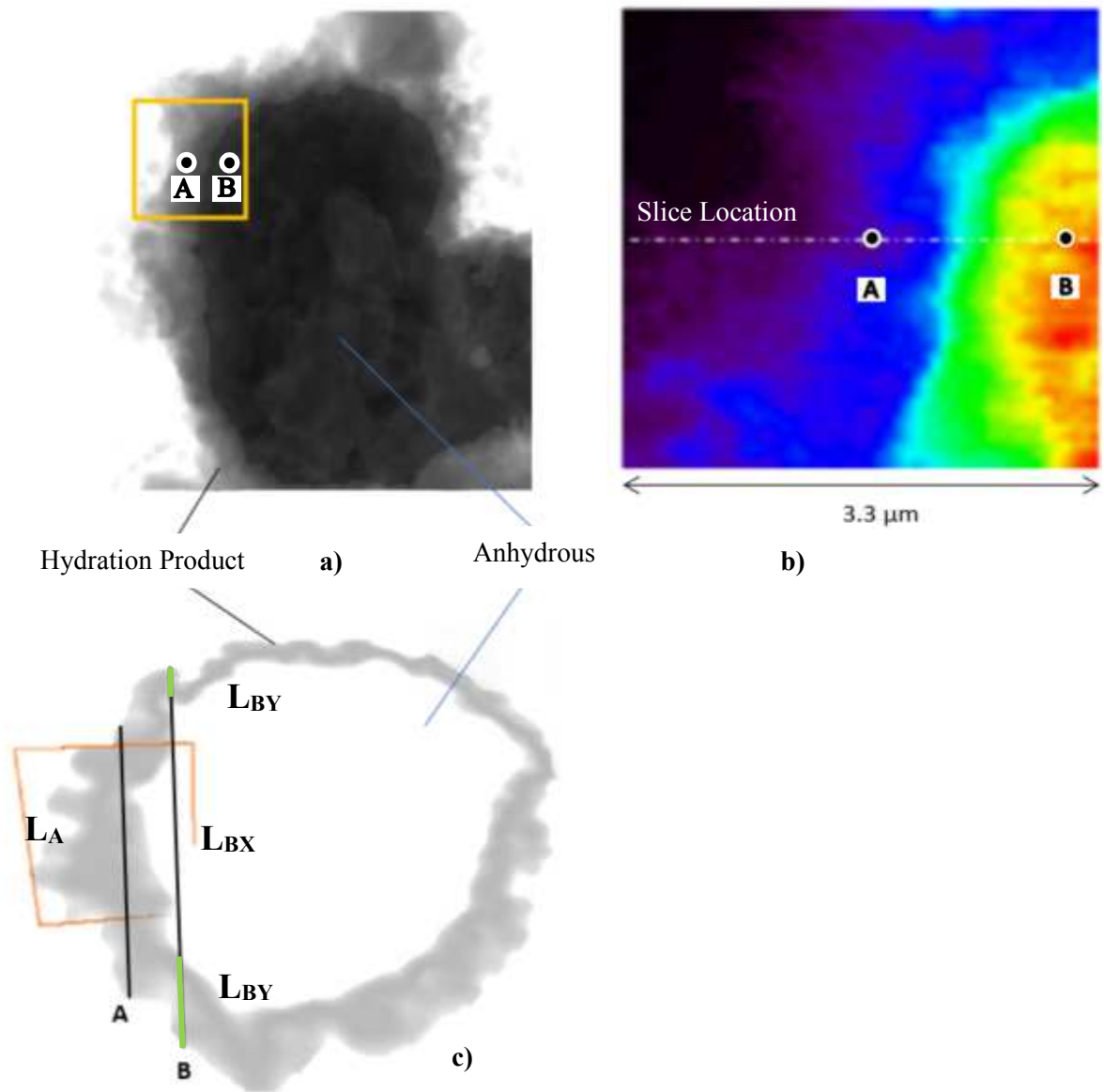
Figure 5-3. Overview of combining nXRF and nCT for particle 1 after 2 h hydration. a) the radiograph shows where the nXRF scan is captured on the particle. Figure 3b shows the nXRF scan and two specific points, A and B, are highlighted. Figure 3c shows a cross-section of the particle and it highlights the path of two points from the nXRF scan that are shown in Figure 3b.

5.3 Results and Discussion

5.3.1 Analysis of Particles Hydrated for 2-hours

The nCT data for particle groups 1 and 2 are shown in Figures 5-4 and 5-5. The images show the radiographs, 3D structure, and slice images before and after 2 h of hydration. The 3D models show the particle separated by color, anhydrous is orange, hydration product 1 is green, and hydration product 2 is red. A slice from the 3D tomograph shows the cross-section for the particles. The slice location is indicated by the blue line on the 3D models. The inner structure of this particle can be seen with a quadrant removed so the internal structure can be observed in Figure 5-8. Particle group 1 seems to have more particles in the after scan as seen in red in the 3D model at 2 h. These additional particles are likely from particles that could have floated near the C_3A particles during hydration and became stuck in the needle formations, thus showing up in the nXRF and nCT scans.

Particle group 2, as shown in Figure 5-5, had many particles that are no longer found in the scan after hydration. These particles may have separated when the samples were added to the saturated CH and $CaSO_4$ solution. Because of this, particle 2 was chosen for a more in-depth analysis.
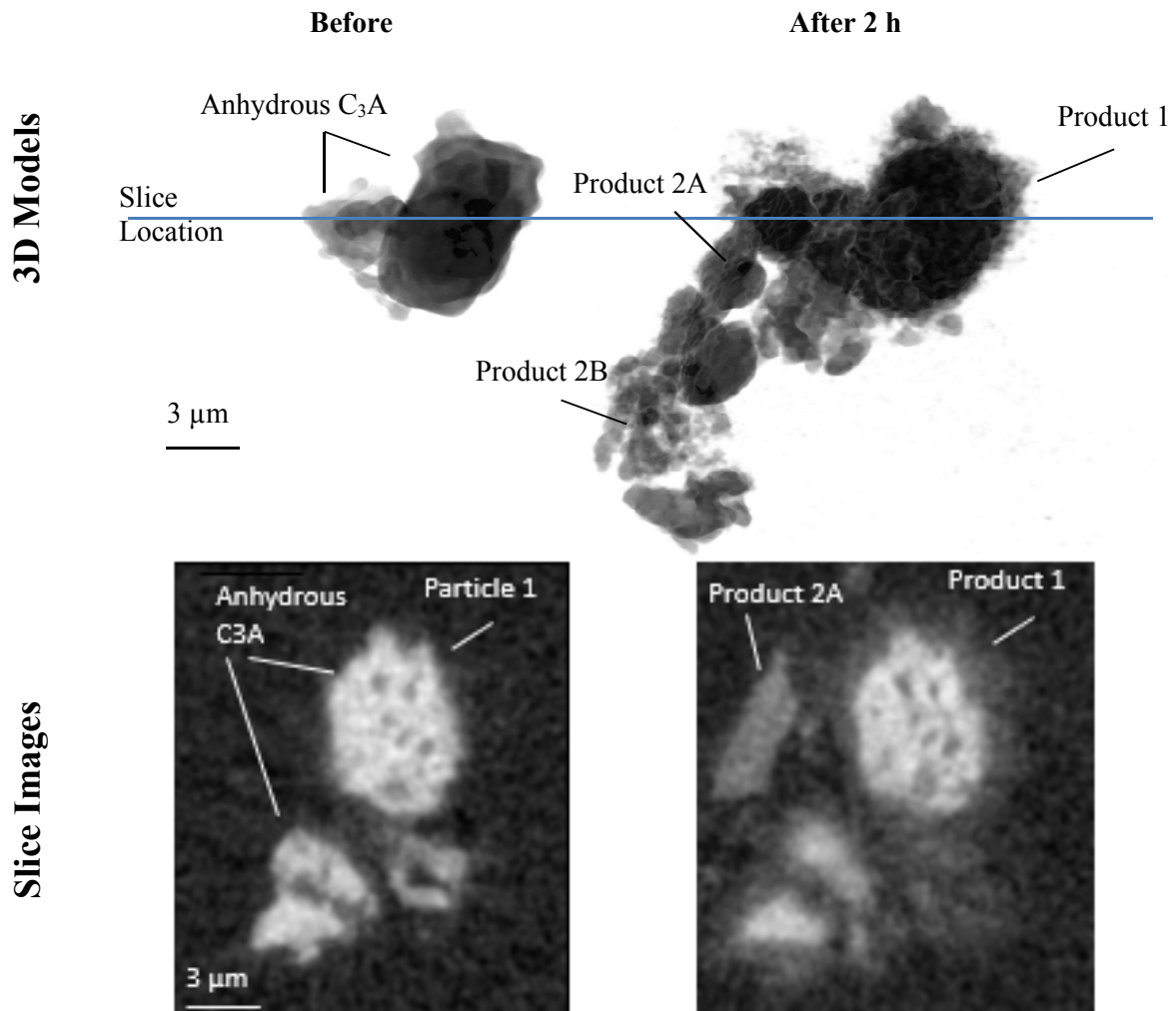
Figure 5-4. The nCT dataset showing 3D radiographs, tomographs, and slice images for particle group 1 and particle 1 before and after 2 h hydration.
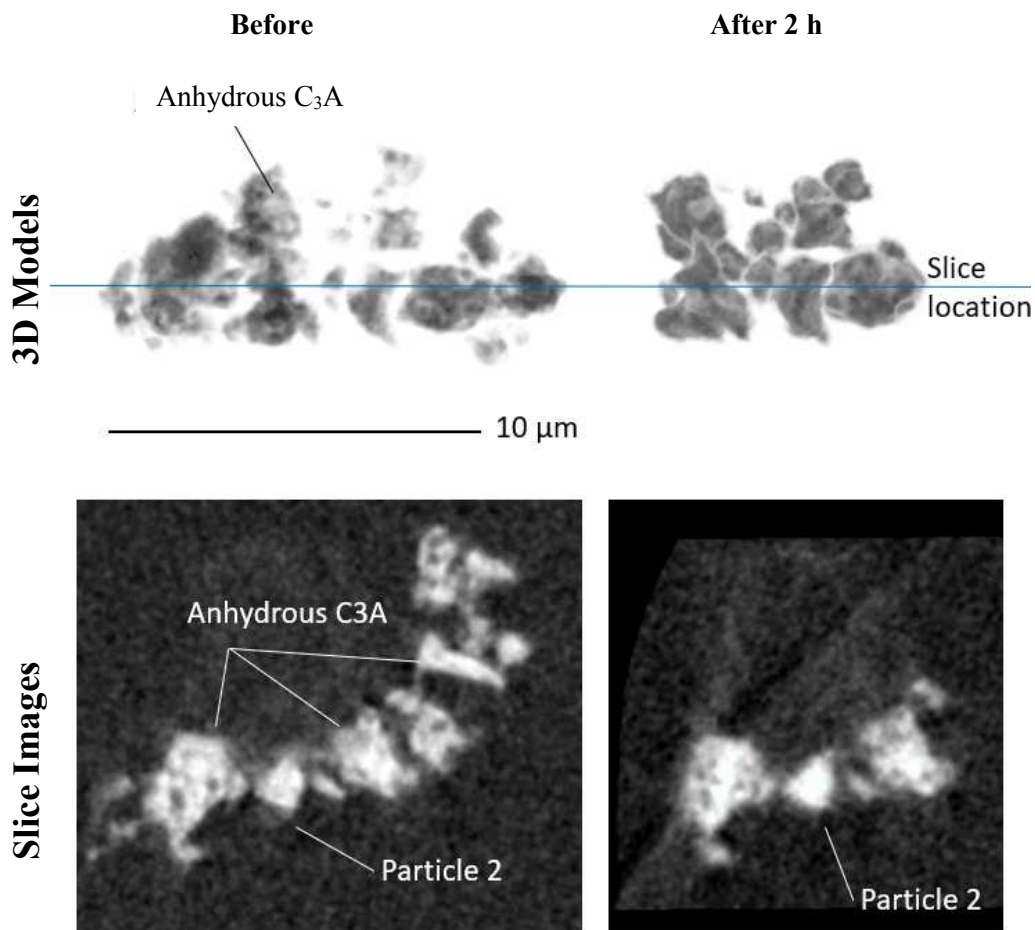
Figure 5-5. The nCT dataset showing 3D tomograph and slice image for particle group 2 and particle 2.

The volumetric changes of the particles 1 and 2 before and after hydration are summarized in Table 5-3. Particle 1 had two different hydration products that formed as seen in Figure 5-4. Including product 2A that formed away from the particle. The nXRF data will be used to provide more insight into these products later in this paper. As seen in Table 5-3, particle 1 had an original volume of 29.5 μm^3. After 2 h of hydration, the particle reduced in volume by 23.5%.

Particle 2 had an original volume of 2.52 μm^3. After 2 h of hydration, the volume reduced by 6.7%. From Figure 5-6, notice Site 1 completely dissolves leaving only hydration product. This could be

due to the increased surface area of Site 1 versus the remaining surface of the particle. This could also be a fast-reacting region of the particle, as discussed in previous studies [21, 22].

5.3.2 Analysis of Particle Hydrated for 10-hours

The nCT data for particle group 3 are shown in Figure 5-6, particle 3 is also identified. The volumetric changes of particle 3 before and after hydration are summarized in Table 5-3. Due to the extensive movement of particle 3 from the original position data cannot easily be taken after the reaction. The larger particle in the after-hydration scan was assumed to be particle 3. The values in Table 5-3 are based on this assumption.

	Before	After 10 h
3D Models		
Slice Images		
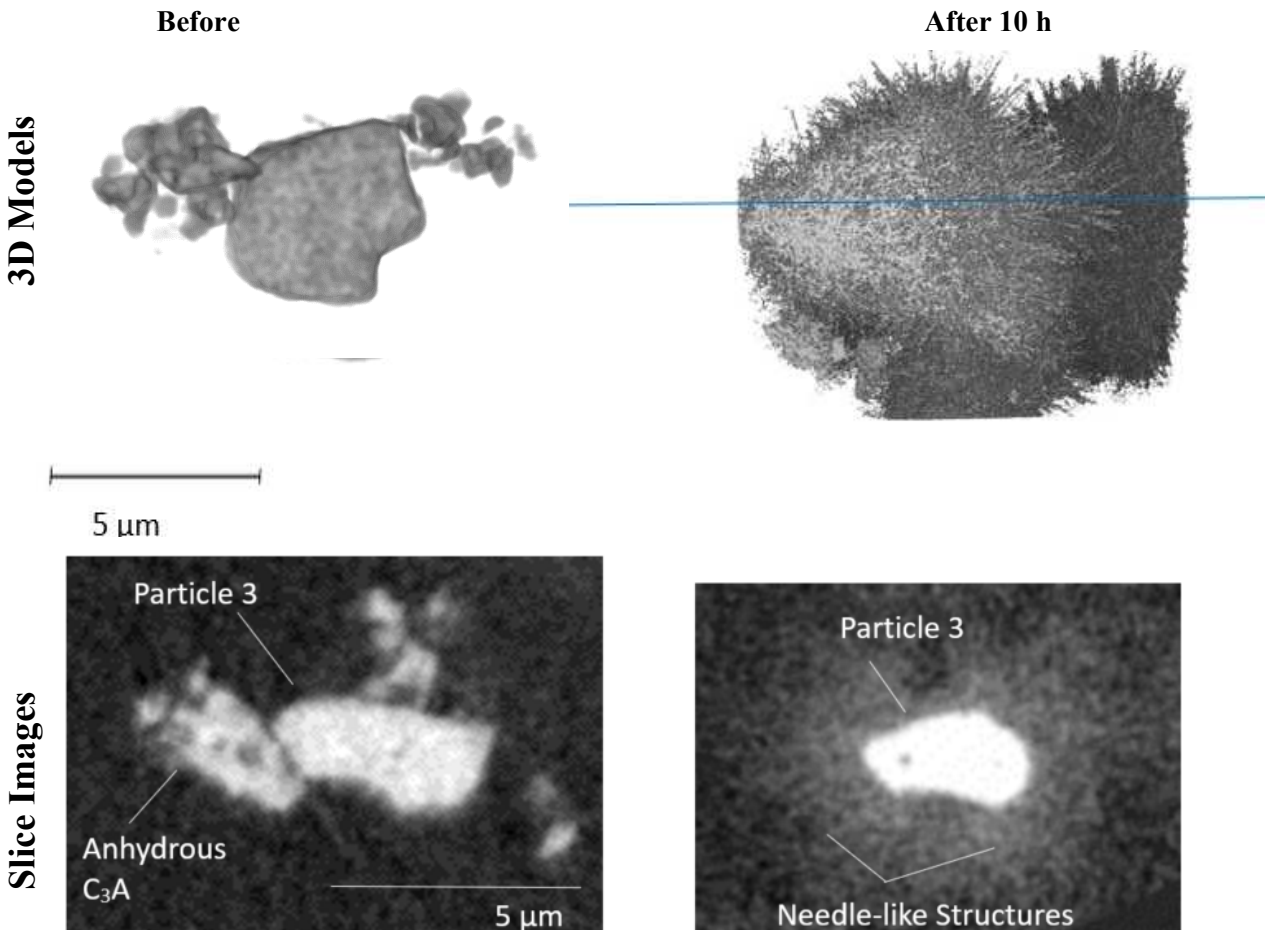
Figure 5-6. nCT results for particle group 3 and particle 3 after 10 h hydration.

Table 5-3. Summary of the measurements of volume three particles.

Particle	Original (μm³)	Hydration Time (h)	After hydration Anhydrous C_3A (μm³)	Percentage of change	Hydration Product (μm³)
1	29.50	2	22.56	23.5%	97.27*
2	2.52	2	2.35	6.7%	1.76
3	29.37	10	19.74	32.8%	123.31

*Sum of both hydration products, product 1 (40.24 μm³) and product 2 (57.03 μm³)

Particle 3 had 123.31 μm³ of hydration product form after 10 hours of hydration with needle-like

structures in much of the viewing window, an increase of 320% from the original particle volume.

These might be ettringite needles that have extended from the surface of the particles. After 10 h of

89

hydration in saturated CH and $CaSO_4$ solution with the continual presence of $CaSO_4$, ettringite crystals could form as observed [97, 133, 134]. Particle 3 had an original volume of 29.37 μm^3. After 10 h of hydration, the particle reduced volume by 32.8%. Particles 1 and 3 had similar volumes but there is only 9.3% less anhydrous material at 10 h compared to the 2 h sample. This seems to agree with the isothermal calorimetry data shown in Figure 5-1. These results show that there is minimal heat release between 2h and 10 h.

5.3.3 Particle Reaction Depth Results

The depth of reaction for Particle 1 can be seen in Figure 5-7. The inner structure of the particle can be seen with a quadrant removed. A line is shown from the original centroid of the particle to a voxel at the surface of the modified region. The distance along this line from the anhydrous particle is recorded from each voxel at the surface. The histograms for Particle 1, 2, and 3 can be seen in Figure 5-8.

After 2 h

3D structure from nCT

Hydration Product

Anhydrous Particle

~0.5 μm

Depth of Hydration Product

3 μm

a)

Distribution of Reaction

Number of voxels on the reacted surface

— Particle 1, 2 h
- - - Particle 2, 2 h
········· Particle 3, 10 h

Depth of Reaction (μm)

b)
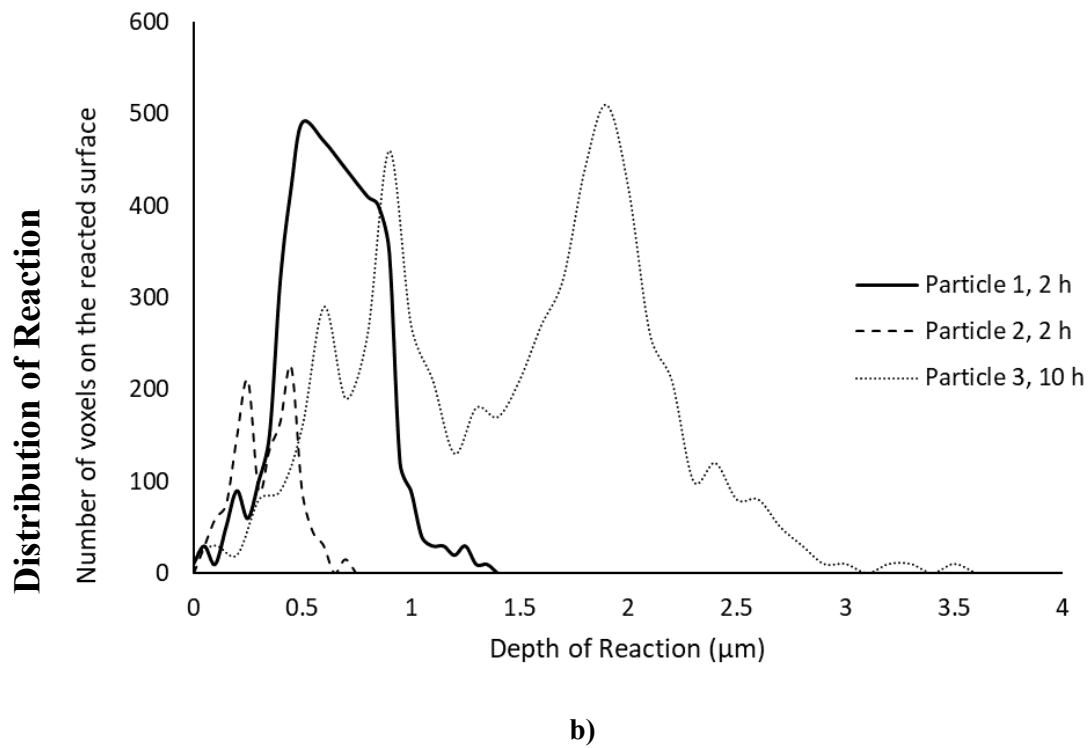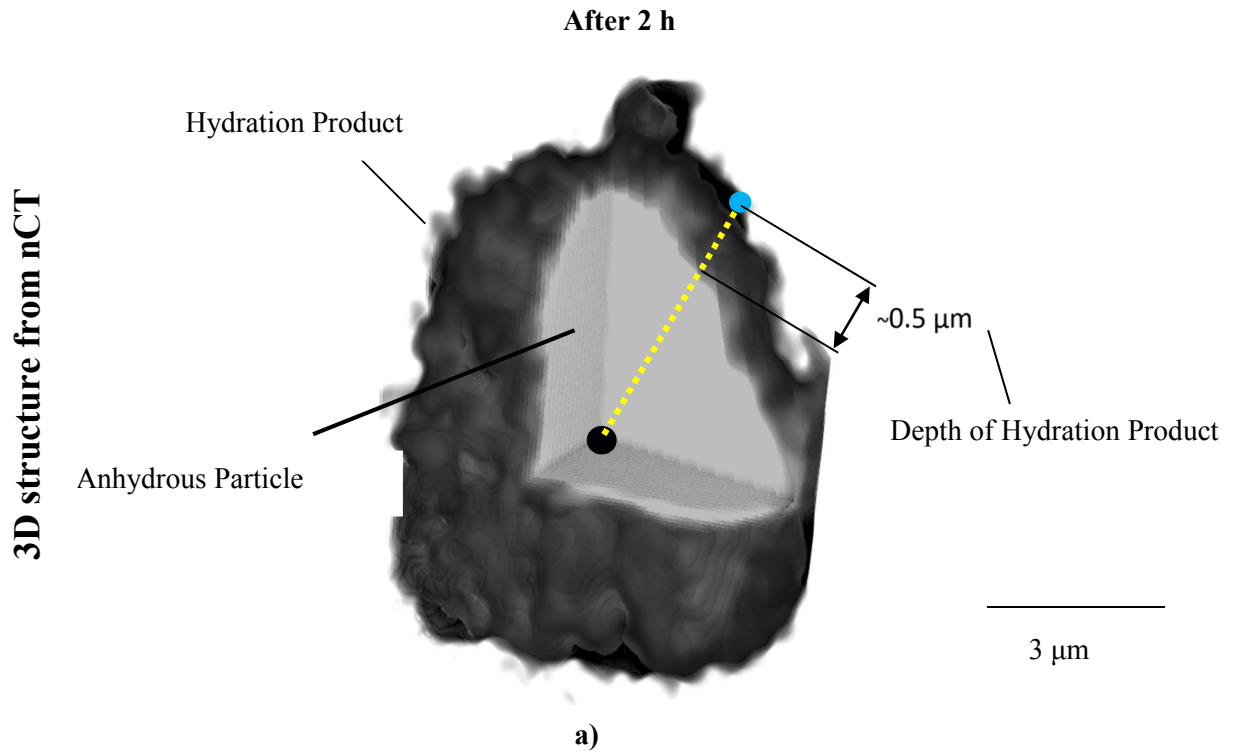
Figure 5-7. a) The nCT depth of reaction of particle 1 after 2-hours of hydration. b) depth of reaction histograms for individual particles.

The depth of reaction data provides a histogram of the reaction depths for all the surfaces of the particles. This shows that particle 1 has a normal distribution and particles 2 and 3 have binomial distributions. Particle 1 has a reaction depth average and one standard deviation of 0.66 +/- 0.22 μm. Since Particles 2 and 3 are binomially distributed, they do not have a clear average depth of reaction. This could be from irregular shapes, highly reactive regions, or both. The particle modification is not uniform but based on reaction sites, density, and reactivity of the sites. This was observed with previous C_3S particles [20-22].

Particles hydrated for 2 h had a reaction depth average and one standard deviation of 0.50 +/- 0.24 μm compared to Particle 3 which hydrated for 10 h and had an average reaction depth of 1.56 +/- 0.56 μm. This shows that Particle 3 had a maximum reaction depth that was on average 2.5x greater than particle 1 and particle 2. This is likely caused by the needle-like materials surrounding the particles that may be ettringite crystals. More information can be observed in Figure 5-6.

5.3.4 Chemical Composition of Particle 1

The elemental densities, mass density, and the Ca/Al, Ca/S, and Al/S molar mass ratios for hydration products and anhydrous C_3A have been obtained with the nTACCo method as previously shown in Figure 3. The maps from three nXRF scans for Particle 1 are given in Figure 5-8. The average densities and one standard deviation for each constituent of particle 1 can be seen in Table 5-4.

3D Model	Elemental Maps

Product 1

Region for nXRF

Ca — Max: 733.6 µg/cm²
Al — 311.4 µg/cm²
S — 101.4 µg/cm²

3.3 µm

Needle-like Structures

Product 2A

3 µm

Ca — Max: 514.6 µg/cm²
Al — 42.0 µg/cm²
S — 11.0 µg/cm²

3.3 µm

Product 2B

Ca — Max: 264.2 µg/cm²
Al — 38.7 µg/cm²
S — 34.3 µg/cm²

Figure 5-8. Particle group 1 view of nCT radiographs showing nXRF elemental maps and at 2 h hydration.

Table 5-4. Elemental densities of the constituents for particle group 1 at 2 h hydration.
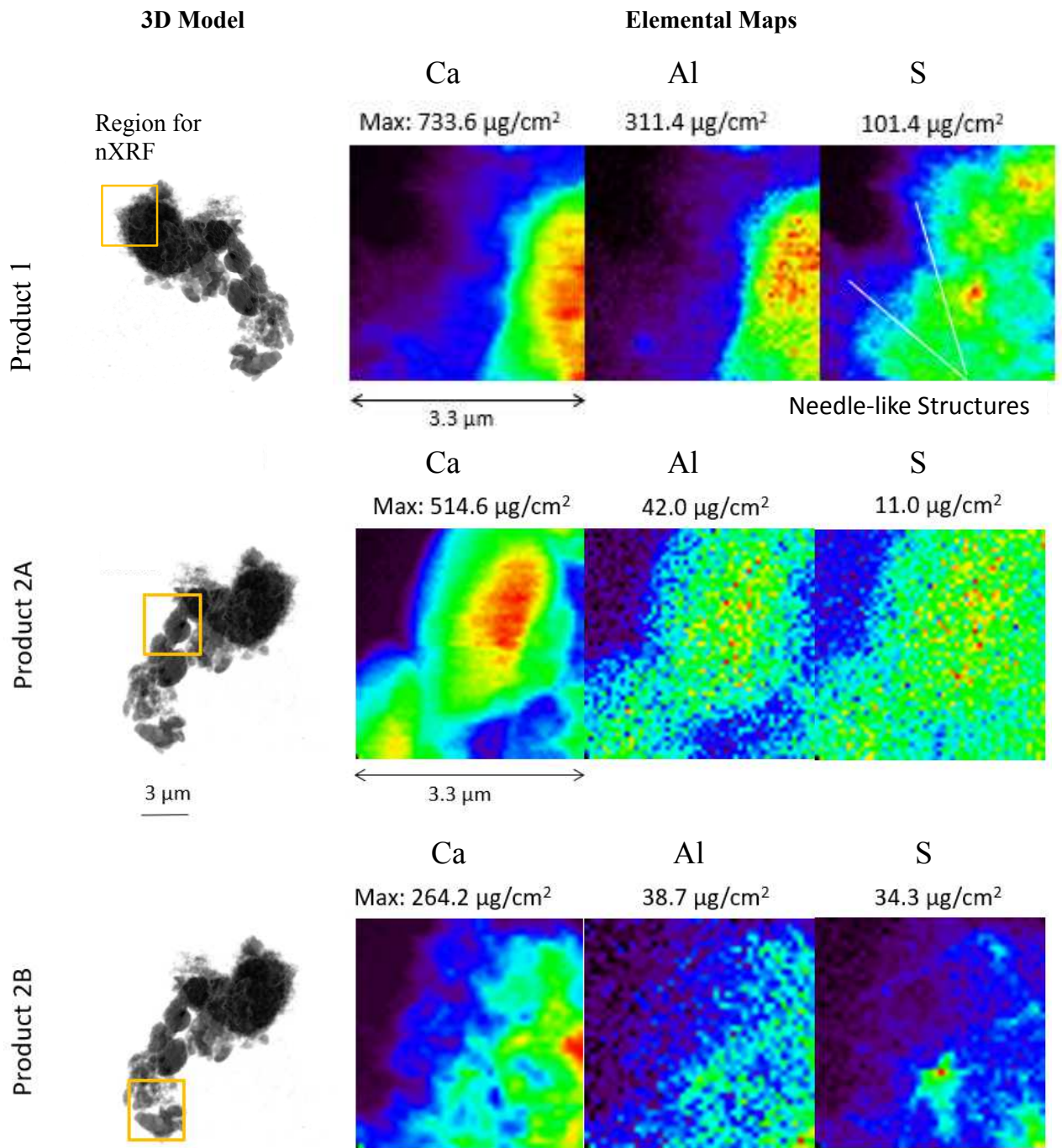
Constituent	Anhydrous C_3A	Product 1	Product 2A	Product 2B
Ca (g/cm^3)	1.41 ± 0.31	0.92 ± 0.22	2.01 ± 0.46	1.21 ± 0.18
Al (g/cm^3)	0.81 ± 0.23	0.32 ± 0.15	0.23 ± 0.09	0.25 ± 0.10
S (g/cm^3)	0.38 ± 0.18	0.31 ± 0.03	0.15 ± 0.04	0.21 ± 0.11
Ca/Al (molar)	2.59 ± 0.73	4.27 ± 0.61	12.98 ± 1.33	7.19 ± 1.26
Ca/S (molar)	4.64 ± 1.61	3.71 ± 1.28	16.75 ± 1.32	7.44 ± 2.45
Al/S (molar)	1.79 ± 0.50	0.86 ± 0.49	1.29 ± 0.73	1.00 ± 0.41
Likely Material	Tricalcium Aluminate	Ettringite	Calcium Hydroxide	Calcium Hydroxide
Formula	C_3A	$C_6A\overline{S}_3H_{32}$	CH	CH
Ca/Al (molar)	2.23	4.46	16.93*	16.93*
Ca/S (molar)	-	2.50	-	-
Al/S (molar)	-	0.56	-	-

*[20]

(-) Value divided by zero

As seen in the table above, product 1 has an average density of Ca of 0.92 μg/cm^3 compared to

product 2A at 2.01 μg/cm^3. The Ca/Al molar ratio for product 1 and product 2A are 4.27 and 12.98,

respectively. This shows a difference between hydration product 1 and 2A. Product 2A also has

different densities of other elements compared to product 2B but the Ca/Al molar ratio for each is

12.98 and 7.19 respectively. Based on the Ca/Al, Ca/S, and Al/S molar ratios and likely hydration

products with C_3A hydrated with saturated CH and $CaSO_4$ water, product 1 is likely ettringite.

Ettringite has a Ca/Al molar chemical composition of 4.46, this is similar to 4.27 for product 1. It is

not unreasonable to observe ettringite as the solution contains $CaSO_4$ [97, 133, 134].

Product 2A and 2B have high Ca concentrations and low Al and S concentrations. These indicate

product 2A and 2B are CH. CH has been measured with nTACCo in a C_3S particle with a Ca/Al

molar ratio of 16.93 [20]. This is similar to 12.98 and 7.19 for products 2A and 2B respectively. The

differences may be because CH previous

ly measured was mixed in with CSH and was a by-product of a C_3S hydrated in a 15 mmol/L lime solution. Due to these products not existing before hydration and having similar Ca concentrations to the C_3A particles but much lower Al and S, this also suggests these particles would be CH from the hydration solution that floated into the sample during hydration.

5.4 Conclusions

This paper shows a study of three individual particles before and after 2 h and 10 h of hydration. These particles were studied by nCT, and one particle was studied with nXRF. The samples were mixed with a w/s = 5 in saturated CH and $CaSO_4$ solution. The nCT was utilized to show the comparison of regions of change precisely with 3D models. This includes the inner structure of the materials, the products formed, and the volumes of the changes. The nXRF data is then combined with the nCT to characterize the chemical composition and mass density of one particle. The following conclusions have been found:

- At 2 h of hydration, CH, ettringite, and anhydrous C3A were observed simultaneously.
- At 10 h of hydration, needle-like structures have formed and extended from the original particle, filling much of the viewing window.
- Two similar-sized particles were subjected to 2 h and 10 h of hydration with volumes of hydration product as a percentage of the original particle volume being 230% and 320%, respectively.
- Two particles had similar original volumes but there is only 9.3% less anhydrous material at 10 h compared to the 2 h particle.
- One particle's reaction depth at 2 h was normally distributed with an average and one standard deviation of 0.66 +/- 0.22 μm.
- Two particles had binomial distributions for reaction depth at 2 and 10 h of hydration. This could be from irregular shapes, highly reactive regions, or both.

95

- Particles hydrated for 2 h had a reaction depth average and one standard deviation of 0.50 +/- 0.24 μm compared to a particle hydrated for 10 h with an average reaction depth of 1.56 +/- 0.56 μm.

Additional work is underway to further investigate the mechanisms that caused the unexpected binomial distributed depth of reactions for two particles. This would provide more insights into the hydration mechanisms of C_3A and further increase knowledge of hydration for Portland cement.

CHAPTER VI

CONCLUSIONS

6.1 Overview

The main tasks of this research were to establish a fresh w/cm test method that is efficient, rapid, and accurate. Determine the accuracy of slump, unit weight, compressive strength, resistivity, and petrography concerning the impact of water on properties of concrete. Establish sample testing times within the new w/cm test method, this included the following two objectives. Establish the maximum amount of time between when a sample is mixed and when it is tested and minimize the amount decomposition in samples tested. Finally, to study C3A hydration during early hydration periods,

6.1.1 Determining the Water to Cement Ratio of Fresh Concrete by Evaporation

- A volume > 1236 cm^3 was needed to precisely and accurately determine the density and water to cement ratio of fresh concrete. This is important because a minimum volume of material is needed in a testing protocol.

- The tested sample was simultaneously used to determine the density and water to cement ratio of fresh concrete. The accuracy of the water to cement ratio is highly dependent on the tested sample density.

- A maximum temperature of 815°C was used to accurately determine the water to cement ratio of fresh concrete. Temperatures that exceed this would evaporate more than water.

97

- The material was tested at a uniform thickness of 19 mm +/- 13 mm. This ensures a consistent testing time.

- By using heat from multiple faces and an insulated chamber the water content of the sample could be found within 15 min.

- For the laboratory mixtures with w/cm between 0.30 and 0.60, the average measured w/cm was within 0.01 from the batched w/cm and on average the difference was 0.001 for the dual heating elements and 0.004 for the furnace.

- For six mixtures with a batched 0.45 w/cm, the AASHTO T 318 microwave oven test was within 0.045 w/cm while the introduced test method was within 0.015 w/cm for the dual heating elements and 0.013 for the furnace.

- The average standard deviation and COV for the laboratory and field mixtures were comparable. The dual heating elements had a standard deviation of the water to cement ratio of 0.012 and COV of 3.0% and the furnace a standard deviation of 0.009 and COV of 1.8% for laboratory and field standard deviation of 0.010 and COV of 1.2%.

- The COV of the introduced w/cm for dual heating elements and furnace was approximately three and five times lower respectively than the AASHTO T-318 microwave oven test (3.0% and 1.8% compared to 8.9%). This is likely caused by the larger volume of sample investigated in both devices.

- For the field testing, 15% of the mixtures were found to have a 0.02 w/cm or higher than the batched w/cm.

6.1.2 Measuring the Change in Water to Cement Ratio in Fresh and Hardened Concrete

- Concrete batch plants and field water adjustments can be used to produce concrete mixtures with a w/cm of a range of +/- 0.02 w/cm of a target value.

- The slump, unit weight, and compressive strength at 7-day and 28-day did not provide a statistically significant measure of the change in the w/cm of the concrete mixture of 0.04.

- The Phoenix measurements are within +/- 0.01 w/cm of the target value for 88% of the measurements and 100% of the measurements are within +/- 0.02 w/cm of the target value.

- The Phoenix is able to observe a change in w/cm of 0.04 for 63% of the investigations.

- The 28-day surface resistivity test is statistically significant for 50% of the mixtures investigated and 7-day surface resistivity is statistically significant for 38% of the mixtures.

6.1.3 Development of Time & Temperature Testing Limits for a Field Water to Cement Ratio Test

- The Phoenix test provided accurate w/cm results within +/-0.01 for 100% of the mixtures investigated if the test was completed before the increase in the rate of heat release known as the acceleration period. The acceleration period occurred after 3h for the mixtures investigated.

- The TGA analysis shows that there is approximately a 2.5% loss in the mass of the paste from 200oC to 800oC. This will cause a negligible mass loss for a concrete mixture.

- For the concrete mixtures investigated the primary material that decomposed after 600°C is the coarse aggregate.

- Based on concrete mixtures with the 10 coarse aggregates tested, the maximum amount of time that the sample should spend in the furnace is 40 min before decomposition begins.

6.1.4 Three-Dimensional Observation of the Microstructure and Chemistry of Tricalcium Aluminate Hydration

- At 2 h of hydration, CH, ettringite, and anhydrous C_3A were observed simultaneously.

- At 10 h of hydration, needle-like structures have formed and extended from the original particle, filling much of the viewing window.

- Two similar-sized particles were subjected to 2 h and 10 h of hydration with volumes of hydration product as a percentage of the original particle volume being 230% and 320%, respectively.

- Two particles had similar original volumes but there is only 9.3% less anhydrous material at 10 h compared to the 2 h particle.

- One particle's reaction depth at 2 h was normally distributed with an average and one standard deviation of 0.66 +/- 0.22 μm.

- Two particles had binomial distributions for reaction depth at 2 and 10 h of hydration. This could be from irregular shapes, highly reactive regions, or both.

- Particles hydrated for 2 h had a reaction depth average and one standard deviation of 0.50 +/- 0.24 μm compared to a particle hydrated for 10 h with an average reaction depth of 1.56 +/- 0.56 μm.

6.2 Further Research Needs

Continued development of the Phoenix w/cm test method. Although many aggregates, SCMs, and admixtures were analyzed, these may not represent materials that are prevalent elsewhere for concrete construction. Unforeseen issues or corrections may need to be implemented in the future to accommodate other materials that have not been tested to date.

Additional work is underway to further investigate the mechanisms that caused the unexpected binomial distributed depth of reactions for two of the C_3A particles. This would provide more insights into the hydration mechanisms of C_3A and further increase knowledge of hydration for Portland cements.

REFERENCES

1. Abrams, D., *Design of Concrete Mixtures* Structural Material Research Laboratory, Lewis Institute, 1918.
2. Cordon, W.A., *Properties, Evaluation, and Control of Engineering Materials*. McGraw-Hill College, 1979.
3. Feret, R., *Etude sur la constitution intime des mortiers hydrauliques.* Bulletin de la Societe d'Encouragement pour 1'Indutrie Nationale, Vol. 96, pp. 1591-1625, 1897.
4. Concrete Manual, *8th ed., US Bureau of Reclamation, Denver, CO, pg 34-39.* 1981.
5. Neville, A.M., *Properties of concrete*. Vol. 4. Longman London, 1995.
6. Daniel, D.G., *Factors Influencing Concrete Workability.* Significance of Tests and Properties of Concrete and Concrete-Making Materials, ASTM International, West Conshohocken, PA, pp. 59-72, 2006.
7. Mehta, P.K. and P.J. Monteiro, *CONCRETE Microstructure, Properties and Materials*. New York, 2017.
8. Powers, T.C., L.E. Copeland, and H. Mann, *Capillary continuity or discontinuity in cement pastes*. 1959.
9. Whiting, D., *Strength and Durability of Residential Concretes Controlling Fly Ash.* RD099, Portland Cement Association.–Skokie: IL, 1989.
10. Powers, T.C. and T. Willis. *The air requirement of frost resistant concrete*. in *Highway Research Board Proceedings*. 1950.
11. Kosmatka, S.H. and M.L. Wilson, *Design and Control of Concrete Mixtures*. 16th Edition. Portland Cement Association, Skokie, IL, 2016.
12. Peterson, R.T. and D. Leftwich, *Determination of water content of plastic concrete using a microwave oven.* NASA STI/Recon Technical Report N, 1978. **79**.
13. AASHTO T 318, *Standard Method of Test for Water Content of Freshly Mixed Concrete Using Microwave Oven Drying*. American Association of State and Highway Transportation Officials, Washington DC, 2015.
14. Hover, K.C., J. Bickley, and R.D. Hooton, *Phase II Report of Preparation of a Performance-Based Specification for Cast-in-Place Concrete.* Guide to Specifying Concrete Performance, NRMCA, March, 2008.
15. ASTM C143 / C143M-15a, *Standard Test Method for Slump of Hydraulic-Cement Concrete, ASTM International*, in *West Conshohocken, PA, 2015.*
16. ASTM C138/C 138 -17a, Standard Test Method for Density (Unit Weight), Yield and Air Content (Gravimetric) of Concrete. ASTM Int, West Conshohocken, PA, 2017.
17. ASTM C39/C39M-18, *Standard Test Method for Compressive Strength of Cylindrical Concrete Specimens, ASTM International, West Conshohocken, PA, 2018.*
18. AASHTO TP95, *Standard Method of Test for Surface Resistivity Indication of Concrete's Ability to Resist Chloride Ion Penetration.* American Association of State Highway and Transportation Officials, Washington DC, 2011.

19.   Robertson, J.B., Ley, M. T., *Determining the Water to Cement Ratio of Fresh Concrete by Evaporation.* Construction and Building Materials, Vol 242, May 2020.

20.   Hu, Q., et al., *Direct three-dimensional observation of the microstructure and chemistry of C3S hydration.* Cement and Concrete Research, 2016. **88**: p. 157-169.

21.   Hu, Q., et al., *Direct Measurements of 3D Structure, Chemistry and Mass Density During the Induction Period of C3S Hydration.* Cement and Concrete Research, 2016. **89**: p. 14-26.

22.   Hu, Q., et al., *Combined three-dimensional structure and chemistry imaging with nanoscale resolution.* Acta materialia, 2014. **77**: p. 173-182.

23.   ACI 211.1-91. *Standard Practice for Selecting Proportions for Normal, Heavyweight, and Mass Concrete*. American Concrete Institute Farmington Hills, Michigan, 1991.

24.   Bentz, E.C., *Probabilistic modeling of service life for structures subjected to chlorides.* Materials Journal, 2003. **100**(5): p. 391-397.

25.   Hime, W. and R.A. Willis, *A method for the determination of the cement content of plastic concrete*. 1955.

26.   Kelly, R. and J. Vail, *Rapid Analysis of Fresh Concrete-Part 1.* Concrete (London), 1968.

27.   Howdyshell, P.A., *Revised Operations Guide for a Chemical Technique to Determine Water and Cement Concrete of Fresh Concrete*. 1977, CONSTRUCTION ENGINEERING RESEARCH LAB (ARMY) CHAMPAIGN ILL.

28.   Whiting, D. and M. Nagi, *Laboratory evaluation of nuclear gage for measurement of water and cement content of fresh concrete.* Materials Journal, 1999. **96**(1): p. 101-108.

29.   Popovics, S. and J.S. Popovics, *Ultrasonic testing to determine water-cement ratio for freshly mixed concrete.* Cement, concrete and aggregates, 1998. **20**(2): p. 262-268.

30.   Mancio, M., et al., *Instantaneous in-situ determination of water-cement ratio of fresh concrete.* ACI Materials Journal, 2011. **108**(5): p. 566-567.

31.   Wei, X. and Z. Li, *Early hydration process of Portland cement paste by electrical measurement.* Journal of materials in civil engineering, 2006. **18**(1): p. 99-105.

32.   ASTM C150/C150 M-18, *Standard Specification for Portland Cement.* ASTM International, West Conshohocken, PA, 2018.

33.   ASTM C33 / C33M-18, *Standard Specification for Concrete Aggregates.* ASTM International, West Conshohocken, PA, 2018.

34.   Ley, M.T., et al., *Determining the air-void distribution in fresh concrete with the Sequential Air Method.* Construction and Building Materials, 2017. **150**: p. 723-737.

35.   C566, A., *Standard Test Method for Total Evaporable Moisture Content of Aggregate by Drying* 2013.

36.   ASTM C231 / C231M - 17a, *Standard Test Method for Air Content of Freshly Mixed Concrete by the Pressure Method*. West Conshohocken, PA, 2017.

37.   ASTM C172 / C172M-17, *Standard Practice for Sampling Freshly Mixed Concrete*. West Conshohocken, PA, 2017.

38.   ASTM C31 / C31M-18b, *Standard Practice for Making and Curing Concrete Test Specimens in the Field, ASTM International, West Conshohocken, PA,.* 2018.

39.   ODOT, *Oklahoma Department of Transportation, Standard Specifications, Oklahoma City, OK.* 2009.

40.   ASTM C1202 - 18, *Standard Test Method for Electrical Indication of Concrete's Ability to Resist Chloride Ion Penetration*. West Conshohocken, PA, 2018.

41.   Taylor, H.F.W., *Cement Chemistry, 2nd edition*. Heron Quay, London, 1997.

42.   Taylor, P.C., et al., *Integrated Materials and Construction Practices for Concrete Pavement: A State-of-the-Practice Manual. Second Edition*, I.S.U. National Concrete Pavement Technology Center, Ames, IA., Editor. 2019.

43.   ACI Committee 318, *Building Code Requirements for Structural Concrete and Commentary (ACI 318-19)*, in *American Concrete Institute*. Farmington Hills, MI, 2019.

44.   Obla, K., & Lobo, C. L., *Mixing Water Control.* Concrete in Focus, Vol 10, pp23-27, 2011.

45.   Koehler, E.P. and M.S. Roberts. *Automated Measurement and Control of Slump and Water Content for Concrete Quality Assurance*. in *Transportation Research Board 92nd Annual Meeting*. Washington D.C., 2013.

46.   ASTM C856-18a, *ASTM C856-18a, Standard Practice for Petrographic Examination of Hardened Concrete, ASTM International, West Conshohocken, PA, 2018.*

47.   Cook, M.D., *Aggregate proportioning for slip formed pavements and flowable concrete*. Oklahoma State University, 2015.

48.   Powers, T.C., *Structure and physical properties of hardened Portland cement paste.* Journal of the American Ceramic Society, Vol. 41, (1), pp 1-6, 1958.

49.   Obla, K.H. and C.L. Lobo, *Acceptance criteria for durability tests.* Concrete International, Vol. 29 (5), 2007.

50.   Spragg, R., et al., *Factors that influence electrical resistivity measurements in cementitious systems.* Transportation research record, Vol 2342 (1), pp 90-98, 2013.

51.   Cook, M.D. and M.T. Ley, *Concrete Reports & Submittals*. lulu.com, 2018.

52.   Suprenant, B.A. and W.R. Malisch, *How to evaluate petrographic reports.* Concrete Construction, 1999.

53.   Ley, M., T., J.B. Robertson, and K. Leflore, J., *Rapid Field Method to Determine the Water to Cement Ratio of Fresh Concrete by Evaporation.* U.S. Provisional Patent Application No. 62/879,965, 2019.

54.   Robertson, J.B., Ley, M. T., *Development of Concrete Mixtures to Mitigate Bridge Deck Cracking*, in *Annual Project Status Report*. Oklahoma Department of Transportation, Oklahoma City, OK, 2019.

55.   Obla, K.H., *Improving Concrete Quality*. CRC Press, 2014.

56.   ASTM C618-19, *Standard Specification for Coal Fly Ash and Raw or Calcined Natural Pozzolan for Use in Concrete, West Conshohocken, PA.* 2019.

57.   ASTM C1017, *Standard Specification for Chemical Admixtures for Use in Producing Flowing Concrete, West Conshohocken, PA, 2013*.

58.   ASTM-C494, *Standard Specification for Chemical Admixtures for Concrete, ASTM International: West Conshohocken, PA.* 2019.

59.   ASTM C94/C94M, *Standard Specification for Ready-Mixed Concrete, West Conshohocken, PA, 2019*.

60.   ASTM C566, *Standard Test Method for Total Evaporable Moisture Content of Aggregate by Drying.* West Conshohocken, PA, 2013.

61.   Cox, D. and D. Hinkley, *Theoretical Statistics Chapman and Hall, London.* 1974.

62.   Moses, L.E., *Graphical methods in statistical analysis.* Annual review of public health, Vol. 8, Issue 1, pp 309-353, 1987.

63.   Goldstein, H. and M.J. Healy, *The graphical presentation of a collection of means.* Journal of the Royal Statistical Society: Series A (Statistics in Society), Vol 158, pp. 175-177, 1995.

64.   Rice, J.A., *Mathematical statistics and data analysis, 3rd Edition*. Cengage Learning, Thomson Brooks/Cole, 2006.

65.   Kalinowski, P., *Understanding Confidence Intervals (CIs) and effect size estimation.* APS Observer, Vol 23, Issue 4, 2010.

66.   Knezevic, A., *Overlapping confidence intervals and statistical significance.* StatNews: Cornell University Statistical Consulting Unit, Vol. 73, Issue 1, 2008.

67.   Wolfe, R. and J. Hanley, *If we're so different, why do we keep overlapping? When 1 plus 1 doesn't make 2.* Canadian Medical Association, Vol. 166, pp. 65-66, 2002.

68.   Snedecor, G.W. and W.G. Cochran, *Statistical Methods, eighth edition.* Iowa State University Press, Ames, Iowa, 1989.

69.   Armitage, P., G. Berry, and J.N.S. Matthews, *Statistical methods in medical research*. John Wiley & Sons, 2008.

70.   Nakagawa, S. and I.C. Cuthill, *Effect size, confidence interval and statistical significance: a practical guide for biologists.* Biological Reviews, Vol. 82, (4), pp. 591-605, 2007.

71.   DeGroot, M.H. and M.J. Schervish, *Probability and statistics*. 2012: Pearson Education.

72.   Rosner, B., *Fundamentals of biostatistics*. 2015: Nelson Education.

73.   ASTM C670, *Preparing Precision and Bias Statements for Test Methods for Construction Materials.* ASTM International, West Conshohocken, PA, 2015.

74.   Mehta, P., *Scanning electron micrographic studies of ettringite formation.* Cement and Concrete Research, 1976. **6**(2): p. 169-182.

75.   Robertson, J.B., M.T. Ley, and M.D. Cook, *Measuring the Change in Water to Cement Ratio in Fresh and Hardened Concrete.* Construction and Building Materials (Submitted), 2020.

76.   Thomas J. T., et al., *State of Water in Hydrating Tricalcium Silicate and Portland Cement Pastes as Measured by Quasi-Elastic Neutron Scattering.* Journal of the American Ceramic Society, 2019.

77.   Lea, F.M. and P.C. Hewlett, *Lea's Chemistry of Cement and Concrete, 4th Edition*. New York: Elsevier Butterworth-Heinmann, 2004.

78.   Jennings, H. *The physical and chemical development of calcium silicate hydrate during the setting and hardening of Portland cement*. in *RILEM PROCEEDINGS*. Chapman & Hall, 1992.

79.   Nilsson, L.-O., *Hygroscopic Moisture in Concrete-Drying, Measurements & Related Material Properties.* Division of Building Materials, LTH, Lund University, Lund Sweden, 1980.

80.   Kocaba V., *Development and evaluation of methods to follow microstructural development of cementitious systems including slags.* PhD Thesis. Lausanne, Switzerland, Ecole Polytechnique Federale De Lausanne, 2009.

81.   Ramachandran V. S., B.J.J., *Handbook of Analytical Techniques in Concrete Science Technology - Principles, Techniques and Applications.* Norwich, NY, pp. 127-173, 2001.

82.   Hager, I., *Behaviour of Cement Concrete at High Temperature. Bulletin of the Polish Academy of sciences, Technical Sciences 61, pp. 1-10.* 2013.

83.   Bensted, J. and S.P. Varma, *Some Application of Infrared and Raman Spectroscocy in Cement Chemistry. Part 3 - Hydration of Poraland Cement and its Consituents.* Cement Technology, September, 5(5), pp 440-445, 1974.

84.   Prochon, P., & Piotrowski, T., *Bound Water Content Measurement in Cement Pastes by Stoichiometric and Gravimetric Analyses.* Journal of Building Chemistry, 1, pp 18-25, 2016.

85.   Dubberke, W., & Marks, V. J., *Thermogravimetric Analysis of Carbonate Aggregate, Final Report for Iowa Highway Research Board*. Reasearch Project HR-336, Office of Materials Highway Division, Iowa Department of Transportation, Ames, IA, 1994.

86. Razafinjato, R.N., Beaucour, A.L. Hebert, R. Ledesert, B. Bodet, R. Noumowe, A. , *High temperature behaviour of a wide petrographic range of siliceous and calcareous aggregates for concretes. Construction Building Materials, Vol 123, pp. 261–273, 2016.*

87. ASTM C1702-17, *Standard Test Method for Measurement of Heat of Hydration of Hydraulic Cementitious Materials Using Isothermal Conduction Calorimetry*. ASTM International, West Conshohocken, PA, 2017.

88. Fordham, C.J. and I.J. Smalley, *A Simple Thermogravimetric Study of Hydrated Cement.* Cement and Concrete Research, Vol 15, pp. 141-144, 1985.

89. Brown, M.E., *Introduction to thermal analysis: techniques and applications*. Vol. 1. 2001: Springer Science & Business Media.

90. Gabbott, P., *Principles and applications of thermal analysis*. 2008: John Wiley & Sons.

91. Haines, P.J., *Thermal methods of analysis: principles, applications and problems*. 2012: Springer Science & Business Media.

92. Heikal, M., *Effect of Temperature on the Structure and Strength Properties of Cement Pastes Containing Fly Ash Alone or in Combination with Limestone.* Ceramics – Silikáty 50 (3) 167-177, 2006.

93. Aruja, E., *The unit cell and space group of 4CaO. Al2O3. 19H2O polymorphs.* Acta Crystallographica, 1961. **14**(12): p. 1213-1216.

94. Black, L., et al., *Hydration of tricalcium aluminate (C 3 A) in the presence and absence of gypsum—studied by Raman spectroscopy and X-ray diffraction.* Journal of Materials Chemistry, 2006. **16**(13): p. 1263-1272.

95. Bullard, J.W., et al., *Mechanisms of cement hydration.* Cement and concrete research, 2011. **41**(12): p. 1208-1223.

96. Christensen, A.N., et al., *Hydrolysis of Pure and Sodium Substituted Calcium Aluminates and Cement Clinker Components Investigated by in Situ Synchrotron X-ray Powder Diffraction.* Journal of the American Ceramic Society, 2004. **87**(8): p. 1488-1493.

97. Collepardi, M., et al., *Tricalcium aluminate hydration in the presence of lime, gypsum or sodium sulfate.* Cement and Concrete Research, 1978. **8**(5): p. 571-580.

98. Hampson, C. and J. Bailey, *The microstructure of the hydration products of tri-calcium aluminate in the presence of gypsum.* Journal of Materials Science, 1983. **18**(2): p. 402-410.

99. Holly, R., et al., *Magnetic resonance in situ study of tricalcium aluminate hydration in the presence of gypsum.* Journal of the American Ceramic Society, 2006. **89**(3): p. 1022-1027.

100. Minard, H., et al., *Mechanisms and parameters controlling the tricalcium aluminate reactivity in the presence of gypsum.* Cement and Concrete Research, 2007. **37**(10): p. 1418-1426.

101. Myers, R.J., et al., *Role of adsorption phenomena in cubic tricalcium aluminate dissolution.* Langmuir, 2017. **33**(1): p. 45-55.

102. Quennoz, A. and K.L. Scrivener, *Hydration of C3A–gypsum systems.* Cement and concrete research, 2012. **42**(7): p. 1032-1041.

103. Roberts, M., *New calcium aluminate hydrates.* Journal of applied chemistry, 1957. **7**(10): p. 543-546.

104. Skalny, J. and M.E. Tadros, *Retardation of Tricalcium Aluminate Hydration by Sulfates.* Journal of American Ceramic Society, 1977. **60**: p. 174-175.

105. Geng, G., et al., *Synchrotron X-ray Nanotomographic and Spectromicroscopic Study of the Tricalcium Aluminate Hydration in the Presence of Gypsum.* Cement and Concrete Research, 2018. **111**: p. 130-137.

106.	Bazzoni, A., M. Cantoni, and K.L. Scrivener, *Impact of annealing on the early hydration of tricalcium silicate.* Journal of the American Ceramic Society, 2014. **97**(2): p. 584-591.

107.	Chen, J.J., et al., *A Coupled nanoindentation/SEM-EDS study on low water/cement ratio Portland cement paste: evidence for C–S–H/Ca (OH) 2 nanocomposites.* Journal of the American Ceramic Society, 2010. **93**(5): p. 1484-1493.

108.	Constantinides, G. and F.-J. Ulm, *The effect of two types of CSH on the elasticity of cement-based materials: Results from nanoindentation and micromechanical modeling.* Cement and concrete research, 2004. **34**(1): p. 67-80.

109.	Diamond, S. *Cement paste microstructure-an overview at several levels*. in *Proc. Conference held at University of SheffieldHydtaulic Cement Paste-Their structure and properties'*. 1976. Cement and Concrete Association.

110.	Gallucci, E., P. Mathur, and K. Scrivener, *Microstructural development of early age hydration shells around cement grains.* Cement and Concrete Research, 2010. **40**(1): p. 4-13.

111.	Garrault, S., et al., *Study of CSH growth on C 3 S surface during its early hydration.* Materials and structures, 2005. **38**(4): p. 435-442.

112.	Goto, S., et al., *Composition and morphology of hydrated tricalcium silicate.* Journal of the American Ceramic Society, 1976. **59**(7-8): p. 281-284.

113.	Jennings, H.M., *A model for the microstructure of calcium silicate hydrate in cement paste.* Cement and concrete research, 2000. **30**(1): p. 101-116.

114.	Juilland, P., et al., *Dissolution theory applied to the induction period in alite hydration.* Cement and Concrete Research, 2010. **40**(6): p. 831-844.

115.	Kumar, A., J. Reed, and G. Sant, *Vertical scanning interferometry: a new method to measure the dissolution dynamics of cementitious minerals.* Journal of the American Ceramic Society, 2013. **96**(9): p. 2766-2778.

116.	Ménétrier, D., et al., *ESCA and SEM studies on early C3S hydration.* Cement and concrete research, 1979. **9**(4): p. 473-482.

117.	Peled, A., J. Castro, and W. Weiss, *Atomic force and lateral force microscopy (AFM and LFM) examinations of cement and cement hydration products.* Cement and Concrete Composites, 2013. **36**: p. 48-55.

118.	Richardson, I., *Tobermorite/jennite-and tobermorite/calcium hydroxide-based models for the structure of CSH: applicability to hardened pastes of tricalcium silicate, β-dicalcium silicate, Portland cement, and blends of Portland cement with blast-furnace slag, metakaolin, or silica fume.* Cement and Concrete Research, 2004. **34**(9): p. 1733-1777.

119.	Richardson, I.G., *The nature of CSH in hardened cements.* cement and concrete research, 1999. **29**(8): p. 1131-1147.

120.	Richardson, I.G., *The calcium silicate hydrates.* Cement and concrete research, 2008. **38**(2): p. 137-158.

121.	Tennis, P.D. and H.M. Jennings, *A model for two types of calcium silicate hydrate in the microstructure of Portland cement pastes.* Cement and concrete research, 2000. **30**(6): p. 855-863.

122.	Vandamme, M., F.-J. Ulm, and P. Fonollosa, *Nanogranular packing of C–S–H at substochiometric conditions.* Cement and Concrete Research, 2010. **40**(1): p. 14-26.

123.	Brisard, S., et al., *Morphological quantification of hierarchical geomaterials by X-ray nano-CT bridges the gap from nano to micro length scales.* American Mineralogist, 2012. **97**(2-3): p. 480-483.

124.   Geng, G., et al., *Atomic and nano-scale characterization of a 50-year-old hydrated C3S paste.* Cement and Concrete Research, 2015. **77**: p. 36-46.

125.   Kilcoyne, A., et al., *Interferometer-controlled scanning transmission X-ray microscopes at the Advanced Light Source.* Journal of synchrotron radiation, 2003. **10**(2): p. 125-136.

126.   Shapiro, D.A., et al., *Chemical composition mapping with nanometre resolution by soft X-ray microscopy.* Nature Photonics, 2014. **8**(10): p. 765.

127.   Winarski, R.P., et al., *A hard X-ray nanoprobe beamline for nanoscale microscopy.* Journal of Synchrotron Radiation, 2012. **19**(6): p. 1056-1060.

128.   Yu, Y.-S., et al., *Dependence on crystal size of the nanoscale chemical phase distribution and fracture in Li x FePO4.* Nano letters, 2015. **15**(7): p. 4282-4288.

129.   Levitz, P. and D. Tchoubar, *Disordered porous solids: from chord distributions to small angle scattering.* Journal de Physique I, 1992. **2**(6): p. 771-790.

130.   Hewlett, P. and M. Liska, *Lea's chemistry of cement and concrete*. 2019: Butterworth-Heinemann.

131.   Taylor, H.F., *Cement chemistry*. Vol. 2. 1997: Thomas Telford London.

132.   Taylor, P.C. and G.F. Voigt, *Integrated materials and construction practices for concrete pavement: A state-of-the-practice manual*. 2007, United States. Federal Highway Administration. Office of Pavement Technology.

133.   Schwiete, H.E., U. Ludwig, and P. Jager, *Symposium on Structure of Portland Cement Paste and Concrete* Highway Research Board, 1966: p. 353.

134.   Stein, H., *Some Characteristics of the Hydration of 3CaO·Al2 O3-CaSO4-CaO-H2O.* Silcates Industriels 1963. **28**: p. 141-145.

135.   Bailey, J. and C. Hampson, *The microstructure and chemistry of tricalcium aluminate hydration.* Philosophical Transactions of the Royal Society of London. Series A, Mathematical and Physical Sciences, 1983. **310**(1511): p. 105-111.

136.   Corstanje, W., H. Stein, and J. Stevels, *Hydration reactions in pastes C3S+ C3A+ CaSO4. 2aq+ H2O at 25° Cl.* Cement and Concrete Research, 1973. **3**(6): p. 791-806.

137.   Scrivener, K.L. and P. Pratt. *Microstructural studies of the hydration of C 3 A and C 4 AF independently and in cement paste*. in *Proc. Br. Ceram. Soc.* 1984.

138.   Tang, F.J. and E.M. Gartner, *Influence of sulphate source on Portland cement hydration.* Advances in Cement Research, 1988. **1**(2): p. 67-74.

139.   Snoeck, D., et al., *The influence of different drying techniques on the water sorption properties of cement-based materials.* Cement and Concrete Research, 2014. **64**: p. 54-62.

140.   Zhang, J. and G.W. Scherer, *Comparison of methods for arresting hydration of cement.* Cement and Concrete Research, 2011. **41**(10): p. 1024-1036.

141.   ORS. *Dragonfly version 3.6*. 2019; Available from: https://www.theobjects.com/dragonfly/.

142.   Vogt, S. *MAPS: A set of software tools for analysis and visualization of 3D X-ray fluorescence data sets*. in *Journal de Physique IV (Proceedings)*. 2003. EDP sciences.

143.   Hubbell, J., *Photon mass attenuation and energy-absorption coefficients.* The International Journal of Applied Radiation and Isotopes, 1982. **33**(11): p. 1269-1290.

APPENDICES

A.1 Statistical Significance

Table A-1 shows the percentage of tests that passed the t-test.

Table A-1. T-Test Results (Percentage of tests)

	Increase in w/cm		
	0.04	0.08	0.12
Slump	0%	0%	0%
UW	0%	0%	0%
Phoenix w/cm	88%	88%	88%
7-day Compressive strength	13%	38%	50%
7-day resistivity	63%	25%	38%
28-day compressive strength	38%	38%	38%
28-day resistivity	63%	50%	63%

Table A-2 shows the percentage of tests with no overlap comparing 95% confidence intervals between water increases per truck tested.

Table A-2. 95% Confidence Interval Results (Percentage of tests)

	Increase in w/cm		
	0.04	0.08	0.12
Slump	0%	0%	13%
UW	25%	38%	25%
Phoenix w/cm	63%	75%	50%
7-day Compressive strength	0%	0%	0%
7-day resistivity	63%	63%	50%
28-day compressive strength	0%	0%	0%
28-day resistivity	88%	75%	75%

VITA

John Bret Robertson

Candidate for the Degree of

Doctor of Philosophy

Thesis: THE IMPACT OF WATER AND C3A ON PORTLAND CEMENT
HYDRATION

Major Field: Civil Engineering

Biographical:

Education:

Completed the requirements for the Doctor of Philosophy in Civil Engineering
at Oklahoma State University, Stillwater, Oklahoma in July 2020.

Completed the requirements for the Master of Science in Civil Engineering at
Oklahoma State University, Stillwater, Oklahoma in May 2010

Completed the requirements for the Bachelor of Science in Civil Engineering at
Oklahoma State University, Stillwater, Oklahoma in December 2008

Experience:

Civil Engineer at Bureau of Reclamation in Denver, CO, from 2010-2016.

Professional Memberships:

Professional Engineer, Colorado, No. 50590
American Concrete Institute (ACI), 2010-present
American Society for Testing and Materials, 2010-present
Strategic Development Council, ACI, 2010-2016
Rocky Mountain Chapter – ACI, 2010-2016